# COMPLIANT CENTRIFUGAL CLUTCHES: DESIGN, ANALYSIS, AND TESTING

by

Nathan B. Crane

A thesis submitted to the faculty of

Brigham Young University

in partial fulfillment of the requirements for the degree of

Master of Science

Department of Mechanical Engineering

Brigham Young University

December 1999

BRIGHAM YOUNG UNIVERSITY

**GRADUATE COMMITTEE APPROVAL**

of a thesis submitted by

Nathan B. Crane

This thesis has been read by each member of the following graduate committee and by majority vote has been found to be satisfactory.

| | |
|---|---|
| _____ | _____ |
| Date | Larry L. Howell, Chair |
| _____ | _____ |
| Date | Kenneth W. Chase |
| _____ | _____ |
| Date | Timothy W. McLain |

BRIGHAM YOUNG UNIVERSITY

As chair of the candidate's graduate committee, I have read the thesis of Nathan B. Crane in its final form and have found that (1) its format citations, and bibliographical style are consistent and acceptable and fulfill university and department style requirements; (2) its illustrative materials including figures, tables, and charts are in place; and (3) the final manuscript is satisfactory to the graduate committee and is ready for submission to the university library.

_____ _____

Date

Larry L. Howell
Chair, Graduate Committee

Accepted for the Department

_____

Craig C. Smith
Graduate Coordinator

Accepted for the College

_____

Douglas M. Chabries
Dean, College of Engineering and Technology

ABSTRACT

COMPLIANT CENTRIFUGAL CLUTCHES: DESIGN, ANALYSIS, AND TESTING

Nathan B. Crane

Department of Mechanical Engineering

Master of Science

Existing classes of centrifugal clutch concepts were reviewed. The pseudo-rigid-body model (PRBM), rigid-body replacement synthesis, force-deflection analysis, compliance potential evaluation, and compliant concept evaluation were used to develop effective new centrifugal clutch concepts. These methods helped develop and model four novel compliant centrifugal clutch designs, model two existing designs, and identify a concept with excellent potential for low-cost centrifugal clutch applications. This concept, the floating opposing arm (FOA) clutch, doubles the torque capacity metric relative to existing compliant designs. Torque and engagement speed models for this clutch were developed and verified against four prototype clutches. Additional novel designs developed through this work have lower torque capacities, but also show good potential because of other unique characteristics. All of the designs were prototyped and tested to measure their torque-speed relationships.

# ACKNOWLEDGEMENTS

The author wishes to acknowledge the gracious support of the many people that contributed to this work both directly and indirectly.

A great debt is owed to Dr. Larry L. Howell for his guidance and instruction in helping me through all of the phases of this work. His mentoring and example have been and will yet be invaluable. The time and effort of Dr. Kenneth Chase and Dr. Timothy McLain as committee members are greatly appreciated.

Brent Weight helped tremendously in his long efforts to prototype the many odd geometries developed, develop testing software, and assist in the testing. Scott Lyon's skills were invaluable in developing the signal conditioning circuits and going to great lengths to solve problems with the data acquisition equipment. Everyone in the lab has been a great support suggesting solutions to occasional problems and setting a fine example through their research and love of learning.

Without my parents early support and encouragement, I never would have made it this far. Most of all, thanks to my supportive wife for her continual support and encouragement as well as her many hours of careful proofreading. Her work both in proofreading and encouraging me to do my best, has greatly improved this thesis.

This work has been funded in part through a National Science Foundation graduate fellowship and by a National Science Foundation Career Award, No. DMI-9624574.

# Table of Contents

# List of Tables

# List of Figures

CHAPTER 1

# Introduction

## 1.1 Thesis Statement

This thesis shows that the principles of compliant mechanism technology can be used to develop and analyze cost-effective centrifugal clutch configurations. Two pre-existing and four novel compliant centrifugal clutch configurations are presented. A basic model of each design is developed and the results of prototype testing are discussed. The relative merits of the different designs are discussed and several applications are demonstrated.

## 1.2 Background

### 1.2.1 Centrifugal Devices

A centrifugal device is actuated by centrifugal force. However, in a strict sense, centrifugal force does not exist, but the term is used because it provides an intuitive way to consider normal accelerations due to constant rotational velocity. Other related terms include centripetal forces, D'Alembert forces, inertial forces and centripetal acceleration. To avoid confusion, each of these terms is reviewed.

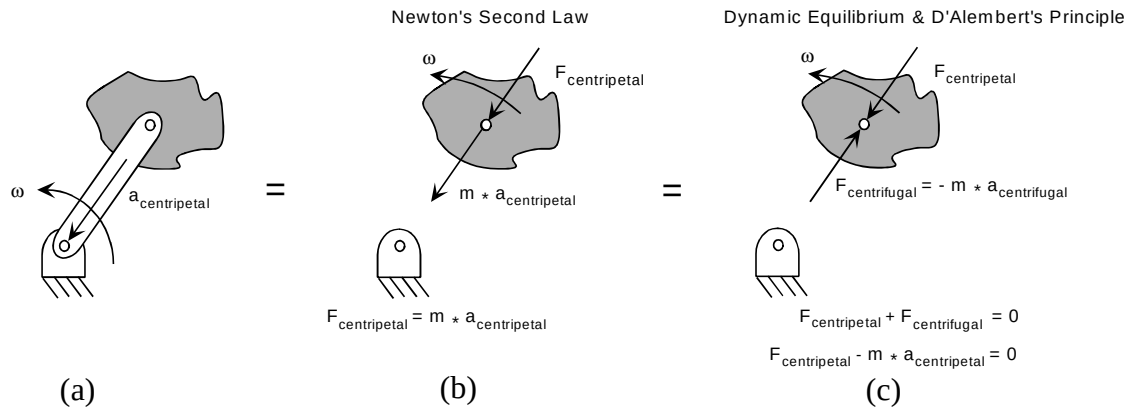


**Figure 1-1** (a) Body rotating at a constant angular velocity and pinned at its center of mass. (b) The motion equations using the standard form of Newton's Second Law. (c) The motion equations using D'Alembert's Principle and centrifugal forces are shown.

A body moving in a circular motion with a constant angular velocity ($\omega$) accelerates continuously due to its constantly changing direction of motion. Figure 1-1(a) shows such a body. The acceleration vector is oriented toward the center of the circular motion and its magnitude is

$$a = \omega^2 r \qquad \textbf{(1.1)}$$

This acceleration is termed *centripetal* or *normal acceleration*. The force exerted to cause this acceleration is called *centripetal force (*Figure 1-1(b)). Applying Newton's second law, the centripetal force is

$$F_{centripetal} = m\omega^2 r \qquad \textbf{(1.2)}$$

Centripetal forces are also directed toward the center of rotation.

The equilibrium equation for a body rotating at a uniform angular velocity with arbitrary additional forces is

$$\sum F = ma = m\omega^2 r \quad \textbf{(1.3)}$$

This equation may be rearranged as

$$\sum F + (-m\omega^2 r) = 0 \quad \textbf{(1.4)}$$

where the term $(-m\omega^2 r)$ is termed an *inertial* or *D'Alembert force*. It has the units of force, and is directed opposite to the centripetal acceleration. D'Alembert's principle states the equivalency of equations (1.3) and (1.4). *Centrifugal force* is the D'Alembert force caused by the centripetal acceleration of a rotating body. It is expressed as

$$F_{centrifugal} = -m\omega^2 r \quad \textbf{(1.5)}$$

For most solid objects, the centrifugal force can be considered a function of rotational velocity only because mass is constant and generally, the radius is nearly constant. Thus centrifugal force is a useful actuation force for many applications requiring a response to rotational velocity. Centrifugal force actuated devices are simple, inexpensive solutions to clutch and switch applications since they require no outside power source or signal for control or actuation.

Many thousands of centrifugal devices are produced annually. Their applications range from yoyos to industrial facilities. Many of these devices are relatively simple and have changed little over the past twenty years. This work systematically applies the principles of compliant mechanism design to these centrifugal devices so that they may benefit from recent advances in compliant mechanism technology.

### 1.2.2 Centrifugal Clutches

Centrifugal clutches transmit torque as a function of the driving speed. The actuation force and control are provided by centrifugal forces on the clutch. This work seeks to develop novel centrifugal clutch configurations with increased torque capacity and/or load acceleration smoothness while maintaining a cost advantage over rigid-body designs. A successful design increases these performance parameters and/or decreases production costs. Centrifugal clutches are constrained by many factors such as heat, wear, load capacity, and space.

Centrifugal clutches reduce starting torques on AC motors, reduce loads on internal combustion engines at idle speeds, and provide overload protection. They can also isolate torsional vibrations. In many applications, the clutches provide adequate load acceleration and control with minimal expense. Their use can also decrease required motor size by decreasing the current draw of motors accelerating a high-inertia load. This is accomplished by reducing the required torque output at speeds where the motor is least able to generate torque. Figure 1-2 compares torque output and current draw of an electric motor with and without a centrifugal clutch.

Each year, centrifugal clutches provide power transmission and/or control for thousands of string trimmers, chainsaws, radio-controlled cars and helicopters, and go-karts. They also control torque transmission in large industrial motors transmitting hundreds or even thousands of horsepower. These applications use centrifugal clutches due to their simplicity and low cost relative to competing solutions such as magnetic, electric, and pneumatic clutches. However, the simplicity of the centrifugal clutch also

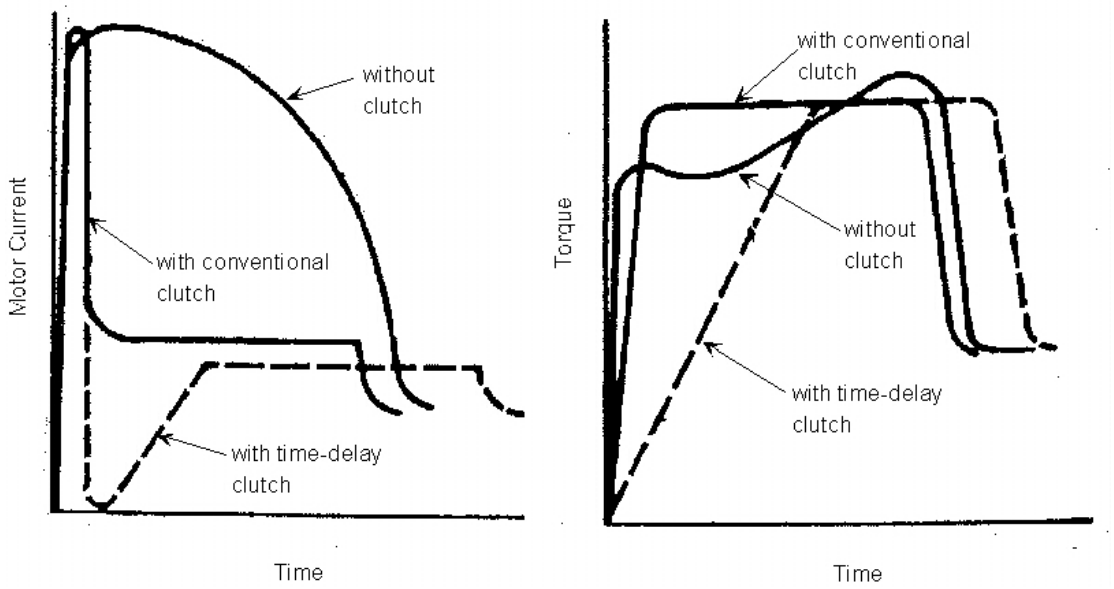


**Figure 1-2** Torque and current versus time of an AC motor with a conventional and a time-delay centrifugal clutch. Current draw is dramatically reduced for both clutch types. The time-delay clutch reduces initial torques to increase the starting smoothness (St. John, 1979).

limits the range of torque control possible from a given clutch. This limits their use in applications demanding smoother starts, or with varying starting conditions.

The squared relationship between torque and speed means there is a cubic relationship between speed and transmitted power. This can be an advantage or disadvantage depending on the application. An apparently small deviation in operating speed can result in a very large change in maximum transmitted power. A clutch should be sized so that no components will be damaged if the clutch transmits its maximum torque.

Centrifugal clutches are friction clutches. As such, wear and heating during load acceleration is an important concern. Clutches may also have problems due to variation in the friction conditions that modify the expected torque-speed relationship. However, centrifugal clutches are very efficient under operating conditions because there is no slippage in the clutch after the load is accelerated. However, if torque increases beyond

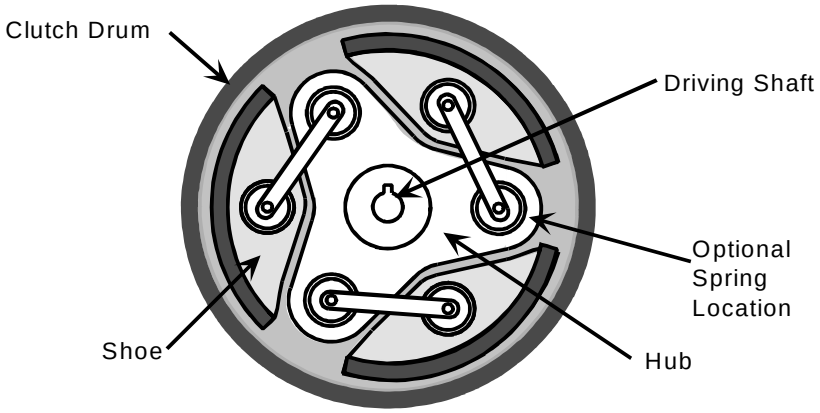


**Figure 1-3** A rigid-body connected-shoe clutch with three shoes.

the clutch's capacity, it will slip harmlessly. This protects motors and other more expensive components from damage due to excessive torque.

A common centrifugal clutch design is the connected shoe design shown in Figure 1-3. As the clutch speeds up, the arms deflect outward. The movement may be resisted by springs to raise the speed at which the clutch begins transmitting torque. When the arms contact the cylindrical drum that surrounds them, they begin to transmit torque. Torque transfer capacity will continue to increase as the speed increases.

### 1.2.3 Overspeed Brakes

Some overspeed brakes are based on centrifugal clutches. Centrifugal clutches are well suited to this applications since speed is the input. The variation of centrifugal force with the speed squared can be a very positive factor in these devices. This relationship would ensure that the brake torque and power dissipation increase quickly until the brake halts the acceleration of the system. This effect could be amplified by the use of a brake

with centrifugal switching action so that the brake “snapped” on. However, this could also cause significant shock loading.

Overspeed brakes are not addressed in detail here because they are simply a kinematic inversion of a centrifugal clutch. A centrifugal overspeed brake is a centrifugal clutch with the output fixed to a frame. Any of the clutches discussed in this work could be modified for use as an overspeed brake.

### 1.2.4 Compliant Mechanisms

Compliant mechanisms are mechanisms that obtain some or all of their motion through the deflection of their members. In a compliant mechanism, a single flexible link often replaces two or more rigid links of an equivalent rigid-body mechanism. This decreases the mechanism’s part count, wear points, and backlash. Due to these advantages, compliant mechanisms have been used in both inexpensive mass-produced parts and low-volume precision parts. Compliant configurations of centrifugal devices may decrease manufacturing costs compared to rigid-body designs. Their lower cost may also allow new applications of centrifugal devices in low-cost products. Compare the rigid-body and compliant clutch designs in Figure 1-4. This clutch demonstrates part count reduction through compliant mechanism technology.

The advantages of compliant mechanisms come with increased design challenges. These challenges include analyzing nonlinear deflections and increased fatigue-failure concerns. The pseudo-rigid-body model (PRBM) translates compliant mechanisms into nearly equivalent rigid-body mechanisms for early analysis and synthesis. Figure 1-5 shows a compliant mechanism and its PRBM. Using the PRBM, compliant mechanisms

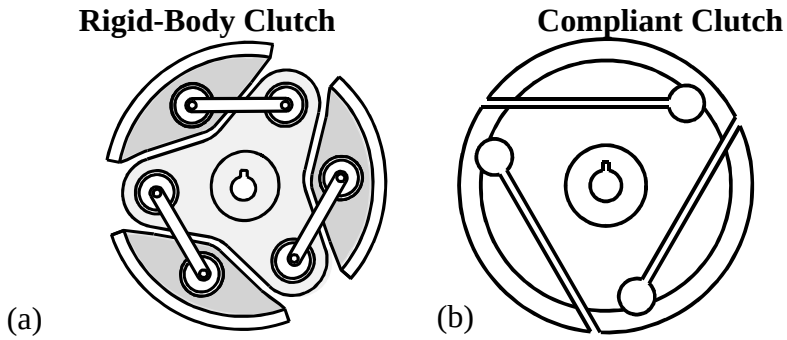


**Figure 1-4** Two centrifugal clutches. (a) The rigid-body clutch consists of at least 13 parts while (b) the compliant clutch is just one piece. Both clutches transmit torque when clutch members move outward due to centrifugal force. As they move outward, they contact a drum and transmit torque.

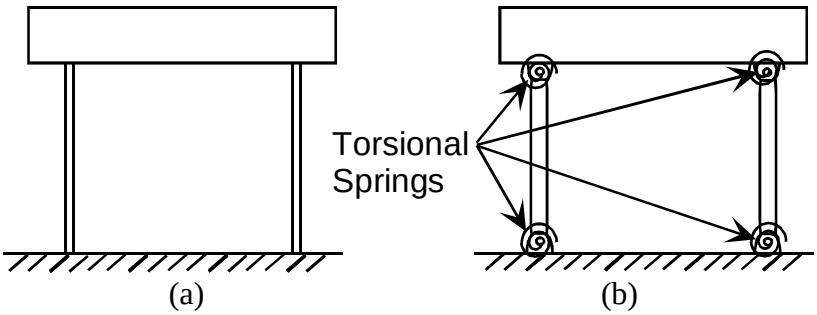


**Figure 1-5** (a) A complaint parallel motion mechanism and (b) its pseudo-rigid-body model.

can be designed and analyzed as rigid-body mechanisms without calculating large beam deflections.

## 1.3 Research Approach

This work brings together many recent developments in compliant mechanism design. The work combines the basic PRBM techniques with rigid-body replacement synthesis, recent work in evaluation of compliance potential, and new tools for evaluating different compliant designs. The research procedure and the relationship of these different procedures are outlined in Figure 1-6 and discussed below.

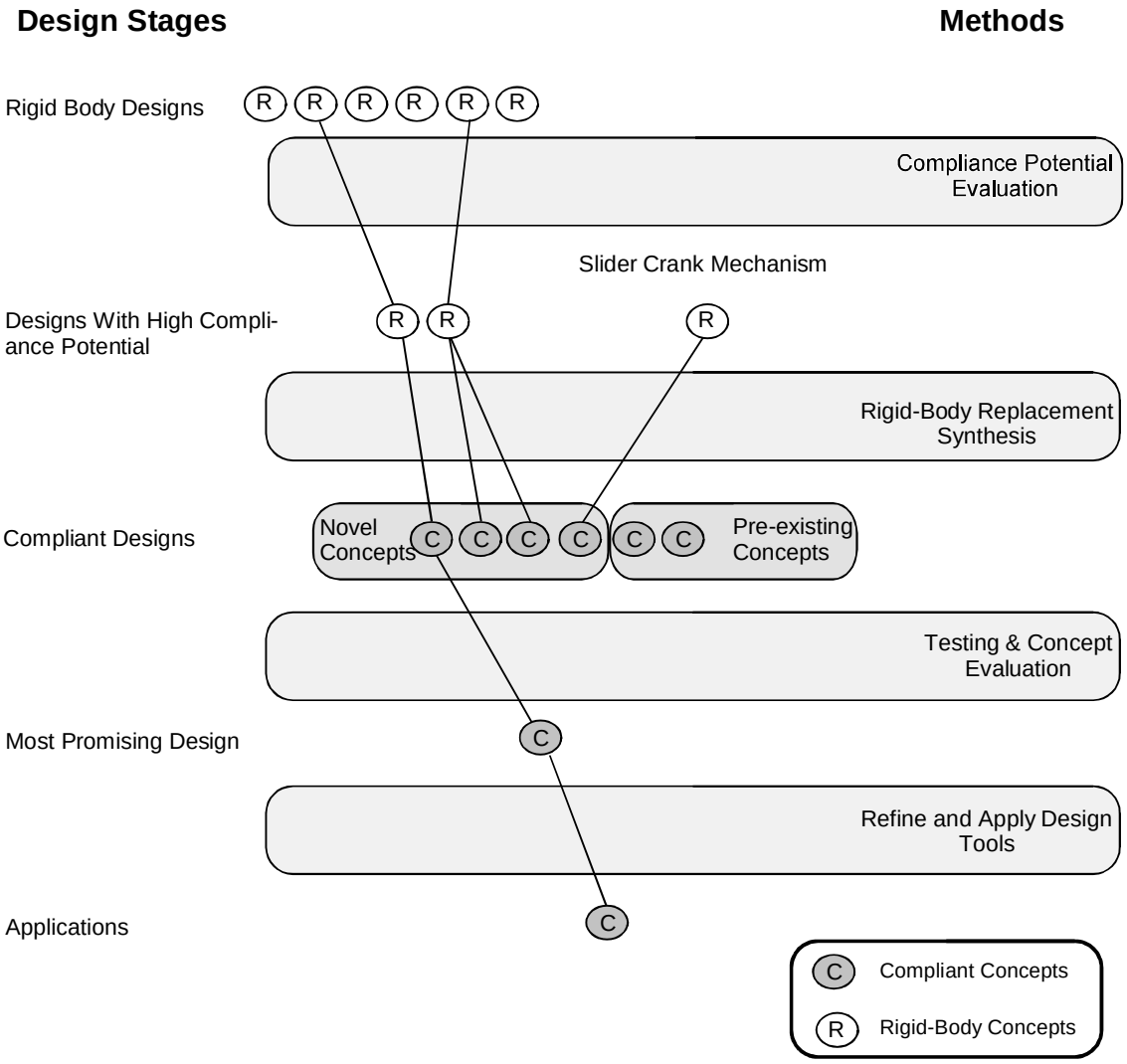


**Figure 1-6** Flowchart of the research approach.

Development proceeded through the following steps.

1. *Survey existing designs*

   Current centrifugal clutch concepts were identified and reviewed. The primary advantages of each concept are discussed.

2. *Develop evaluation criteria*

   Important challenges and limitations of centrifugal clutches were identified by reviewing technical and commercial literature. This information was used to develop evaluation criteria for the compliant-centrifugal clutches.

3. *Evaluate compliance potential of the rigid-body designs*

   Compliance potential criteria developed by Roach & Howell (1999) and Berglund (1998) were used to identify which centrifugal clutch concepts are most adaptable to compliant mechanisms.

4. *Develop compliant designs by rigid-body replacement*

   Compliant centrifugal clutches were developed from concepts that scored well in the compliance criteria evaluation. They were developed by rigid-body-replacement synthesis. Using this method, multiple compliant mechanisms were be generated from a single rigid-body concept.

5. *Explore other novel compliant configurations*

   As the mechanisms generated above were evaluated, other concepts were developed to overcome their limitations. Common mechanism types such as four-bars and double sliders were surveyed for other promising compliant designs.

6. *Prototype designs and collect test data to identify any unique characteristics of a design*

   The new designs were prototyped from sheets of polypropylene using an NC mill. All of the prototype clutches were designed to maximize the actuation mass within a cylinder 4.40 inches in diameter and 0.25 inches long.

   The torque-speed relationships of the clutches were measured. This data was reviewed for unique characteristics such as exceptional torque capability, a non-quadratic torque-speed relationship, or potential for smoother load starting.

7. *Evaluate designs relative to the design criteria*

   The information gleaned from the models and testing were used to rate the different designs relative to the design criteria through a scoring matrix.

8. *Develop torque models for promising clutch types*

   The clutches that scored well in the evaluation were analyzed and the PRBM was applied to develop approximate torque models for parameterized clutches.

9. *Demonstrate potential applications for new centrifugal clutch concepts.*

   A current application for centrifugal clutches was selected. The ideas developed from this thesis were applied to this application to show how they may improve cost and/or performance.

Centrifugal clutches interact with a complex, varied environment. This environment requires similarly broad analysis and testing to complete the design and development of a workable device. In developing a device for a commercial application,

no part of the analysis can safely be ignored. However, the primary purpose of this work is to assess potential and to identify principles rather than develop a design for an application. Therefore, the scope of the issues and concerns addressed in this work are limited to those that fulfill this purpose. Many concerns inherent in the centrifugal clutches studied cannot be analyzed here. Such concerns include wear, material selection, fatigue life, vibration modes, heat transfer, and manufacturing concerns.

## 1.4 Research Benefits

Compliant mechanism technology has advanced significantly in recent years. These advances have simplified the design of compliant mechanisms, making it more practical for many applications. The primary benefit of this work is further demonstration of this technology's potential. Also, the work demonstrates that the varied techniques developed for specific parts of the compliant mechanism design process can be integrated into an effective, coherent development method.

Centrifugal clutches have received very little treatment in the technical literature. Therefore, there is little publicly available analysis of centrifugal clutch concepts. While this work will not completely fill this void, it will represent a step forward.

Novel centrifugal clutch configurations developed through this work may have practical value. Previous work, such as the development of the compliant ratchet and pawl clutch (see also page 13, Roach, et al, 1998), has shown that compliant mechanisms can dramatically reduce part counts while maintaining functionality. Similar improvements may be achieved in the centrifugal clutches. Further, these designs may be directly applicable to the design of overspeed brakes since a brake is frequently a kinematic

inversion of a clutch. Lessons from this work may also apply to other mechanisms that are actuated by centrifugal or other inertial forces.

Moreover, this work advances the state of the art in compliant mechanism design by demonstrating the value of the pseudo-rigid-body model (PRBM) in synthesizing and designing dynamically loaded mechanisms. Some of these mechanisms have PRBM's with multiple inputs and multiple degrees of freedom. The PRBM approach facilitates design and analysis of these highly nonlinear applications because it decouples the solution of nonlinear deflections of compliant mechanisms from the solution of nonlinear force-deflection equations. The PRBM is also a helpful tool for converting complicated geometries and interactions into simpler, more familiar forms that the designer can understand more intuitively.

This work also illuminates some weaknesses of the PRBM. Specifically, the work shows the need for a usable PRBM of a fixed-fixed flexible segment. This segment type is frequently encountered in fully compliant devices. However, the designer is left to choose an approximate PRBM of the segment by intuition or use a numerical technique to solve the deflections.

## 1.5 Literature Review

### 1.5.1 Centrifugal Devices

Clutches and brakes have been used for centuries. In the last century, general design equations for clutches and brakes have been well developed. Most modern machine design textbooks contain such equations and discuss their development (Norton, 1998; Shigley & Mischke, 1989). A more complete treatment of their design can be found in

Orthwein (1986) and South & Mancuso (1994). Goodling (1977) developed equations for torque transfer of a flexible trailing shoe centrifugal clutch.

Many of these books apply these general clutch/brake equations to centrifugal clutches. Additionally, several authors have presented discussions of centrifugal clutch applications and their benefits such as low cost, automatic operation, overload protection, and motor cost reduction (Goodling, 1974; St. John, 1975, 1979; Town, 1988).

Several researchers have sought to mitigate some of the undesirable performance characteristics of centrifugal clutches. Dekhanov & Makhtinger (1987) devised a way to switch a clutch from nonaggressive to aggressive shoe orientation after load acceleration. This increases operating torque transfer while maintaining a reasonably smooth start. Achi (1986) showed how centrifugal clutches may be used to improve simple industrial operations in developing countries where equipment cost is critical. A centrifugally actuated continuously variable transmission and the development of improvements thereto is discussed by Chase et al. (1991).

Industry has also been working on developing centrifugal clutches as evidenced by patents in the area (Gruden & Brooks, 1999; Schultz, 1996; Shimizu & Ogura, 1987; Weiss, 1984). Several patents reference a compliant, one piece design (Figure 1-7) that is well suited to low-cost gasoline-engine applications (Kellerman & Fischer, 1976; Dietzsch et al., 1977; SuchDev & Campbell, 1989).

Roach et al. (1998) reported a compliant ratchet and pawl one-way clutch with centrifugal throw-out (Figure 1-8). This device shows that compliant mechanisms can be successfully employed in mechanical power transmission devices. It also demonstrates,

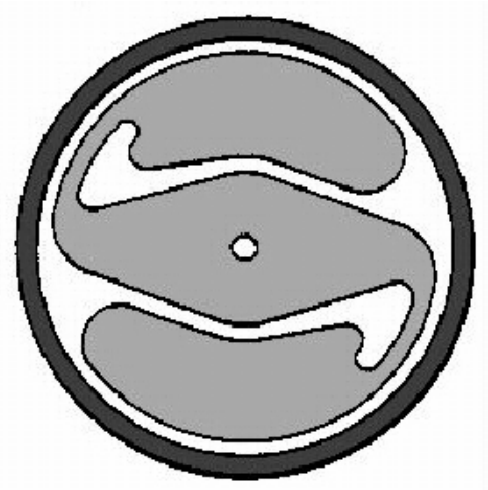

**Figure 1-7** A compliant centrifugal clutch. This clutch is well suited to production by powder metallurgy. It is commonly referred to as an "S-clutch" (Suchdev & Campbell, 1989).

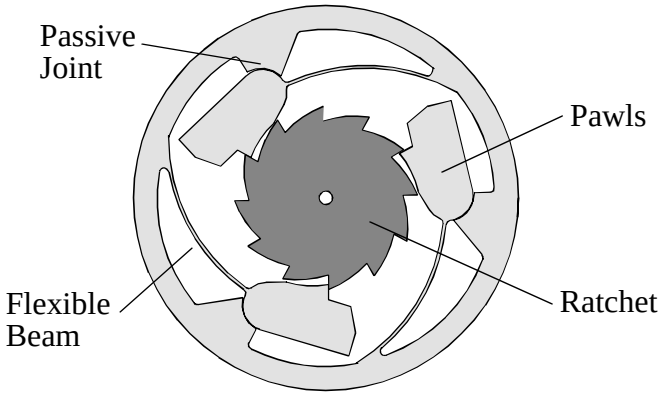


**Figure 1-8** A Compliant ratchet and pawl clutch with centrifugal throw-out (Roach, 1998)

together with the existing compliant centrifugal clutches, the potential to develop additional compliant centrifugal devices.

Centrifugal switches have also been the subject of several patents (Moore, 1980; Kramer et al., 1982). However, no compliant designs are currently found in the patent or technical literature.

### 1.5.2 Mechanism Synthesis and Design

The kinematics fundamental to this research are described in any basic kinematics textbook (Norton, 1999; Erdman & Sandor, 1997; Paul, 1979; Hartenberg & Denavit, 1964;). An efficient method for developing force-deflection relationships is the method of virtual work (Paul, 1979; Norton, 1999).

Recent research in bistable mechanisms support the study of centrifugal switches. Howell & Midha (1995c) observed that the required input force of a toggle mechanism acting on a compliant workpiece reaches a maximum before passing through the toggle point. Opdahl et al. (1998) reviewed and classified the mechanism types that can generate bistable behavior. Jensen (1998) identified the spring locations that generate bistable behavior in four-bar mechanisms.

### 1.5.3 Compliant Mechanisms

Compliant mechanisms are mechanisms that obtain some or all of their motion from the deflection of their members. They frequently require fewer parts than comparable rigid-body designs since revolute joints are often replaced by flexible segments. The potential energy stored in the flexible segments can replace springs and the reduction in revolute joints reduces problems with backlash and wear. In many applications, compliant mechanisms can maintain or even improve performance relative to conventional rigid-body designs. (Sevak & McLarnan, 1974; Her 1986; Salamon, 1989)

These advantages are bought with the price of greater design difficulty. Frequently, these mechanisms undergo large, nonlinear deflections. The mechanical advantage of the mechanism is reduced because some of the input work deflects the

members (Salamon & Midha, 1998). Further, stress analysis and fatigue become much more important in the basic design of the mechanism.

Compliant mechanisms frequently deflect far beyond the linear range. The deflection of these members must be calculated and understood to analyze and design them. Bisshopp and Drucker (1945) laid the foundation for consideration of compliant mechanisms by their application of elliptical integrals to solve problems involving large deflection of cantilever beams. Shoup and McLarnan (1971a) examined the range of mechanisms that can have one or more flexible segments and lower pairs. Efforts were also made to develop qualitative understanding of flexible segment deflections (Shoup & McLarnan, 1971b; Shoup, 1972). Burns (1964) and Burns and Crossley (1968) developed rigid-link approximations for flexible link deflections. Gorski (1976) provides a good review of analytical methods for the calculations of elastic deflection of bars. Boronkay & Mei (1970) made an early effort to analyze a compliant mechanism using finite element analysis. Gandhi & Thompson (1980) developed the equations to apply finite element analysis using a mixed variational principle to flexible link mechanisms. Hill & Midha (1990) developed a graphical Newton-Raphson technique to aid in the solution of compliant mechanism deflections.

Some researchers have built on these numerical analysis techniques in developing compliant mechanism synthesis techniques. They have employed topological synthesis methods based on optimization techniques that remove material or adjust material properties until the optimal force or deflection characteristics are achieved (Anathasuresh et al., 1994; Anathasuresh et al., 1995; Frecker et al., 1996; Frecker et al., 1997). Parkinson et al. (1997) defined compliant mechanisms by a series of splines. The location

of the control points and the section properties at the points were design variables modified to find an optimal mechanism. These techniques can yield unique designs outside the design space considered by the human designer.

A new approach to compliant mechanism design began with the development of the pseudo-rigid-body model (PRBM) through which a compliant mechanism is modeled as a rigid-body mechanism. The PRBM predicts the displacement and force characteristics of the compliant mechanism accurately enough to support preliminary analysis and synthesis of compliant mechanisms. The rules for creating a PRBM of a compliant mechanisms or vice versa were developed to make this approach feasible (Howell & Midha, 1994a, 1994b, 1995a, 1995b, 1996a; Howell et al., 1996). These conversions replace flexible segments with rigid segments connected by lower pairs. Torsional springs are placed at joints to model the effects of the compliance on the force deflection characteristics of the mechanism. A summary of the basic rules for creating a PRBM is included as Appendix A.

Recently, Saxena and Kramer (1998) proposed an approximation for a flexible segment subject to both end forces and moments. This loading condition occurs in fixed-fixed flexible segments. This work yields insight into the relationship between force and moment loading, but does not represent a full PRBM that permits application of rigid-body kinematic techniques to analyze compliant mechanisms with fixed-fixed segments.

The PRBM allows the wealth of knowledge of rigid-body kinematics to be employed in the analysis and synthesis of compliant mechanisms. An example of the application of rigid-body approaches to compliant mechanism design via the PRBM is the

application of Burmester theory for dimensional synthesis of mechanisms (Mettlach & Midha, 1996).

There are two primary synthesis methods associated with the PRBM: rigid-body replacement and synthesis for compliance. In rigid-body replacement, a rigid-body mechanism design is converted through the PRBM into a compliant design. This process usually generates multiple compliant designs equivalent to the original rigid-body design. Further considerations such as stress, fatigue life, and manufacturability may be used to select a specific design. Synthesis with compliance introduces energy equations. The energy equations are solved with the rigid-body loop closure equations to meet the design goals. The designer using this method can solve for variables such as the equivalent spring constants of compliant members. Through synthesis with compliance, mechanisms with specific force-deflection relationships may be synthesized. (Howell et al., 1994; Howell & Midha, 1996b)

The PRBM has been applied to several design problems. It has been used in the design of parallel mechanisms (Derderian et al., 1996), functionally binary pinned-pinned segments (Edwards, 1999), and pantographs (Nielson & Howell, 1998).

The PRBM is the basis for extending rigid body type synthesis techniques to compliant mechanisms. Murphy et al. (1994a, 1994b) proposed a systematic way of identifying all possible compliant mechanism configurations that would be equivalent to an existing rigid-body design. Midha et al. (1994) assisted synthesis efforts by developing a more rigorous and thorough terminology for discussing compliant mechanism configurations. They suggested a definition of links compatible with traditional rigid-body

definitions. Additionally, segments, segment kinds and categories, and their structural and functional types are defined to describe the compliant mechanism design space.

The mechanical advantage of compliant mechanisms does not follow directly from rigid-body-mechanism theory. In rigid-body mechanisms, work is generally assumed to be conserved between the input(s) and the output(s), making mechanical advantage a function of position only. However, Salamon & Midha (1998) showed that these assumptions do not hold for compliant mechanisms. In compliant mechanisms, mechanical advantage is a function of position *and* applied forces. Each of several possible mechanical advantage definitions yields insight into different characteristics of the mechanism.

Roach & Howell (1999) have developed criteria for evaluating the degree of benefit possible from replacing an existing rigid-body mechanism with a compliant version. These techniques help to systematically identify those mechanisms in which compliance would be of greatest benefit. These procedures capture some of the intuition of experienced engineers in assessing proposed designs so that less experienced engineers may more easily design compliant mechanisms. Berglund (1998) has also proposed criteria for evaluating compliance potential, comparing compliant mechanism concepts, and comparing compliant and rigid designs. These criteria with some modifications will be used in this work.

## 1.6 Thesis Outline

The thesis proceeds as described next. Chapter 1 introduces the work and surveys previous work in the area. Chapter 2 reviews centrifugal clutches and summarizes existing

centrifugal clutch types. Chapter 3 discusses the design criteria by which the clutches were evaluated and the methods used to test them. Chapter 4 presents and evaluates the compliant clutch designs studied in this project. Chapter 5 applies the floating opposing arm (FOA) clutch to a string trimmer. It develops and tests the accuracy of necessary design models for these tests. Finally, Chapter 6 reviews the important aspects of the work and recommends future areas of study.

CHAPTER 2

# Centrifugal Device Background

This chapter discusses some important issues in designing centrifugal devices and then reviews in more detail rigid-body centrifugal clutches and their basic operating characteristics. Criteria for evaluating potential for conversion of rigid-body mechanisms to compliant mechanisms are presented. These criteria are applied to the rigid-body centrifugal clutch types.

## 2.1 Centrifugal Device Design

### 2.1.1 Important Issues in Centrifugal Device Design

Centrifugal devices share many design issues due to their common actuation source. It is helpful to recognize these similarities so that lessons learned from one type of mechanism design may be more easily recognized as applicable to other mechanisms.

*Actuation Force is Dependent on Mass*

Generally, in mechanism design, the link lengths of the mechanism are designed separately from the geometry. In most cases, the necessary link lengths and ground locations are calculated given the constraints imposed by the application. Later, the links

can be sized for stresses, appropriate springs may be added, and provisions made for actuating the mechanism.

Compliant mechanisms couple the geometry more closely to the kinematics since significant stresses are caused by mechanism movement alone. However, through the use of the pseudo-rigid-body model (PRBM), the kinematics and stress analysis can be largely decoupled for initial design work. Synthesis can be accomplished by generating a rigid-body design that meets kinematic constraints. Then, the design space of equivalent compliant mechanisms can be explored for designs that meet other constraints such as stress.

Centrifugal devices couple the kinematics and the geometry even more closely than do compliant mechanisms. Every portion of the mechanism not located at the center of rotation is subjected to an applied force. The magnitude of this applied force is dependent on the mass of the link and the distance of its center of mass from the axis of rotation. Thus, the shape of the links controls the magnitude and location of the actuation force. The path and force characteristics of a compliant mechanism can vary significantly with different loading locations. The mass dependent nature of the actuation force can sometimes lead to trade-offs between increasing the segment flexibility and increasing the mass to increase the actuation force.

Figure 2-1 shows a mass connected to fixed supports on both sides by curved flexible segments. The flexible segments can deflect to allow the mass to move upwards. If centrifugal force is used to actuate the mechanism, the designer must choose between flexibility and available input force. The flexibility of the segments increases as they are

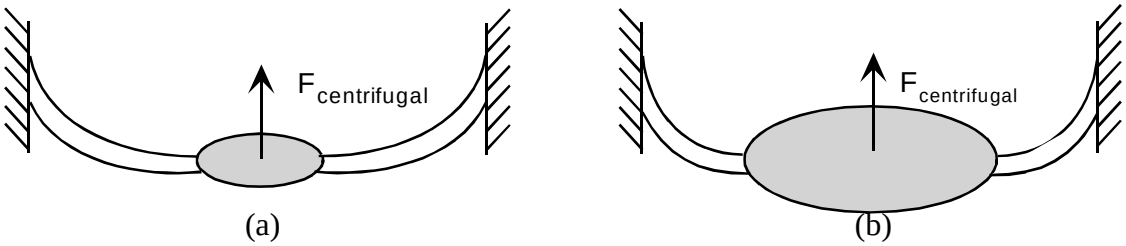


**Figure 2-1** Compliant-centrifugal device trade-offs. (a) The compliant mechanism is more flexible due to the longer segments, but has a smaller actuation force due to the smaller mass. (b) The mechanism has a larger actuation force, but shorter, stiffer members.

lengthened as shown in Figure 2-1(a). To increase the input force, the mass must be increased. However, as illustrated in Figure 2-1(b), it is difficult to increase the input force without making the segments shorter due to the space constraints.

*Mechanism Performance is Speed Dependent*

Unlike most mechanisms, the input to a centrifugal mechanism is speed rather than force or displacement. This means that a centrifugal clutch only transmits its rated power when operated at the rated speed. The necessary speed-deflection relationships are developed by adjusting the stiffness of any springs, mass of the links, and the location of the links' centers of mass.

*Multiple Inputs*

Centrifugal force acts on every body not rotating about its center of mass. No link of the mechanism is entirely without an applied force. Therefore, a multi-link centrifugal mechanism usually has multiple inputs. However, the forces on some links may be small enough to neglect.

*Centrifugal Device Nonlinearities*

Centrifugal devices have multiple sources of nonlinearities beyond the general nonlinearity of kinematic equations. First, the actuation force is proportional to the

rotational velocity squared. Second, the force magnitude may change due to changes in the distance to the center of mass during mechanism operation. Third, the direction of the force is radially outward from the center of rotation through the center of mass of the object in question. Therefore, the direction of input force changes as parts of the mechanism deflect or rotate. For some mechanisms, the deflections are small enough that the magnitude and direction of the forces can be assumed constant. However, care must be taken as these assumptions can introduce significant error in some cases.

### 2.1.2 Advantages

The primary advantage of centrifugal devices is their simplicity. They do not require any external signal or power for actuation or control. They generally use fewer components than competing solutions. This simplicity leads to lower costs and high reliability. Often, centrifugal devices are the lowest cost solution to a problem. This cost difference can be quite significant in some applications. Many years of experience in designing and using centrifugal devices has permitted steady improvements in their performance.

Another advantage is their sensitivity to small changes in speed since the actuation force varies with the speed squared. This sensitivity can be very advantageous in applications such as centrifugal switches and overspeed brakes. A small increase in speed can cause a larger increase in actuation force. This helps an overspeed brake stop a larger than expected load at only slightly higher speeds.

### 2.1.3 Disadvantages

The largest disadvantage of centrifugal devices is their lack of versatility. Centrifugal force is always proportional to the square of the speed. This relationship is set

by the laws of physics and cannot be modified to meet the needs of a specific application. Most centrifugal devices are designed or modified for a specific application with specific operating conditions. They cannot easily be modified to operate under different operating conditions. By comparison, many electric or magnetically actuated devices can be precisely controlled for nearly optimal performance under varying conditions.

The lack of flexibility requires that centrifugal devices be custom designed for many applications. This can increase the cost for applications with unusual requirements. The expense is reduced by designs that use a series of standard parts with built in adjustments. This approach reduces the device cost but sacrifices some performance since the standard parts won't provide optimal performance for every situation.

The nonlinearities of the actuation and the coupling of geometry and kinematics discussed earlier are also challenges. Many designs have been developed as much by testing and intuition as by engineering design.

## 2.2 Types of Centrifugal Clutches

Centrifugal clutches are actuated by the centrifugal force resulting from rotating the clutch. They transfer torque through frictional contact, but there are different methods for transmitting their power and controlling their engagement. Goodling (1974) reviewed seven basic clutch types, their characteristics, capabilities, limitations, and typical horsepower ratings. A brief review of that discussion is provided.

### 2.2.1 Flexible Trailing Shoe

This clutch type has a flexible band lined with friction material that is pulled around by its leading edge (Figure 2-2). The flexible band is weighted appropriately by

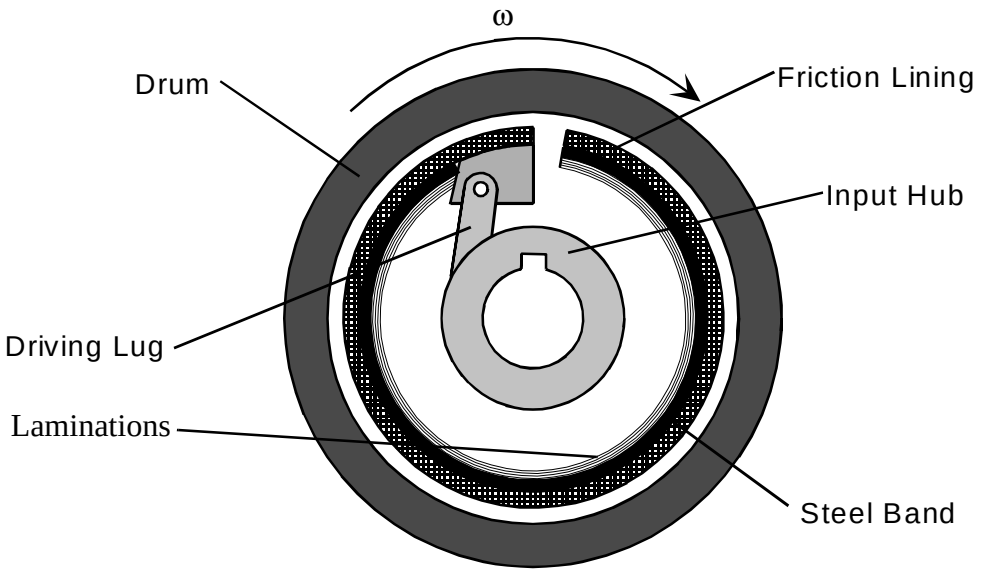


**Figure 2-2** Flexible Trailing Shoe Centrifugal Clutch. The weighted steel band deflects to contact the drum as the clutch accelerates. The clutch torque output is less sensitive to changes in the coefficient of friction than are most types.

laminations so that the band is pushed out into contact with the clutch drum as the clutch accelerates. This clutch type is less sensitive to changes in the coefficient of friction than most types (Goodling, 1977). It is used in applications requiring between ten to two-thousand horsepower. The clutch band mounting can be modified so that it is reversible.

### 2.2.2 Connected Shoes

This clutch is perhaps the most common centrifugal clutch type (Figure 2-3). The friction shoes are held by a rotating link. This link can be equipped with a spring to delay engagement if required for the application. These clutches have different torque transfer characteristics depending on the direction of rotation. When rotating so that the friction force tends to increase the pressure of the shoes on the drum, the torque transfer can be two to three times as high as in the opposite direction (Dekhanov & Makhtinger, 1987). The high torque direction is referred to as the aggressive or self-energizing mode. The

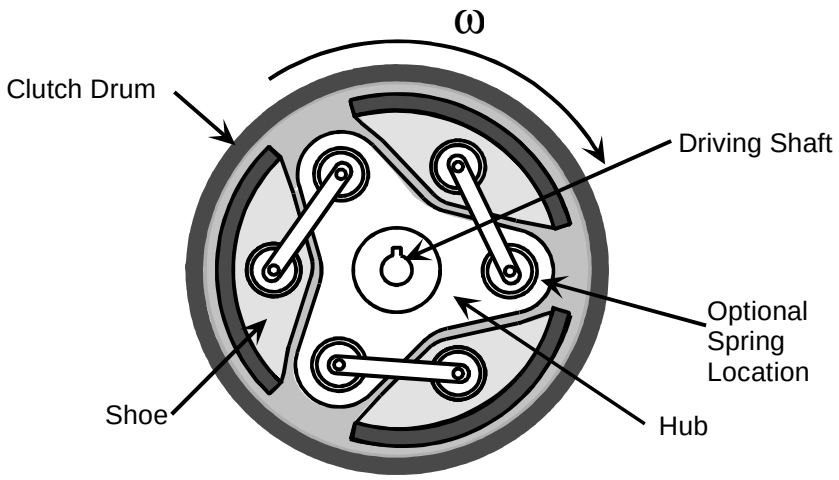


**Figure 2-3** Connected Shoe Centrifugal Clutch. The arrow indicates non-aggressive rotation direction.

lower torque direction is the non-aggressive mode. The aggressive mode sacrifices considerable smoothness of engagement for the increase in torque transfer achieved. Connected shoe clutches commonly transfer one to two-thousand horsepower.

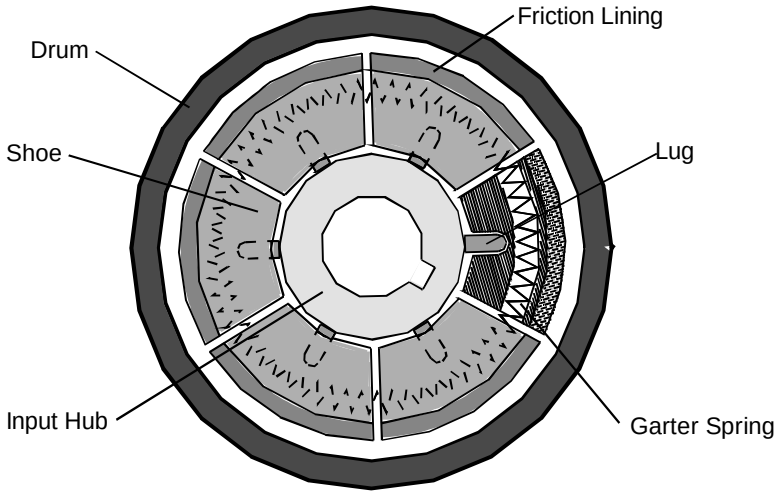


**Figure 2-4** Floating Shoe Centrifugal Clutch.

### 2.2.3 Floating Shoes

Floating shoe clutches (Figure 2-4) contain large wedge-shaped shoes which slide on lugs that project radially outward from the clutch hub. The shoes slide radially outward to contact the clutch drum. A garter spring may be used to increase the speed of engagement. These clutches are very simple and yet they maximize the frictional contact area and centrifugal force for a given volume. These clutches operate the same in both directions. Horsepower ratings from one half to four thousand are common.

### 2.2.4 Oil Clutch

The oil clutch (Figure 2-5) is distinguished from most of the other clutch types. Its distinguishing feature is the inclusion of a capacitance effect that slows down the time response of the clutch's output torque to a change in the input speed. Oil clutch torque output is a function of speed and time. This can significantly increase the starting smoothness of the clutch.

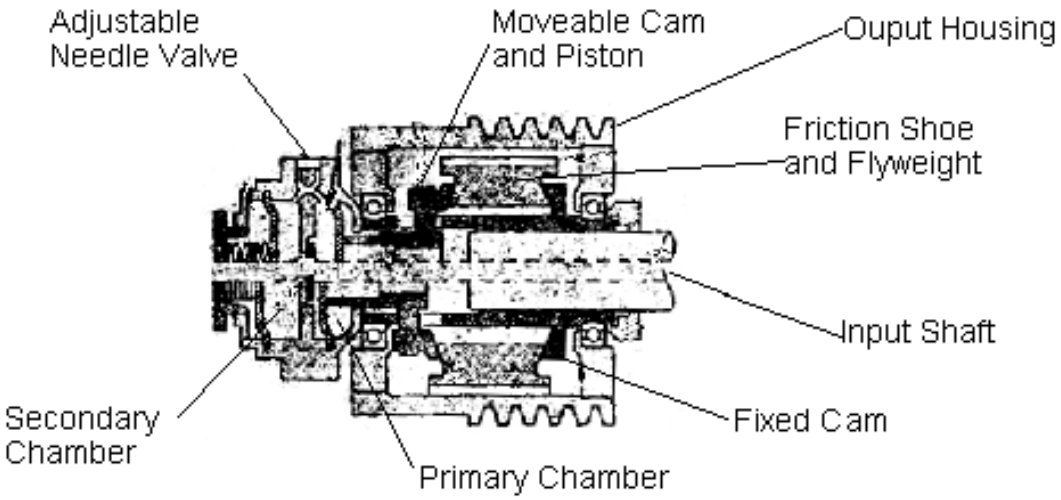


**Figure 2-5** Oil Centrifugal Clutch. (Goodling, 1974)

Oil clutches operate by means of a flyweight that forces oil through a needle valve into a variable volume chamber. The oil flow controls the pressure of the friction shoes against the clutch drum. The volume of the chamber and the orifice size in the needle valve control the torque transferred and the engagement speed respectively. This is probably the most adjustable of the clutch types. They transmit from one to three-hundred and seventy horsepower.

### 2.2.5 Mercury Clutch

Mercury clutches (Figure 2-6) also have the advantage of a capacitance effect that slows the torque response to speed changes. This effect is achieved by the flow of mercury through a small orifice from a reservoir to an expandable shoe. The shoe is restrained by a spring to further retard engagement.

The orifice size and spring stiffness control the engagement characteristics, but their effects can be considered separately. The shoes will respond immediately to speed input much like a floating shoe clutch. However, the mercury will move through the

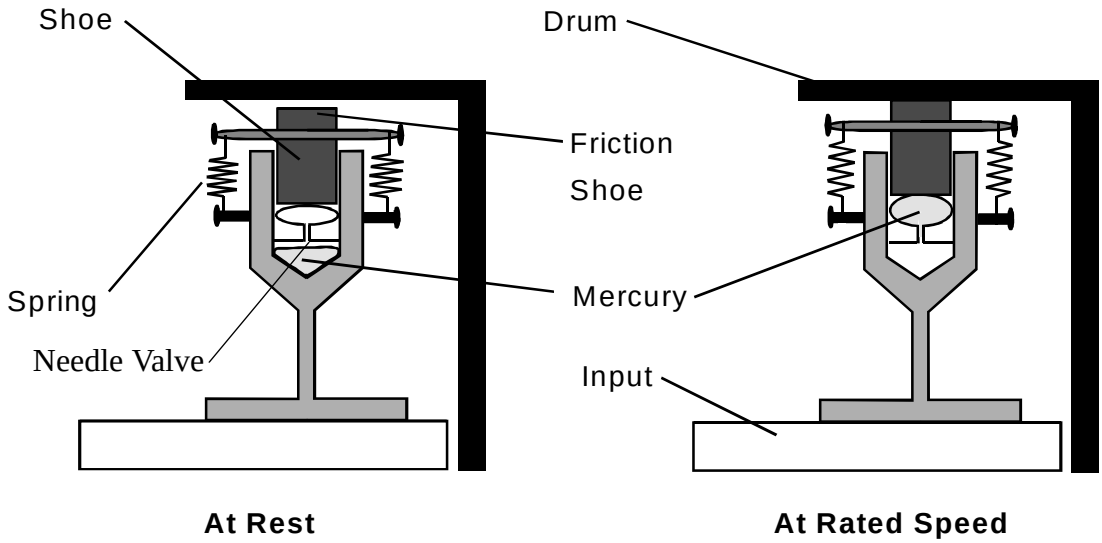


**Figure 2-6** Mercury Centrifugal Clutch. The mercury flows from the reservoir to the expandable shoe to help force the shoe against the drum.

orifice over time and slowly increase the torque transfer. The relative mass of the shoes and mercury determine the relative significance of these two effects. Mercury clutches are capable or transmitting from fractional to seventy-five horsepower.

### 2.2.6 Ball & Cone Clutch

Ball and Cone clutches (Figure 2-7) contain an input member rotating inside of an oil-filled output housing. The torque is transferred as steel balls are forced outward by the centrifugal force and in turn push tapered rings against an angled contact surface. The oil surrounds the mechanism and reduces the heating and wear at the friction surfaces. These clutches transmit two- to nine-thousand horsepower at operating speeds.

### 2.2.7 Dry Fluid

Dry fluid clutches (Figure 2-8) have a rotor on the output member that spins in a housing connected to the input member. The void between the rotor and the housing is partially filled with small steel shot (0.011” to 0.017” in diameter); the amount of shot

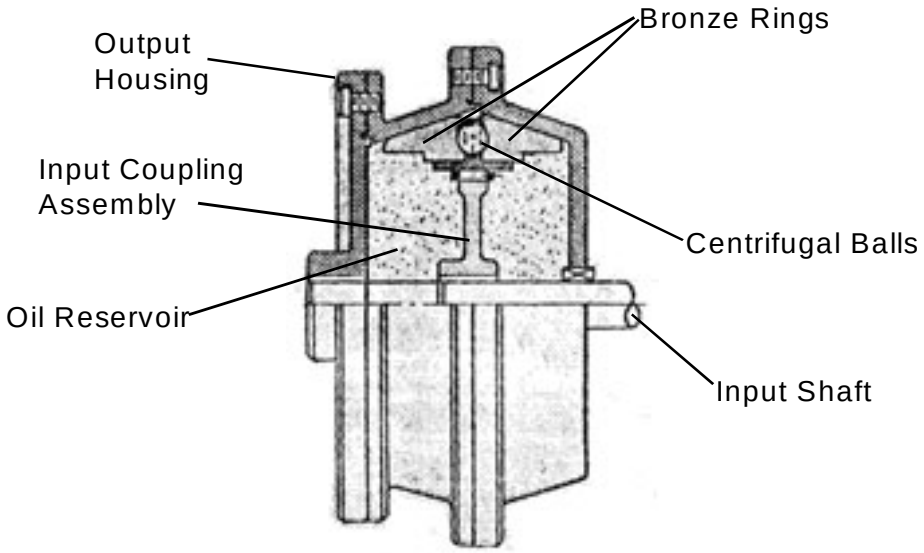


**Figure 2-7** Ball & Cone Centrifugal Clutch. The Centrifugal balls cam the bronze rings outward to transmit torque through friction with the output housing. (Goodling, 1974)

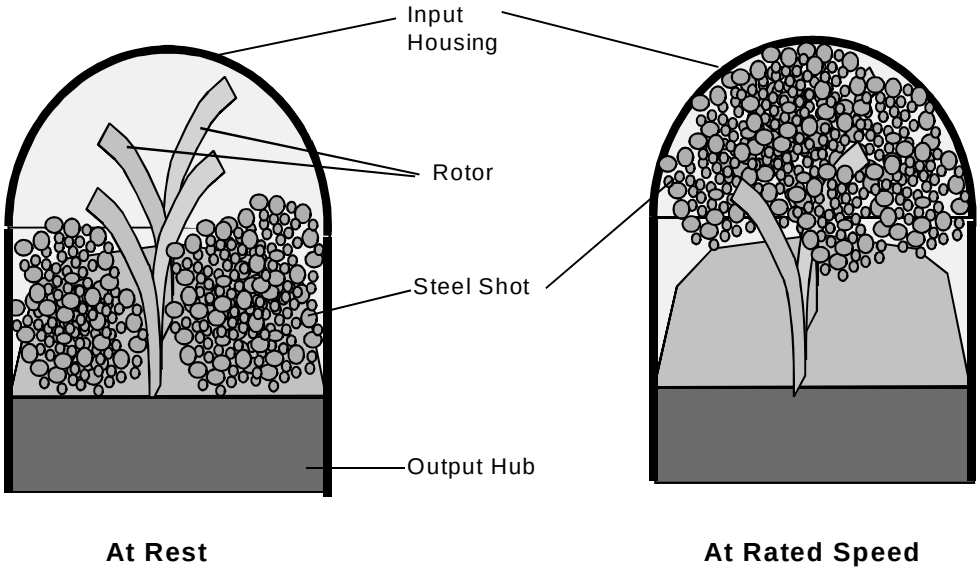


**Figure 2-8** Dry Fluid Centrifugal Clutch. At rated speed, the steel shot packs between the rotor and the output housing to transmit torque.

determines the torque transferred. The centrifugal force packs the shot into the area between the rotor and the housing to transmit torque. The shot forms a static mass with no slipping once the load is accelerated. An advantage of this concept is that the primary wear

point of the clutch is the shot which is easily replaced. Dry fluid clutches commonly transmit between one quarter and four-hundred horsepower.

## 2.3 Two Evaluation Types

The establishment and use of clear evaluation criteria is an effective way to compare different options. The use of such criteria help assure that important issues are systematically considered and provide a natural process for documenting design decisions. When used well, they can also help identify specific weaknesses and/or strengths of concepts. Once recognized, the strengths of different approaches may be combined or weaknesses mitigated.

Roach et al. (1999) and Berglund (1998) proposed similar sets of criteria for evaluating the compliance potential of rigid-body mechanism designs. Berglund also developed a set of criteria for comparing different compliant designs and assessing their value relative to an existing rigid-body design. The criteria translate the common advantages and disadvantages of compliant mechanisms into a series of gauges for measuring a concept's potential.

This work will include two types of evaluations. They are as follows:

- *Compliance Potential* - Assess the potential for improving the performance of an existing rigid-body mechanism by using a compliant mechanism
- *Compliant Concept Comparison* - Compare different compliant concepts for the same mechanism type to identify the most promising alternative.

The rigid-body designs will be reviewed using a compliance potential evaluation. Later, a compliant concept comparison will be conducted to select the best design(s) for further consideration.

## 2.4 Compliance Potential Evaluation

Berglund applied his compliance potential criteria to the seven centrifugal clutch types described above. His evaluation was used for selecting the clutch types with the highest potential benefit from the application of compliant mechanism theory.

He divided the clutch evaluation into two phases. The feasibility phase, composed of the first five criteria, indicates whether a compliant version of a rigid-body mechanism is possible. If selection criteria one and five or three, four, and five are negative then a compliant mechanism is not possible. The screening phase, selection criteria six through eleven, assesses the potential benefits of applying compliant mechanism technology to rigid-body designs. In each phase, a mechanism is given a “+1” for a “yes” answer, and a “-1” for a “no” answer. The scores of each mechanism are tallied. The mechanisms with the highest scores have the greatest compliance potential.

### 2.4.1 Evaluation Results

The results of Berglund’s clutch type evaluation are shown in Table 2-1. The evaluation indicates that the connected shoe and the floating shoe clutches have the greatest compliance potential. The flexible shoe clutch shows significant potential as well. Compliant concepts based on these three clutch types were developed.

### 2.4.2 Discussion of Most Promising Clutch Types

The floating and connected shoe clutches scored highest. However, the floating clutch does not have any components that rotate relative to one another. They move on linear paths extending radially from the axis of rotation. On a positive note, the clutch uses springs that can be replaced by compliance to reduce the design complexity and part count.

The connected shoe clutch appears to be the most promising design. It has kinematic pairs which do not go through a complete revolution and they are often produced with springs. They are also used in lower power rating applications where the potential cost reduction of compliant mechanisms could be a significant advantage.

The flexible shoe clutch also shows promise. Of particular interest is the low sensitivity to coefficient of friction of its torque output. Goodling (1977) reported that a 31% difference in coefficient of friction might result in a torque output change of 6%.

**TABLE 2-1 Compliance Criteria Evaluation of Centrifugal Clutch Types (Berglund, 1998)**

| Selection Criteria | Flexible Shoe | Connected Shoe | Floating Shoe | Mercury | Oil | Ball and Cone | Dry Fluid |
|---|---|---|---|---|---|---|---|
| 1. Do revolute joints exist? | Yes | Yes | Yes | Yes | Yes | Yes | Yes |
| 2. Is the relative motion in each joint necessary? | Yes | Yes | Yes | Yes | Yes | Yes | Yes |
| 3. Does a revolue joint exist with >360 motion? | Yes | Yes | Yes | No | No | No | No |
| 4. Can some motion > 360 be reduced? | No | No | No | No | No | No | No |
| 5. Do springs exist in design? | No | Yes | Yes | Yes | Yes | No | No |
| 6. Will part count be reduced by compliance? | Yes | Yes | Yes | No | No | No | No |
| 7. Will the weight be reduced by compliance? | Yes | Yes | Yes | No | No | Yes | No |
| 8. Do no links cross? | Yes | Yes | Yes | Yes | Yes | Yes | Yes |
| 9. Are any links free from compressive stress? | Yes | Yes | Yes | Yes | Yes | Yes | Yes |
| 10. Are links subject to torque normal to axis of rotation? | Yes | Yes | Yes | Yes | Yes | Yes | Yes |
| 11. Are any links free from prolonged stress or high temperature? | No | No | No | No | No | No | No |
| TOTAL | 5 | 7 | 7 | 1 | 1 | 1 | -1 |

Torque output from a connected shoe or floating shoe clutch would change 31% under the same conditions. In reality, it is already a compliant design since its performance is dependent on the deflection of the flexible shoes. Its performance might be increased or its cost decreased by further application of compliant mechanism theory.

The oil and mercury clutches did not score well on their compliance potential. However, they have a significant advantage over the other clutch types. In both types, fluid flow through an orifice controls the torque application. This flow takes a finite amount of time that slows the clutch engagement and increases the starting smoothness. Any compliant clutches that could achieve a similar effect would have a significant performance advantage over other centrifugal clutch types.

CHAPTER 3

# Centrifugal Clutch Evaluation Procedures and Criteria

One purpose of this work was to systematically apply the techniques of compliant mechanism design to centrifugal clutches, and assess the relative merits of different concepts. This chapter describes the systematic procedures used for developing, and evaluating the different clutches. First, the overall process is outlined. Second, the evaluation criteria and the procedure used for their application are presented. Finally, this chapter documents the apparatus and methods used for physical testing of the concepts. This discussion of methods lays the foundation for all of the work found in the later chapters.

## 3.1 Clutch Evaluation Procedure

**Develop a PRBM of the concept.** The clutches were modeled using the PRBM. The PRBM generally predicts accurately the performance characteristics of the clutches. However, even when the model is not accurate quantitatively, it does help the designer better understand the behavior of the clutch and how it might be improved. The PRBM's of the clutches are included in Chapter 4.

**Prototype the clutch concept.** All of the clutch concepts were prototyped from sheets of polypropylene 1/4” thick using a numerically controlled (NC) mill. The clutches were made to a standard outer diameter of 4.40 inches and designed to fit a standard test mount and drum. In most cases, multiple prototypes were made of the clutch concepts. Although it is unlikely that the optimal design of a particular clutch was obtained, these different designs permitted quick exploration of the concept design space and an indication of the concepts’ potential performance.

**Measure the Clutch’s Torque vs. Speed Relationship.** This is the single most important factor in evaluating the clutch concepts. Multiple measurements of the torque-speed measurements were made of each working prototype. The results of these tests are documented in Chapter 4. The test methods employed are discussed in “Clutch Testing” on page 49.

**Measure the Concept against the Evaluation Criteria.** After modeling and testing the clutches, the clutches were measured against the established design criteria. The combined experience of modeling, prototyping, and testing the clutches provide an adequate experience base for evaluating the potential of each concept.

## 3.2 Evaluation Criteria

### 3.2.1 Berglund Criteria

Berglund (1998) proposed criteria for evaluating the relative value of different compliant mechanism designs. Berglund suggested measuring compliant mechanism designs using these criteria by assigning numbers from 0 to 4 corresponding with a qualitative assessment of the criteria. The scores for the different criteria are then

weighted and summed. The mechanisms with the highest scores have the greatest promise.

Berglund suggested fifteen criteria for comparing specific compliant designs. Since this work focuses on evaluating broad concepts, definite answers are not available for many of the criteria that Berglund proposed. His criteria are better suited to evaluating specific designs for specific applications. Therefore, Berglund's criteria are not used directly in evaluating the compliant centrifugal clutch concepts. Instead, the criteria he suggested are combined with several other criteria specific to centrifugal clutches.

### 3.2.2 Criteria Adapted from Berglund for Use in this Work

The following criteria are adapted from Berglund's work for evaluating the compliant centrifugal clutch concepts.

*Suitability of Loading*

The loading on compliant mechanisms is important for two reasons. First, the deflection path of the mechanism depends on the loading applied. Second, the life of the mechanism depends on the applied stresses. The flexible compliant segments are much more susceptible to fatigue failures than are rigid links. Experience has shown that compliant mechanisms can be designed with adequate fatigue life, but careful consideration of loading is necessary.

Berglund identified four guidelines for evaluating the suitability of loading for flexible segments. For this work, they are evaluated individually so that no factor is overlooked and then combined into one overall factor. The guidelines are:

- Minimal compression in the long, thin flexible segments.

  Long, thin flexible segments are prone to buckling under compressive loads. Buckling should generally be avoided since it is a somewhat unpredictable phenomena, is not accounted for in the PRBM, and may fracture or plastically deform the flexible member.

- Small deflection required in flexible segments.

  Smaller deflections mean the stresses are lower in the flexible segments and the PRBM is most accurate.

- Minimal Tension in the flexible members.

  Most mechanisms must go through a particular path and whatever force necessary to achieve the necessary rotation or displacement is applied. Tensile forces oppose the deflection of flexible members. When they are present larger input forces and thus larger stresses are required.

- Passive joints used instead of rigid-body links in links that require compressive loads.

  Passive joints are cams that act like pin joints but can only receive compressive forces. Passive joints can support large loads through rigid segments without the extra parts and complexity of a pin joint. They should be considered for use in any joints with continual compressive loading.

*Ease of manufacture*

One of the primary advantages of compliant mechanisms is reduced production cost. The relative reduction in manufacturing costs of different compliant mechanisms is an important consideration. However, manufacturing costs are difficult to estimate without making some simplifications. Since the clutch concepts are planar, all of them could be manufactured by a cutting process, and in fact, many compliant clutches are currently produced from flat stock by cutting operations such as laser cutting. If a cutting process is used, the relative costs of different clutches should be proportional to the length of the perimeter of the clutch's profile. The smaller the profile perimeter, the quicker and less expensive the clutch can be manufactured.

Therefore, the total perimeter length of the clutches is used as an index of relative manufacturability. The perimeter was measured from the CAD package used to model the prototypes for manufacturing.

*Retention of resilience in compliant members*

In many clutch applications, the clutch must not transmit torque when the input speed is below a certain level. To prevent torque transfer at slower speeds, the clutch must have springs to resist the centrifugal force without transmitting torque. If the stiffness of the springs changes significantly with time or with normal fluctuations of the operating environment, the clutch will not perform reliably.

The ability of the springs to retain their resilience is dependent on a variety of factors. These factors include the operating temperature, the chemical environment, the stress level in the segments, and how long stress is applied. Many of these factors such as the operating environment are primarily determined by the application rather the mechanism's design. Moreover, the significance of all of these effects is profoundly dependent on the material used. Since the material selection and particular application environments are outside the scope of this work, the influence of these factors on the resilience of the compliant members will not be considered in the evaluation.

This factor will be assessed qualitatively by considering the relative stress level of the flexible segments and the sensitivity of the clutch performance to changes in the resilience of the compliant members.

### 3.2.3 Additional Criteria for Centrifugal Clutches

The most important factors in clutch performance are torque transmission capacity, engagement speed, and smoothness of start. Once these concerns are addressed,

the performance after wear, the wear life, and clutch heating during start-up are the other major concerns to be considered. In specific applications, reversible operation, torque limiting performance under overspeed conditions, or torque output sensitivity to the coefficient of friction may also be important. Since the overall concepts are being evaluated and not the suitability of the concepts for a specific application, these criteria will be simplified in the work.

*Torque Capacity*

In small power, low cost applications, the torque capacity is the single most important factor. Torque capacity is determined by four parameters: the mass of the arms, the mechanical advantage of the resulting centrifugal force, the stiffness of any springs, and the driving speed. Since the position of most clutch types is constant after contact, the mechanical advantage is constant. Therefore, the four factors can be reduced to three by combining the mass and mechanical advantage factors to create a single torque factor. In many clutch designs, an analytical determination of these parameters is unwieldy, but they can be determined quite readily from experimental data. If the actuation mass is maximized while maintaining a uniform size constraint, the torque factor can be used as an index of the absolute torque capacity of the clutch type. Since all of the clutches fit within the same space, a clutch with a higher torque capacity rating can be made more compactly than clutches with lower torque ratings for a given set of application requirements.

Multiple definitions of the three parameters are possible. For this work, the equation reported by St. John (1979) will be used. It is

$$T = T_b(U_o^2 - U_r^2) \quad \textbf{(3.1)}$$

where,

$T_b$ = basic clutch torque, torque output at 1000 rpm without any springs
$T$ = operating torque of the clutch at speed $U_o$
$U_o$ = the operating rpm/1000
$U_r$ = the engagement rpm/1000

Equation (3.1) is valid for speeds greater than $U_r$. Below $U_r$, the equation predicts negative torque transfer which is not possible. The parameters in Equation (3.1) were determined from the experimental data. The equation was solved for $T_b$ to get

$$T_b = \frac{T}{(U_o^2 - U_r^2)} \quad \textbf{(3.2)}$$

This equation was applied to each data point using the measured speed and torque for $U_o$ and $T$ respectively. The value of $U_r$ was selected as that value which minimized the standard deviation of the $T_b$ values calculated from the different data points. The $U_r$ values generally match the observed engagement speed.

The $T_b$ parameter is a helpful concept because it facilitates comparison between clutches with different engagement and operating speeds. In order to meaningfully compare torque outputs, the engagement and test speed of every clutch would have to be identical. The use of a common size envelope for all of the designs, further normalizes the $T_b$ values with respect to clutch size to provide a more equal measure of relative torque capacity.

For most of the clutches, applying Equation (3.1) with the parameter values determined as explained above fit the experimental data quite well. However, this equation is of the form

$$T = a\omega^2 + c \tag{3.3}$$

It neglects any effects that vary linearly with rotational velocity. Some clutches have significant linear terms that cannot be ignored. This equation is not a good fit for these clutch types. The two clutch types affected are the split arm clutches with less-stiff segments and the grounded opposing arm clutches. Figure 3-1 compares the adequacy of the model predictions for a typical clutch and one with a significant linear term.

The linear terms in both of these clutches are likely due to members that continue deflecting with increasing speed and torque even after contact. In the split arm clutch, these deflecting members are non-contacting flexible segments. In the grounded opposing arm clutches, the flexible members connected to the inner hub continue deflecting. The significance of the linear terms will depend on the stiffness of the flexible segments.

*Starting Smoothness*

In some applications starting smoothness is not critical, but generally clutches with smoother starting capability are preferred. The starting smoothness is a function of load inertia, the speed-torque relationship of the driver, and the speed-torque capability of the clutch. The clutch's effect on starting smoothness can be seen by fixing the other two variables. All remaining differences in load acceleration are due to the clutch.

Virtually all centrifugal clutches have a quadratic relationship between output torque and input speed. The only exceptions are those clutches that are dependent on fluid

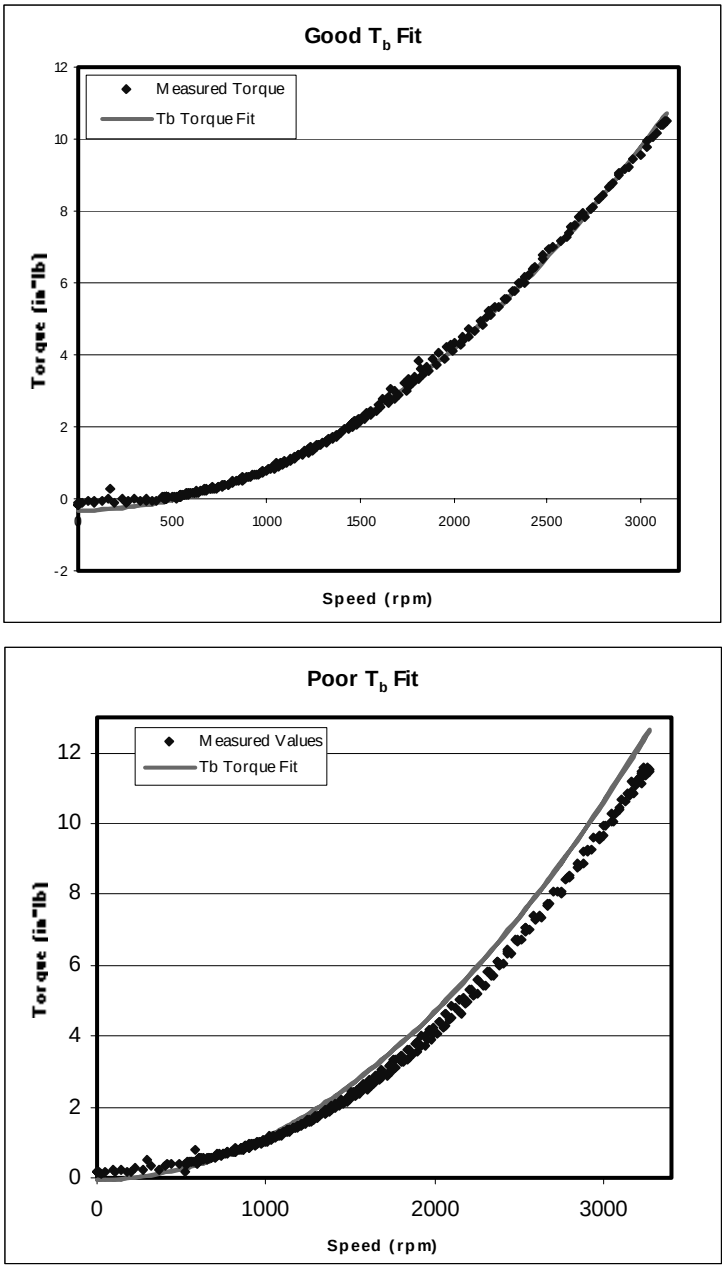


**Figure 3-1** These graphs compare the adequacy of the $T_b$ model in describing the torque performance of the tested clutches. The $T_b$ model has a maximum error of nine percent for the poor fit graph.

flow for torque application. Damping in the fluid flow makes the torque output a function of time as well as input speed. This allows improved starting smoothness as compared to clutches with quadratic torque speed relationships as shown in Figure 1-2 on page 5.

All quadratic relationship clutches that fit Equation (3.1) will have the exact same starting smoothness if designed for the same application. However, clutches that are not adequately approximated by Equation (3.1) will vary from the norm. The basic application requirements specify the operating torque at the required operating speed and the engagement speed where torque is zero. Additionally, the equation for the clutch torque model has its minimum when the speed is zero. These three pieces of information, operating speed and torque, engagement speed, and a zero linear term, completely define the speed-torque relationship.

The load acceleration is a function of the load inertia and the torque-speed relationships of the driver and the clutch. For a given load and driver, the load acceleration is directly related to the torque-speed characteristics of the clutch. Therefore, all clutches with the same torque-speed relationship will have the same starting smoothness for a given application.

However, if a linear term is added to the model, the application requirements do not completely define the clutch torque characteristics. This may allow the clutch to be tuned for improved starting smoothness within the given application constraints, but the amount of variation possible is limited because the starting smoothness and the engagement speed are primarily determined by one design variable: the stiffness of the flexible members. Since the variables are coupled, the potential variation in the starting smoothness of the clutches with linear terms is limited.

Since all of the concepts have relatively small linear torque terms and the linear terms are not independent of engagement speed, there is no appreciable variation in

starting smoothness between the tested clutch concepts. Therefore, this parameter is not used in the concept evaluation

*Wear Performance*

Most well-designed clutches will fail or require service due to excessive wear. Several factors indicate clutch performance under wear conditions. First is contact area. Increasing the contact area with the drum improves the clutch wear characteristics. Second is the sensitivity of clutch torque output to wear. Three reasons a clutch might be sensitive to wear are:

- compliant segments are wear points
- torque is sensitive to the amount of rotation for engagement
- torque is sensitive to the exact contact location

The effects of wear include significant changes in transmitted torque, engagement speed, or operating stresses in the flexible segments.

*Other Performance Advantages*

Many other clutch features are useful in specific applications or groups of applications. Some of these attributes are bi-directional operation, decreased torque sensitivity to the coefficient of friction, and reduced torque output above the operating speed. These advantages are valuable in some applications and are of little importance in others.

To consider these characteristics in this general evaluation, they will be grouped together into one category. The default clutch evaluation with respect to this criteria will be zero. The clutch's score can then be raised by one point for each extra feature incorporated into the design.

### 3.2.4 Clutch Rating Methods

Except as noted under “Other Performance Advantages” the clutch will be rated from 0 to 4 with respect to each criteria. The meaning of the ratings is given in Table 3-1. These ratings are multiplied by a weighting factor between one and five that reflects the importance of the particular criteria. Larger values of the weighting factor indicate more vital criteria. All of these values will be summed for a particular clutch to reach an overall clutch score. Higher scores indicate greater concept potential.

The weights were selected to reflect the relative importance of the criteria for the types of applications that compliant centrifugal clutches would be best suited. These applications would probably be low cost consumer items that aren’t expected to have an extended life. Therefore, the manufacturability was weighted highest with a five. The torque capacity was rated a four since it directly affects the size, weight, and material costs of a clutch. Wear was a three since every clutch must withstand a minimum wear time. Retaining resilience was weighted as a two since loss of resilience might degrade performance but would not cause failure. Similarly Loading was ranked a two since the expected applications do not require indefinite life, and most of the concepts can be

**TABLE 3-1 Definition of Clutch Ratings**

| Rating Definition | Rating |
|---|---|
| **Unacceptable** | 0 |
| **Below Average** | 1 |
| **Average** | 2 |
| **Better than Average** | 3 |
| **Superior Performance** | 4 |

modified to improve the loading if necessary. Other Performance Parameters is weighted as a one since few low cost applications need any of the extra parameters.

## 3.3 Clutch Testing

### 3.3.1 Test Setup

The most fundamental performance metric of the centrifugal clutches is torque transfer at a given speed. The torque was measured by connecting a cylindrical drum to a fixed torque gauge while a clutch rotated inside of the drum. A driving source was selected with much higher power output than the clutch. This makes the torque measurement simple, but introduces an additional problem. Throughout a test, the clutch is dissipating its maximum power capacity through friction at the clutch-drum interface. Plastic at the contact point quickly melts when polypropylene clutches are tested without a friction material on the contact surfaces. This results in viscous rather than coulomb energy dissipation at the contact surfaces.

This problem was resolved by adhering cotton webbing to the contact areas on each polypropylene clutch as shown in Figure 3-2. The webbing provided a consistent friction surface and insulated the plastic clutch from the heat generated during testing. Further, the clutch rubs against a large steel drum that provides an excellent heat sink. Together, the webbing and drum reduced heating in the clutch enough that temperature dependence of the plastic material properties could be disregarded. Temperatures in the clutch did not change noticeably even after several minutes of continuous operation.

The coefficient of friction between the cotton webbing and the steel drum was measured as shown in Figure 3-3. An adjustable inclined plane was made from steel with

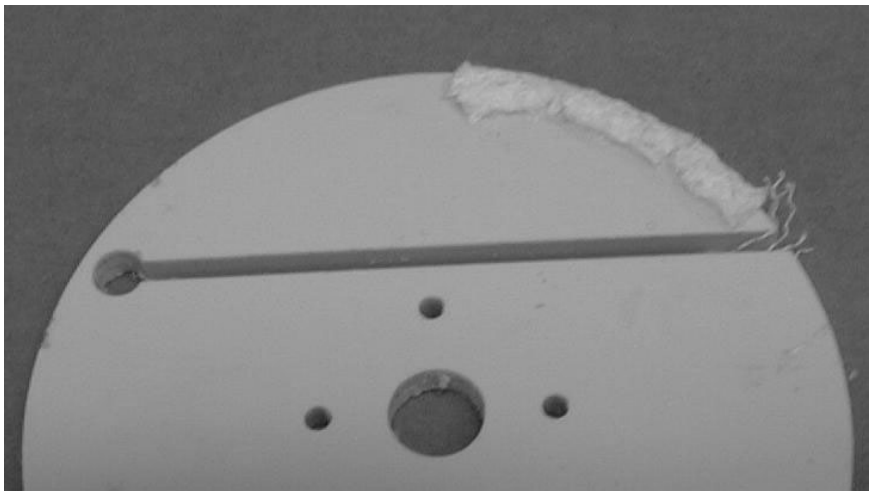

**Figure 3-2** A compliant centrifugal clutch with cotton webbing glued on the contact surface.

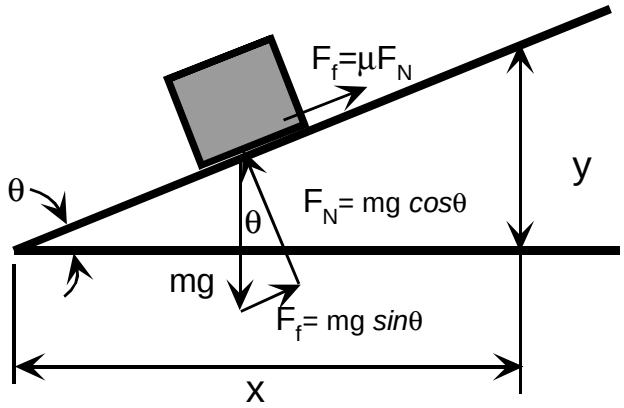


**Figure 3-3** Measuring the coefficient of friction.

a similar surface finish as the clutch drum. The weight lined with cotton webbing was placed on the inclined plane. The angle of the inclined plane was adjusted until the weight would slide down the incline plane at a steady rate (no acceleration). This permitted measurement of the sliding coefficient of friction rather than the static coefficient of friction. To achieve steady sliding, the weight was bumped to overcome the static friction and initiate sliding.

The coefficient of friction (μ) is then found by summing the forces and applying the relationship

$$F_f = \mu F_N \tag{3.4}$$

Summing the forces on the sliding block and solving for the normal and frictional forces gives

$$F_N = mg\cos\theta \tag{3.5}$$

$$F_f = mg\sin\theta \tag{3.6}$$

Equation (3.5) and (3.6) are substituted into Equation (3.4) and solved for μ to find

$$\mu = \frac{\sin\theta}{\cos\theta} = \tan\theta \tag{3.7}$$

which can also be expressed as

$$\mu = \frac{y}{x} \tag{3.8}$$

The clutches were tested on a lathe with continuous speed variation as shown in Figure 3-4. The clutches were rotated inside the fixed steel drum while the torque transfer and driving speed were measured using computer data acquisition. The drum is mounted on the driving shaft with bearings and restrained from rotation by the torque gauge.

APPENDIX B “Experiment Data” contains further data about the test setup and instrumentation.

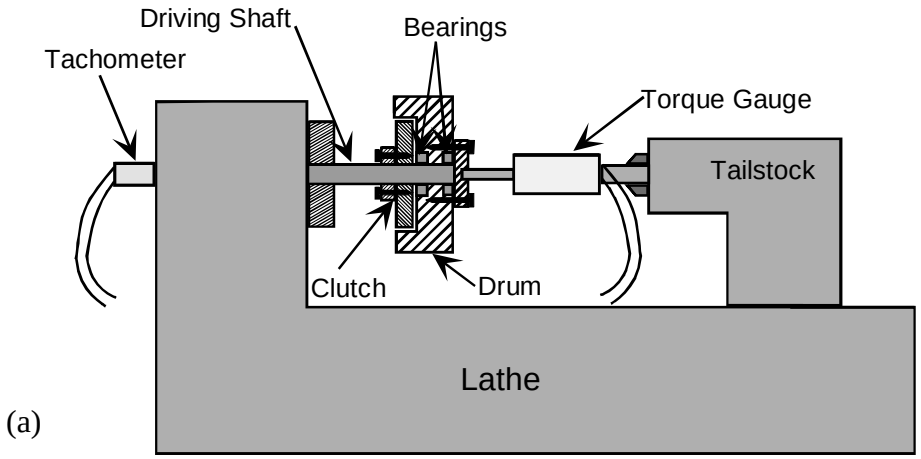


(a)

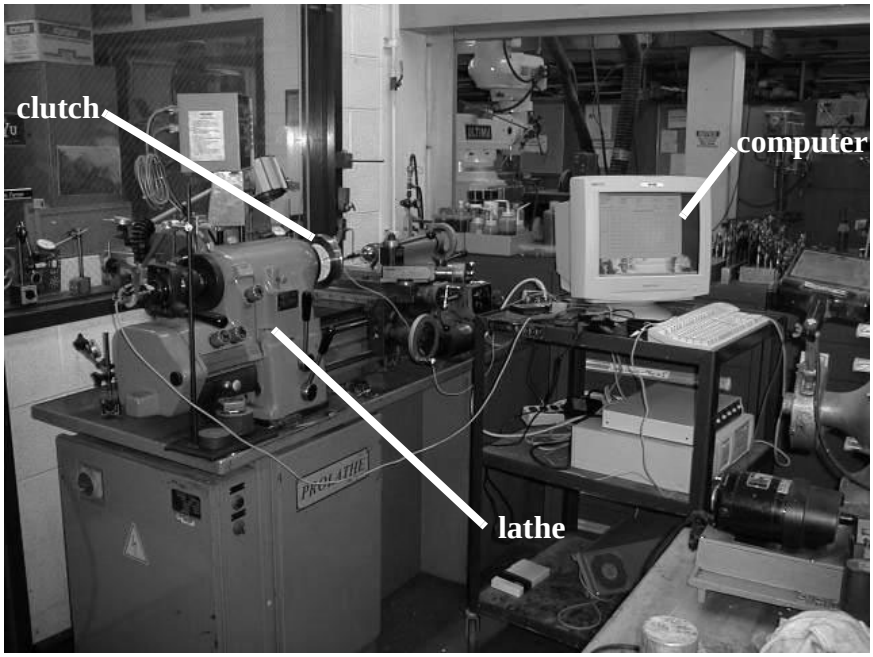


(b)

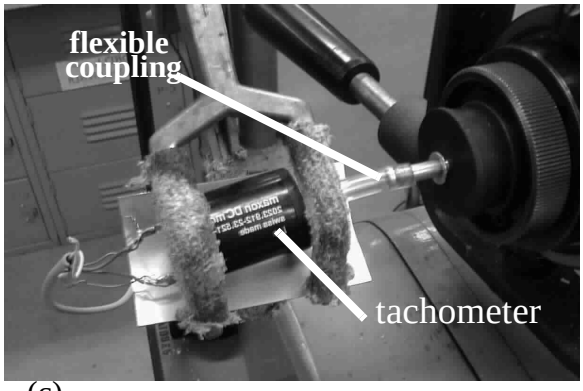


(c)

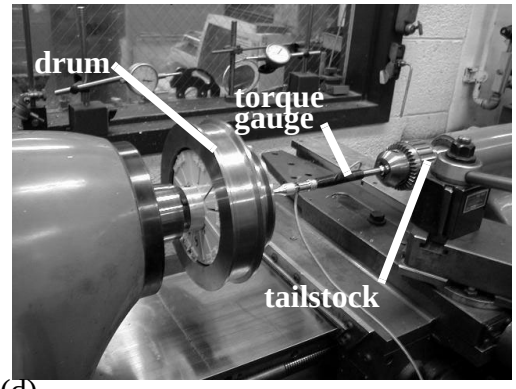


(d)

**Figure 3-4** (a,b) Clutch test setup. (a,c) The tachometer measures the clutch speed. (a,d) The clutch spins inside the stationary clutch drum. (a,d) The output torque is measured be the reaction torque gauge mounted between the tailstock and the clutch drum. The clutch drum is mounted on the driving shaft with bearings.

### 3.3.2 Test Procedures

The torque gauge measures the torque output from the clutch plus the torque due to friction in the bearings. To account for this error, the torque on the drum due to the bearing friction was measured. A linear fit to the bearing torque data was then subtracted from the measured torque values to find the clutch torque output. “Bearing Torques” on page 135 in APPENDIX B contains more information. Each clutch was cycled through the speed range of the lathe two to three times. The data sets from the different cycles were compared to verify that the results were consistent. Each data point is the average of ten readings. No additional filtering was performed on the torque sensor output. The tachometer signal was filtered by a capacitor connected in parallel with the output voltage. Reference “Tachometer” on page 134 for more information. The data was sampled at ten hertz and the data points were recorded in a file for review after the test. Figure 3-5 shows a sample data set from a clutch test. APPENDIX B “Experiment Data” contains representative data sets for each clutch prototype.

### 3.3.3 Error Sources

Every test setup has error sources and it is important to understand what these sources are and how they impact the accuracy of the measured data. The errors in the measurements are discussed and their relative magnitudes are mentioned.

*Coefficient of Friction*

The coefficient of friction directly affects the torque capacity of all of the clutches. However, the coefficient of friction is subject to many variables even under controlled conditions. Dirt or grease contamination on either of the contacting surfaces would have a

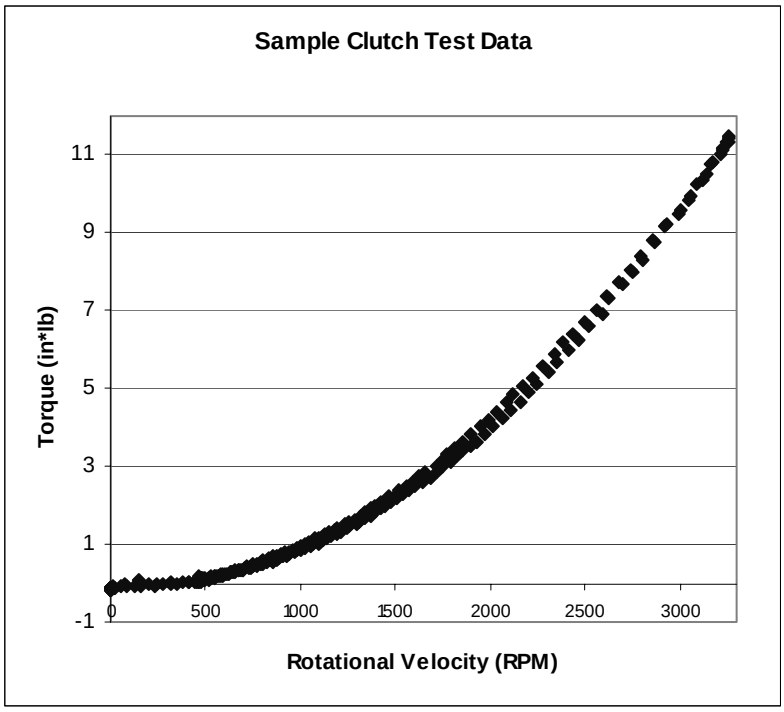


**Figure 3-5** Test data from a representative clutch torque test.

noticeable impact on the torque capacity. The torque error due to the accuracy of the measured coefficient of friction could be ten to fifteen percent.

*Cotton Webbing Thickness*

The cotton webbing has an irregular surface due to the coarse weave, and easily compresses several thousandths of an inch. This makes it very difficult to define the effective outer radius of the clutch. The webbing is also attached with a layer of glue that may vary in thickness. Considering that the total deflection of most of the clutches is only 0.050 inches, a variation of only several thousandths of an inch may cause noticeable error in the engagement speed

*Modulus of Elasticity*

The modulus of elasticity of the flexible segments directly affects their effective spring constant. The effective modulus of elasticity is subject to variation due to

production, light exposure, stress cycling, and exposure to some chemicals. The stress relaxation of the polypropylene is very significant. Cragun, et al. (1998) measured the modulus of elasticity of polypropylene when stressed to half of the yield stress. They measured an initial values of 165 ksi dropping off to a value of about 120 ksi after several minutes. This degree of stress relaxation makes predicting the engagement speed in polypropylene very difficult. This is a significant error source in the engagement speed.

*Density*

The density of polymers can vary between manufacturers and between batches. Density influences both torque capacity and engagement speed. However, this variation and the error it introduces are probably small.

*Machining Tolerances*

Most numerically controlled machines are accurate to within several thousandths of an inch. That error would not have a noticeable impact on the torque capacity, but it would affect the engagement speed significantly. Many flexible segments are only 0.050 to 0.075 inches thick. An error of 0.002 inches on both sides of the segment could decrease the spring constant by fifteen to twenty-two percent. The spring constant is very sensitive to the segment thickness because it is proportional to the thickness cubed.

*Electrical Noise*

The signal from the torque transducer was amplified by 532 times by an analog circuit before it was sampled by the computer. This amplification also amplifies the noise. This problem was mitigated by averaging ten readings for every stored value, and only testing clutches when no other machines were running adjacent to the test lathe. Figure 3-5 shows that the random error is small relative to the magnitude of the measured signals.

CHAPTER 4

# Compliant Centrifugal Clutch Designs

In order to develop new clutch configurations, rigid-body replacement synthesis was applied to the connected shoe, floating shoe, and flexible trailing shoe centrifugal clutches. Modifying these designs and developing original designs from basic mechanism classes such as the slider-crank yielded additional clutch concepts.

The generated concepts comprise four novel compliant centrifugal clutch types. Two of the types are compliant floating-shoe clutches. One type is a flexible trailing shoe, and the other is based on a double-slider mechanism. Two existing compliant versions of the connected shoe clutch are also presented.

The new clutch concepts and two existing clutch designs are described and concept testing results are reported. Further test data is reported in APPENDIX B. The clutch types are evaluated using the method presented in Chapter 3 to identify those with the greatest potential.

## 4.1 Existing Compliant Designs

Two compliant centrifugal clutch concepts are currently manufactured and used for a variety of applications: the conventional compliant centrifugal clutch and the S-clutch. These clutches meet the performance requirements in simple applications much less expensively than competing rigid-body designs. These clutches have been developed and designed largely by trial and error.

A more effective design model will assist in designing these mechanisms so that they may be adapted more readily to new applications. A PRBM of the concepts presents a partial solution to this need. Since much of the model is the same for both clutches, the conventional compliant centrifugal clutch will be presented in full detail. The S-clutch will be discussed more briefly, focusing on its dissimilarity to the first clutch.

### 4.1.1 Conventional Compliant Centrifugal Clutch ($C^4$)

The conventional compliant centrifugal clutch ($C^4$) (Figure 4-1(a)) is already used in low cost applications such as radio-controlled helicopters which do not demand a particularly smooth start or precise torque characteristics. These clutches generally operate at low power ranges characteristic of radio-controlled models and some lawn and garden equipment. The clutch is easily produced in low volumes because it does not require significant specialized tooling. Frequently, the clutch is not lined with friction material to further reduce manufacturing cost.

The PRBM of this design is a connected shoe clutch with a small-length-flexural pivot as illustrated in Figure 4-1(b). The clutch arm is modeled as though it were pinned to

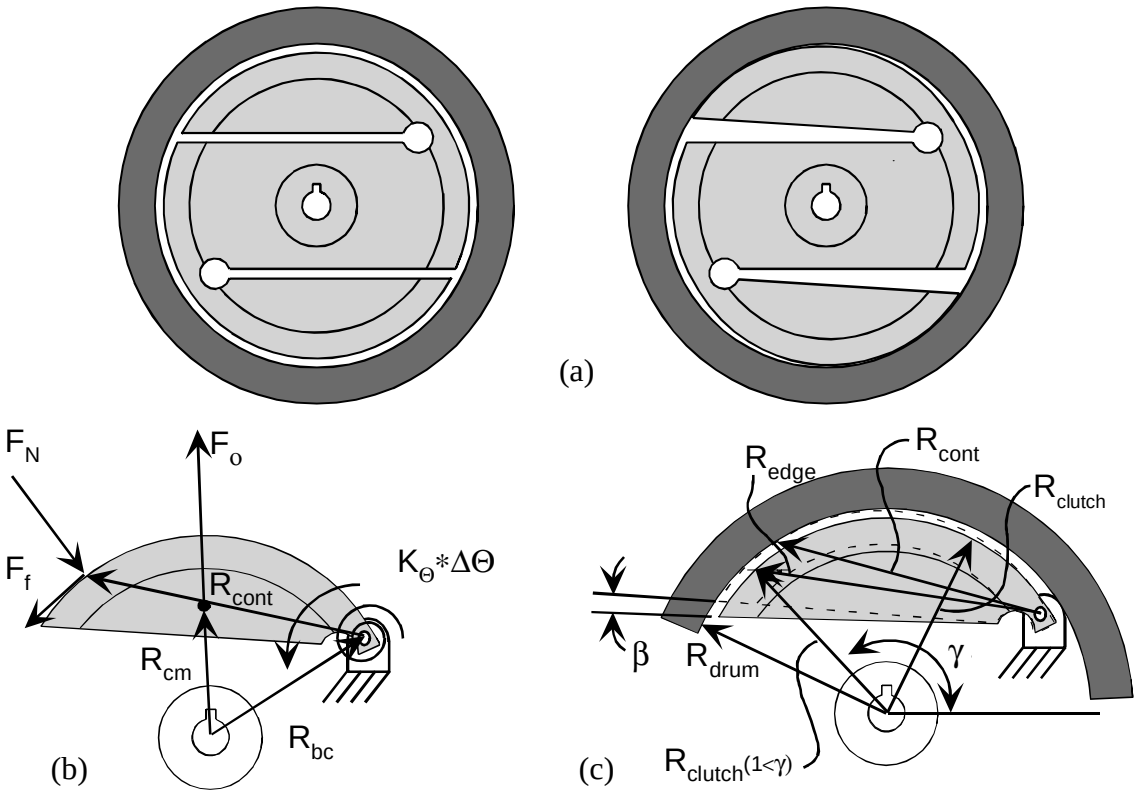


**Figure 4-1** (a)Conventional Compliant Centrifugal Clutch in its undeflected and deflected positions, (b) force and distance vectors for torque equations, (c) vectors and angles used in the contact equations.

the base of the clutch with a torsional spring to model the energy storage of the flexed beam connecting the arm to the clutch base. The characteristic pivot is placed at the thinnest point in the curved beam. The flexible segment is short enough relative to the length of the arm that the displacement at the end of the flexible segment can be disregarded while considering only the angular deflection.

The spring constant for the model can be approximated by modeling the curved segment as several linear beams. The spring constant is often negligible relative to the other forces when the clutch is analyzed at operating speed. Therefore, a simple approximation is often sufficient. However, in considering torque near the engagement speed, a more accurate approximation is essential for model accuracy.

The torque transfer capacity can be estimated by assuming a line of contact on an appropriate point on the clutch drum. The contact line is normal to the page and so it is a point on the profile. The forces on the clutch arm can be summed and solved for the frictional force. Figure 4-1(b) diagrams these forces. The vector summation of moments about the pin is

$$K\Delta\Theta\hat{k} + (\vec{R}_{cm} - \vec{R}_{bc}) \times \vec{F}_o + \vec{R}_{cont} \times \vec{F}_f + \vec{R}_{cont} \times \vec{F}_N = 0 \quad \textbf{(4.1)}$$

where the radial acceleration is treated as an inertial force. By assuming that the frictional force on the clutch drum is proportional to the normal force, the equation can be expressed as

$$K\Delta\Theta\hat{k} + (\vec{R}_{cm} - \vec{R}_{bc}) \times \vec{F}_o + \vec{R}_{cont} \times |\vec{F}_N|\mu\hat{f}_f + \vec{R}_{cont} \times \vec{F}_N = 0 \quad \textbf{(4.2)}$$

where $\mu$ is the friction coefficient and $\hat{f}_f$ is the unit vector in the direction of $\vec{F}_f$. This equation can be solved for the magnitude of the normal force to find

$$|\vec{F}_N| = \frac{K\Delta\Theta\hat{k} + (\vec{R}_{cm} - \vec{R}_{bc}) \times \vec{F}_o}{-\vec{R}_{cont} \times \hat{f}_f\mu - \vec{R}_{cont} \times \hat{f}_n} \quad \textbf{(4.3)}$$

where

$$\hat{f}_n = \frac{\vec{F}_N}{|\vec{F}_N|} \quad \textbf{(4.4)}$$

The torque is then given by

$$T = |\vec{F}_N|\mu R_{drum} n \quad \textbf{(4.5)}$$

where $n$ is the number of clutch arms and $R_{drum}$ is the inner radius of the drum. Other parameters are calculated as follows:

$$\vec{F}_o = M_{arm}\vec{R}_{cm}\omega^2 \quad \textbf{(4.6)}$$

where $M_{arm}$ is the mass of a single clutch arm, and $\omega$ is the clutch speed in radians per second.

The output torque is sensitive to the actual location of contact between the clutch and the drum. This location is given by $\gamma$, an angle measured from the horizontal. Reference Figure 4-1(c) for an explanation of the variables used in the contact equations. At contact, the following vector equation must be satisfied:

$$R_{drum} = \left|\vec{R}_{cont} + \vec{R}_{bc}\right| \quad \textbf{(4.7)}$$

where $\vec{R}_{cont}$ is $\vec{R}_{edge}$ rotated by an angle $\beta$ and $\vec{R}_{edge}$ is defined as

$$\vec{R}_{edge} = \left|R_{clutch}(1\angle\gamma) - \vec{R}_{bc}\right| \quad \textbf{(4.8)}$$

The expression $(1\angle\gamma)$ denotes a unit vector with angle $\gamma$.

The actual contact point is that angle $(\gamma)$ which minimizes the arm rotation for contact $(\beta)$. The contact point can be found by applying an optimization algorithm. The contact angle is the design variable. The objective is to minimize the arm rotation for contact subject to the constraint imposed by Equation (4.8).

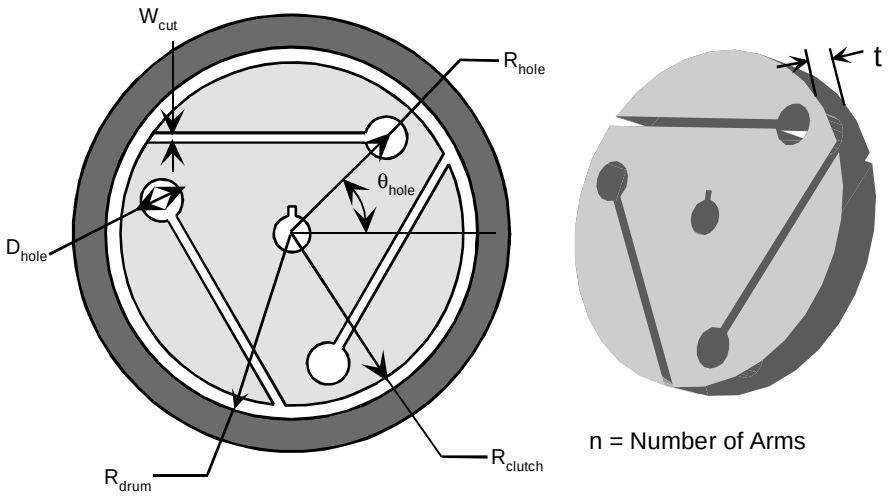


**Figure 4-2** The parameterization of a $C^4$ clutch.

*Test Results*

Figure 4-2 explains the parameterization of the clutch. Refer to Table 4-1 for the parameter values for the three prototype $C^4$ clutches with the measured $T_b$ values and the

**TABLE 4-1 Parameter values for C4 test clutches.**

| Clutch Parameters | $C^4$ #1 | $C^4$ #2 | $C^4$ #3 |
|---|---|---|---|
| $R_{clutch}$ (in) | 2.200 | 2.200 | 2.200 |
| $R_{hole}$ (in) | 2.018 | 1.967 | 1.977 |
| $D_{hole}$ (in) | 0.185 | 0.286 | 0.266 |
| $\theta_{hole}$ (deg) | 36.66° | 28.80° | 31.66° |
| $W_{cut}$ (in) | 0.125 | 0.125 | 0.125 |
| $R_{drum}$ (in) | 2.250 | 2.250 | 2.250 |
| n | 3 | 2 | 2 |
| t (in) | 0.250 | 0.250 | 0.250 |
| $\mu$ | 0.28 | 0.28 | 0.28 |
| $T_b$ (in*lb/1000 rpm) | 1.04 | 1.06 | 0.83 |
| Perimeter (in) | 34.65 | 29.14 | 28.71 |

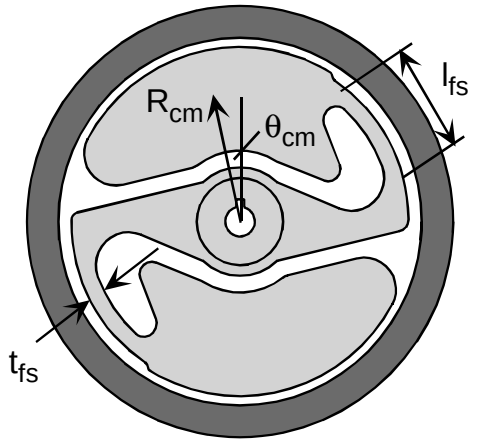


**Figure 4-3** An S-clutch. The longer flexible segments help reduce the bending stress relative to a comparable $C^4$ clutch.

calculated perimeters. The $T_b$ values varied from 0.86 to 1.06 in*lb/1000 rpm. The profile perimeter varied from 28.7 to 34.7 inches.

### 4.1.2 S-Clutch

The S-clutch (Figure 4-3) is another compliant version of the connected shoe clutch. The S-clutch uses longer flexible segments than the $C^4$ clutch. This reduces the stresses in the flexible segments when the arm deflects to contact the drum. The lower stress levels make the design more suitable for lower strength materials like powdered metal. This clutch is used in many low-end gas-powered lawn tools.

The clutch can be modeled in three ways: small deflection beam theory, FEA, and the PRBM. Small deflection beam theory can be applied with reasonable accuracy since the space between the clutch and the drum is generally very small. FEA would be the most accurate method since it can best account for the irregular beam cross section at the ends. The PRBM aids in visualizing the behavior of the clutch, particularly under large deflections. An approximate PRBM is presented for reference.

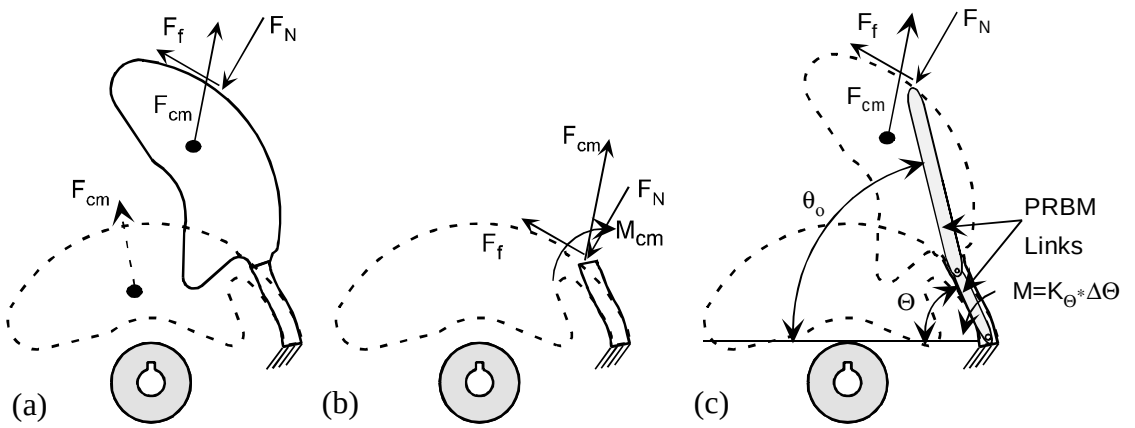


**Figure 4-4** S-clutch analysis. (a) The applied forces on the clutch arm. (b) The applied forces on the flexible segment. A moment is required for equivalence since the forces were moved. (c) The PRBM of the clutch arm. The arm is divided into two segments, one for the rigid segment and one for the flexible segment. However, the angle of the second link ($\theta_o$) is a function of the angle of the first link ($\Theta$).

Since the flexible segment is long, the small-length-flexural-pivot model used for the $C^4$ clutch is not as accurate. However, there is not a general model of a fixed-fixed segment like this one. The fixed-fixed segment is difficult to model because it is subject to both force and moment loads as shown in Figure 4-4(b). The closest PRBM types are for flexible beams loaded either by a force or a moment. An approximate model may be developed by using a value of the characteristic radius factor ($\gamma$) and the stiffness coefficient ($K_\Theta$) between the values predicted by the force and moment load models (Appendix A).

Additional error is introduced by the difference between the pseudo-rigid-body angle ($\Theta$) and the actual angle of the beam tip ($\theta_o$). This error can be reduced by placing another pin at the beam tip to accommodate the difference in angle between the two links. The angle of the final link is given by

$$\Delta\theta_o = \Delta\Theta c_\theta \quad \textbf{(4.9)}$$

The $c_\theta$ parameter is a function of the load type and direction. Approximate values can be developed for mixed force and moment loading from the models for simple loading types.

Like the $C^4$ clutch, the normal force can be found by summing the moments about the characteristic pivot at the ground. The normal force can then be used in Equation (4.5) to predict the torque output.

*Test Results*

Two S-clutch prototypes were constructed and tested. The parameters of the prototypes and the measured $T_b$ values are given in Table 4-2, where the parameters are explained in Figure 4-3. The two prototype clutches are very similar because the simple geometry leaves little room for adjusting the mechanical advantage of the centrifugal

**TABLE 4-2 Parameter values for prototype S-clutches.**

| Clutch Parameters | #1 | #2 |
|---|---|---|
| $R_{clutch}$ (in) | 2.200 | 2.200 |
| Arm Volume ($in^3$) | 0.96 | 0.95 |
| $R_{cm}$(in) | 1.338 | 1.338 |
| $\theta_{cm}$ (deg) | -11.8 | -12.3 |
| $l_{fs}$ (in) | 1.250 | 1.455 |
| $t_{fs}$ (in) | .2072 | 1.25 |
| $R_{drum}$ (in) | 2.250 | 2.250 |
| n | 2 | 2 |
| t (in) | 0.250 | 0.250 |
| $\mu$ | 0.28 | 0.28 |
| $T_b$ (in*lb/1000 rpm) | 1.10 | 1.14 |
| Perimeter (in) | 32.56 | 33.23 |

actuation force. The only significant variation between the two clutches lies in the stiffness of the flexible members, but the purpose of the $T_b$ value is to permit torque capacity comparison of clutches with different effective spring constants. The measured $T_b$ values of 1.10 and 1.14 in*lb/1000 rpm verifies that the $T_b$ value does compare clutch torque capacities even when the clutches have different spring stiffnesses. The profile perimeter values are 32.6 and 33.2 inches. These values are very similar to those from the $C^4$ clutches.

## 4.2 Novel Compliant Designs

### 4.2.1 Floating 1 (F1)

This design is a compliant version of the floating shoe clutch. See Figure 4-5. The design combines the shoes and the spring of a rigid-body floating-shoe clutch to reduce the part count. The shoes are connected by thin flexible segments that provide the spring force. However, the hub rather than the flexible segments bears the torque load. This increases the design space of the concept. The clutch can be designed to engage at very low speeds using very flexible connecting elements while supporting large torque loads through a stiff hub. Many competing designs require that the torque loads pass through the flexible segments. In these cases, torque capacity and engagement speed are not entirely independent. A disadvantage of the stiff hub is that additional parts may be necessary to hold the floating shoes on the hub.

The geometry and loading of the clutch are symmetrical. Therefore, the clutch can be analyzed by considering just one shoe and applying geometric and force constraints imposed by the symmetry of the closed loop. The force exerted by the hub transfers torque

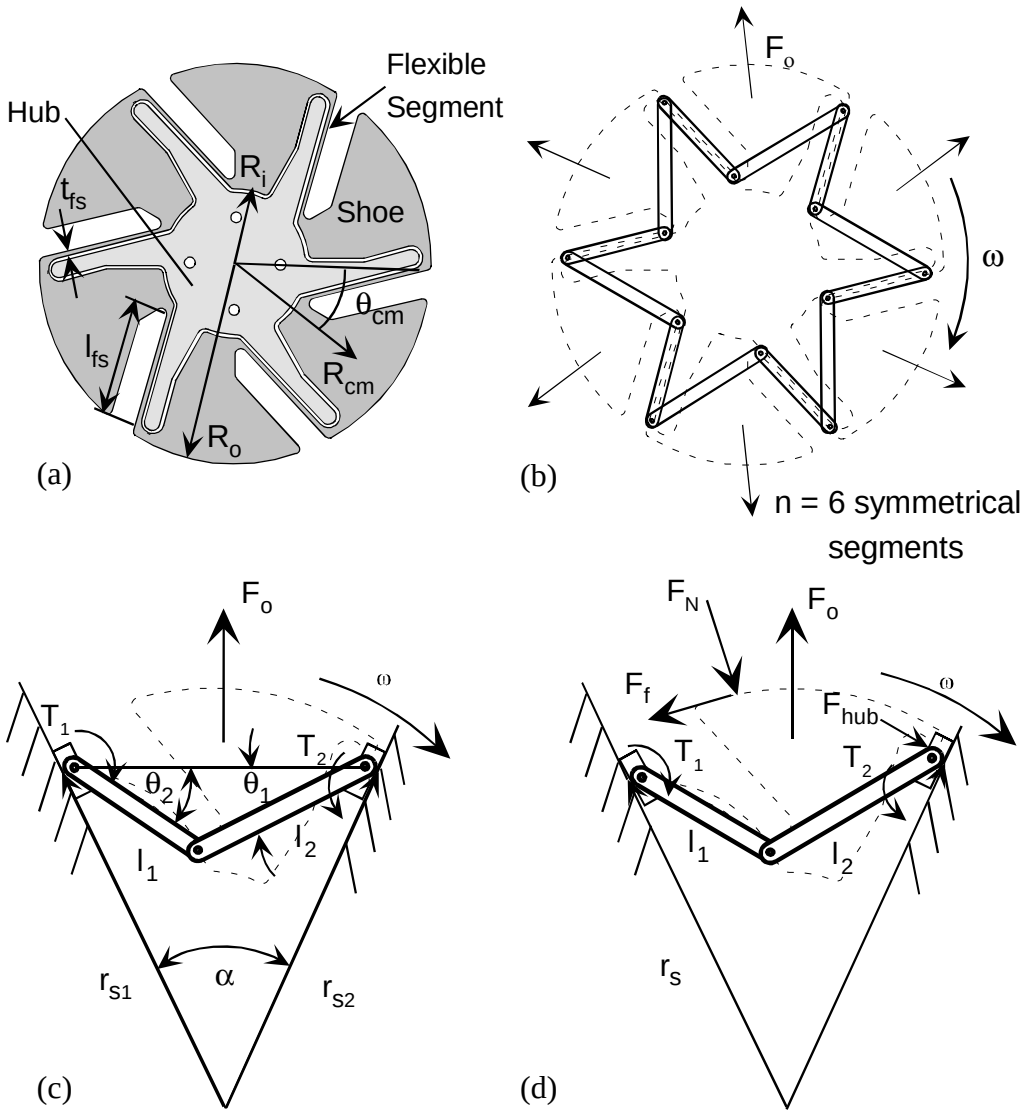


**Figure 4-5** A F1 type centrifugal clutch. (a) The clutch is pictured with its center hub. (b) The clutch's PRBM and applied centrifugal forces are shown. (c) The forces on a clutch segment before engagement and (d) after engagement when the center of mass lies on the bisector of $\alpha$.

from the driving input to the floating member of the clutch. Before the floating member contacts the drum, the torque input through the hub overcomes losses such as air resistance and accelerates the clutch. The hub force is negligible while the clutch is rotating at a constant speed, it has not contacted the drum, and the center of mass is on the line that bisects $\alpha$.

Figure 4-5(c,d) shows the forces acting on one shoe of a clutch rotating with constant angular velocity before and after engagement with the drum. The locations of the pin joints are not directly calculable from the PRBM. The flexible segment is a fixed-fixed segment with combined loading, therefore an approximate PRBM must be used that combines the effects of the force and moment loading. The ends can be modeled as sliders since the pins move along a radial line. Due to symmetry, the two ends are always the same distance from the axis of rotation and the reaction forces are of equal magnitude. Choosing the radius from the center axis ($r_s$) as the generalized coordinate, the position equations are

$$\theta_1 = \operatorname{acos}\left(\frac{2r_s^2(1-\cos\alpha)+l_1^2-l_2^2}{2r_s l_1\sqrt{2(1-\cos\alpha)}}\right) \quad \textbf{(4.10)}$$

$$\theta_2 = \operatorname{acos}\left(\frac{2r_s^2(1-\cos\alpha)+l_2^2-l_1^2}{2r_s l_2\sqrt{2(1-\cos\alpha)}}\right) \quad \textbf{(4.11)}$$

$$\alpha = \frac{2\pi}{n} \quad \textbf{(4.12)}$$

Using these equations, an optimization routine can be applied to find the contact location and position as was done for the $C^4$ clutch.

The force-deflection relationships can be developed through the application of virtual work or free-body diagrams. Consider the case in which the center of mass is on the bisector of the included angle ($\alpha$) between the two sliders. If the clutch segment is

oriented so that the vector from the rotational axis to the center of mass is vertical, the centrifugal force and mechanism position can be related by

$$0 = \left|\vec{F}_o\right|((\vec{r}_{cm} - \vec{r}_{s_1}) \times \hat{j}) + T_1 + T_{21} + l_1\left|\vec{F}_o\right| \frac{\sin\left(\frac{\pi}{n} - (\pi + \theta_1)\right)}{\sin\frac{\alpha}{2} + \sin\left(\pi - \frac{\alpha}{2}\right)} \tag{4.13}$$

$$\vec{F}_o = m\omega^2 \vec{r}_{cm} \tag{4.14}$$

$$T_1 = k_1(\theta_{1o} - \theta_1) \tag{4.15}$$

$$T_{21} = k_{21}[(\theta_{1o} - \theta_1) - (\theta_{2o} - \theta_2)] \tag{4.16}$$

These equations are valid when the change in $r_s$ due to the mechanism movement remains small enough that the resulting change in direction and magnitude of $\vec{F}_o$ can be neglected.

These equations can be used in two ways. The easiest is to first evaluate the position relationships of the clutch for a given value of $r_s$ and then apply the known angle values to Equations (4.13) to (4.16). The direction of $\vec{F}_o$ is known and its magnitude can be evaluated directly from Equation (4.13). The equations can also be evaluated when given a value of $\omega$ to calculate $\vec{F}_o$ and solve for the resulting mechanism position. However, this solution is only possible through numerical methods for systems of nonlinear equations.

A similar approach can be utilized to develop equations for the normal force on the clutch drum. In this case, the mechanism position can be found from the constraints imposed by contact with the drum. A new force-deflection analysis is then performed considering normal, friction, and hub forces. Since the friction force is a known function

of the normal force, the normal and friction force are really just one unknown. The clutch's torque transfer is given by Equation (4.5).

The clutch acts much like a standard floating clutch except that the radial offset between connections on each side of the shoes and the bending of the flexible segments apply a moment to the shoe. Therefore, the shoes rotate as they move radially outward to contact the drum.

*Test Results*

The F1 clutches are parameterized as illustrated in Figure 4-5(a). Table 4-1 lists the parameter values for the F1 prototype tested. The $T_b$ value indicates a significant increase in torque capacity relative to the $C^4$ and S-clutches. However, the clutch also has a

**TABLE 4-3 Parameter values for prototype F1 clutch**

| Clutch Parameters | #1 |
|---|---|
| $R_{clutch}$ (in) | 2.200 |
| Segment Volume ($in^3$) | .3296 |
| $R_{cm}$(in) | 1.618 |
| $\theta_{cm}$ (deg) | 34.5 |
| $l_{fs}$ (in) | 1.16 |
| $t_{fs}$ (in) | 0.045 |
| $R_{drum}$ (in) | 2.250 |
| n | 6 |
| t (in) | 0.250 |
| $R_i$ (in) | 0.81 |
| $T_b$ (in*lb/1000 rpm) | 1.49 |
| Perimeter, One Cut (in) | 44.47 |
| Perimeter, 2 Cuts(in) | 66.5 |

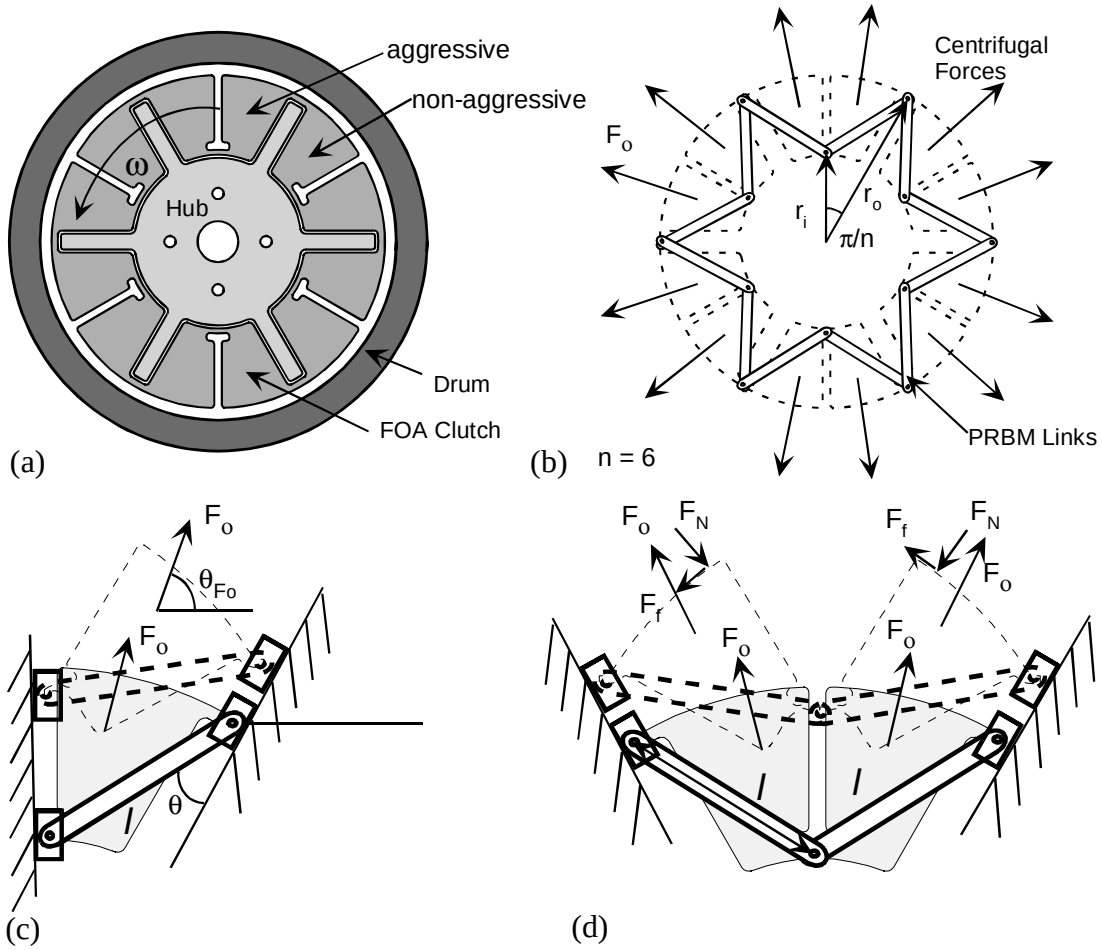


**Figure 4-6** (a) A FOA clutch in its undeflected position. (b) The PRBM of the clutch with the centrifugal forces shown. (c) The applied forces deflection path before contact of a single shoe and its PRBM. (d) The applied forces and deflected position of a single shoe and its PRBM after contact. (Deflections are shown larger than actual deflections.)

significant increase in the profile perimeter to 44.5 inches if the hub can be made from the interior cutout. If not, the value of the profile perimeter term increases to 66.5 inches.

### 4.2.2 Floating Opposing Arm

The floating opposing arm (FOA) clutch (Figure 4-6) gets its name from the fact that adjacent friction surfaces rotate in opposite directions to contact the drum--one rotates clockwise and the other rotates counter clockwise. This means that half of the shoes are aggressively oriented, and half are non-aggressively oriented. The aggressive and non-

aggressive shoes are connected together. This results in a higher torque than a clutch with non-aggressive shoes but a smoother start than if all the shoes were aggressively oriented. The basic clutch consists of just two parts, but additional parts may be necessary to reliably maintain the position of the shoes on the hub.

The PRBMs of the FOA clutch and the F1 clutch are similar. The primary difference is that every link on the FOA clutch has a friction surface and sufficient mass to have a significant centrifugal force. Also, the PRBM links are all the same length in the FOA model and all flexible segments are small length flexural pivots.

The clutch has a high degree of symmetry. Prior to contact with the clutch drum, the deflection of the clutch can be analyzed by considering just one shoe. The force from the hub is small and is not considered in this analysis. Figure 4-6(c) shows the forces on the shoe. Symmetry requires that the centers of the flexible segments move on paths extending radially from the axis of rotation. If $r_i$ is the generalized coordinate and the initial values $r_{i_o}$ and $r_{o_o}$ are known, the displacement of the mechanism is given by

$$l = \sqrt{r_{o_o}^2 + r_{i_o}^2 - 2 r_{o_o} r_{i_o} \cos\frac{\pi}{n}} \tag{4.17}$$

$$\theta = \operatorname{asin}\left(\frac{r_i \sin\frac{\pi}{n}}{l}\right) \tag{4.18}$$

$$r_o = l\left(\sin\theta \cot\frac{\pi}{n} + \cos\theta\right) \tag{4.19}$$

Summation of forces and moments on the link can be used to solve for the relationship between the centrifugal force ($F_o$) and the mechanism position. The resulting equation is

$$\overrightarrow{r_{cm}} \times \overrightarrow{F_o} + T_1 + T_2 + l\angle\left(\frac{\pi}{2} - \frac{\pi}{n} - \theta\right) \times \vec{F}_{So} = 0 \quad \textbf{(4.20)}$$

where the parameters are defined as

$$\overrightarrow{F_o} = m\omega^2(r_i\hat{j} + \overrightarrow{r_{cm}}) \quad \textbf{(4.21)}$$

$$\left|\vec{F}_{So}\right| = -F_o \frac{\sin\theta_{Fo}}{\sin\left(\pi - \frac{\pi}{n}\right)} \quad \textbf{(4.22)}$$

$$\angle\vec{F}_{So} = \pi - \frac{\pi}{n} \quad \textbf{(4.23)}$$

$$T_1 = k_1(\theta_o - \theta) \quad \textbf{(4.24)}$$

$$T_2 = k_2(\theta_o - \theta) \quad \textbf{(4.25)}$$

$F_{So}$ is the reaction force at the outer slider. The spring constants of the flexible segments ($k_1$, $k_2$) are calculated from Equation (A.3). In this work, the mechanism deflections are assumed sufficiently small that the changes in magnitude and deflection of $\vec{F}_o$ can be neglected. With this restriction, Equation (4.20) can be solved directly for the magnitude of $\vec{F}_o$ since its direction is known.

After contact with the drum, the aggressive and non-aggressive shoes will not be loaded symmetrically. The clutch must be modeled with two shoes together as drawn in Figure 4-6(d). After contact, the mechanism position is known. The conditions of force and moment equilibrium can be applied to solve for the normal force. The torque is then given by Equation (4.5).

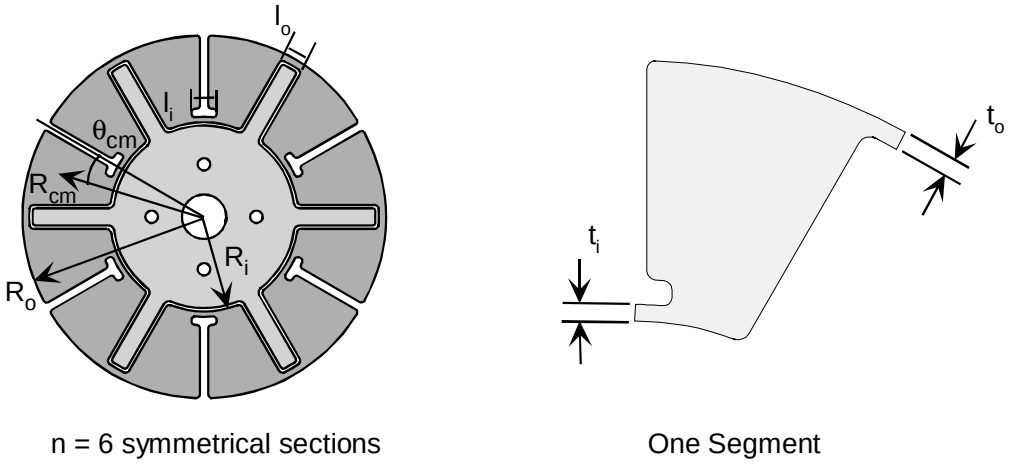


**Figure 4-7** Parameter values for the FOA clutches.

*Testing Results*

Figure 4-7 describes the parameterization of the FOA clutches. Four FOA clutches were prototyped and tested. Table 4-1 summarizes their parameters, measured $T_b$ values, and profile perimeters. These clutches have the highest $T_b$ values of all the clutches tested. The profile perimeters are larger than some of the clutches, but not much larger. The profile perimeters are actually smaller than average for some designs if the hub is made from the center piece left from making the inner cut of the floating piece.

### 4.2.3 Grounded Opposing Arm

The Grounded Opposing Arm (GOA) clutch is represented in Figure 4-8(a). It may be modeled as a double slider. Until contact with the clutch drum, the slider-crank half model is sufficient. However, the non-symmetric frictional forces require that the shoe pairs be modeled together after engagement. This clutch may also be considered a floating opposing arm (FOA) clutch that is fixed to the hub.

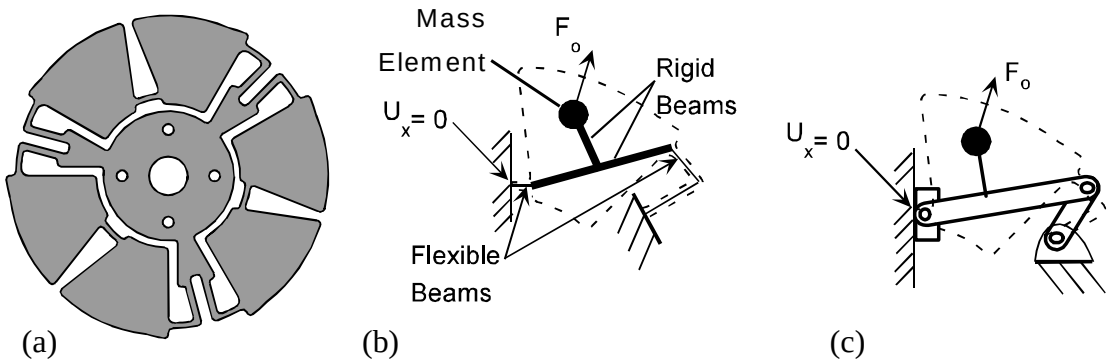


**Figure 4-8** Grounded Opposing Arm (GOA) Clutch. (a) A GOA clutch with three arm pairs. (b) A schematic of a FEA model of the clutch before contact. (c) An approximate PRBM for the clutch before contact.

The GOA design shares the opposing arm torque characteristics with the floating opposing arm design. However, it is all one piece. This reduces the part count while

**TABLE 4-4 Parameter values for prototype FOA.**

| Clutch Parameters | #1 | #2 | #3 | #4 |
|---|---|---|---|---|
| $R_{clutch}$ (in) | 2.200 | 2.200 | 2.200 | 2.200 |
| Arm Volume ($in^3$) | 0.174 | 0.443 | 0.316 | 0.194 |
| $R_{cm}$(in) | 1.710 | 1.569 | 1.604 | 1.6375 |
| $\theta_{cm}$ (deg) | 13.79 | 28.50 | 21.99 | 13.68 |
| $l_i$ (in) | 0.265 | 0.347 | 0.20 | 0.256 |
| $t_i$ (in) | 0.066 | 0.066 | 0.066 | 0.066 |
| $l_o$ (in) | 0.243 | 0.418 | 0.238 | 0.232 |
| $t_o$ (in) | .075 | .075 | .075 | .075 |
| $R_{drum}$ (in) | 2.250 | 2.250 | 2.250 | 2.250 |
| n | 6 | 3 | 4 | 6 |
| t (in) | 0.250 | 0.250 | 0.250 | 0.250 |
| $R_i$ (in) | 1.125 | .875 | .875 | .875 |
| $T_b$ (in*lb/1000 rpm) | 2.17 | 2.22 | 2.62 | 2.66 |
| Perimeter, One Cut (in) | 45.13 | 35.46 | 41.14 | 49.54 |
| Perimeter, 2 Cut (in) | 63.21 | 46.59 | 53.53 | 69.03 |

maintaining reversibility. On the other hand, the connections to ground stiffen the structure and reduce the torque for a given clutch size. The torque is further reduced by the additional mass removed from the shoes to create the connections to ground. The clutch members also continue deflecting with increased torque. Some of the centrifugal force is stored in the member deflection rather than being transferred to the clutch drum. This reduces torque output but increases starting smoothness. Starting smoothness increased only slightly in the prototyped clutches.

This clutch is the only design with a closed-loop PRBM that is connected to ground. This distinction results in several unique characteristics. As a closed-loop mechanism, the GOA clutch can be designed with a variety of force-deflection characteristics by varying the relative stiffness of different segments. Some of the possibilities include bistability and continually increasing force. The continually increasing force option is the standard of all other designs considered in this work. Bistable force-deflection relationships may be appropriate for a centrifugal brake. These potential features may permit this clutch to be utilized as a centrifugal switch or a centrifugal brake. However, these possibilities are not examined in this work.

An accurate analysis of this clutch may be performed using finite element methods. Nonlinear beam elements with a mass can be used as pictured in Figure 4-8(b). Flexible segments are modeled with beam elements assigned the actual section properties. The rigid segments are assigned large section properties to minimize the segment deflection.

The complicated segment type at the ground connection cannot be modeled accurately with the PRBM. However, an approximate PRBM is helpful in visualizing the

general mechanism behavior. Figure 4-8(c) shows an approximate PRBM for an unengaged clutch arm.

*Test Results*

Two versions of the GOA clutch were prototyped and tested. The parameters of the prototypes are presented in Table 4-1 and the parameter definitions are given in Figure 4-9. The $T_b$ values for the GOA clutches are higher than the existing designs but remain significantly lower than the FOA designs. The profile perimeters are approximately the same as most of the other new designs.

**TABLE 4-5 Parameter values for prototype GOA clutches.**

| Clutch Parameters | #1 | #2 |
|---|---|---|
| $R_{clutch}$ (in) | 2.200 | 2.200 |
| Segment Volume ($in^3$) | 0.339 | 0.366 |
| $R_{cm}$(in) | 1.625 | 1.565 |
| $\theta_{cm}$ (deg) | 35.06 | 35.02 |
| $l_i$ (in) | 0.295 | 0.303 |
| $t_i$ (in) | 0.070 | 0.070 |
| $l_1$ (in) | 0.540 | 0.194 |
| $t_1$ (in) | 0.090 | 0.125 |
| $l_2$ (in) | 0.374 | 0.340 |
| $t_2$ (in) | 0.070 | 0.070 |
| $R_{drum}$ (in) | 2.250 | 2.250 |
| n | 3 | 3 |
| t (in) | 0.250 | 0.250 |
| $R_i$ (in) | 0.97 | 0.75 |
| $T_b$ (in*lb/1000 rpm) | 1.64 | 1.73 |
| Perimeter (in) | 48.75 | 47.92 |

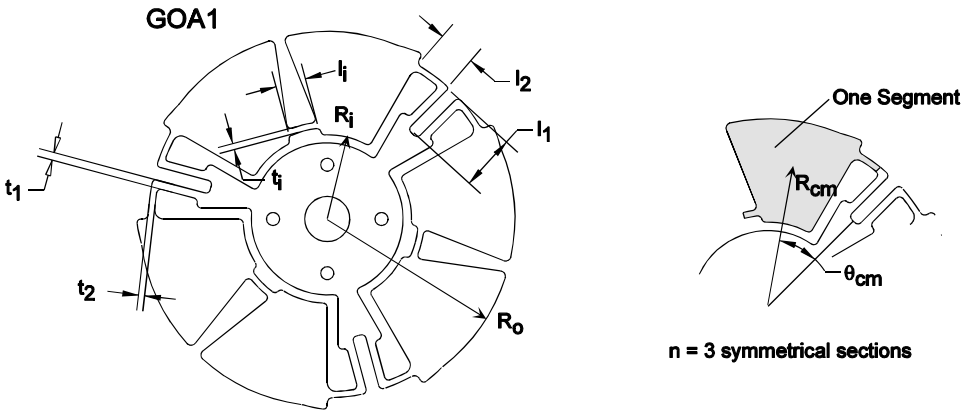


**Figure 4-9** Diagram of parameter definitions for the GOA clutch.

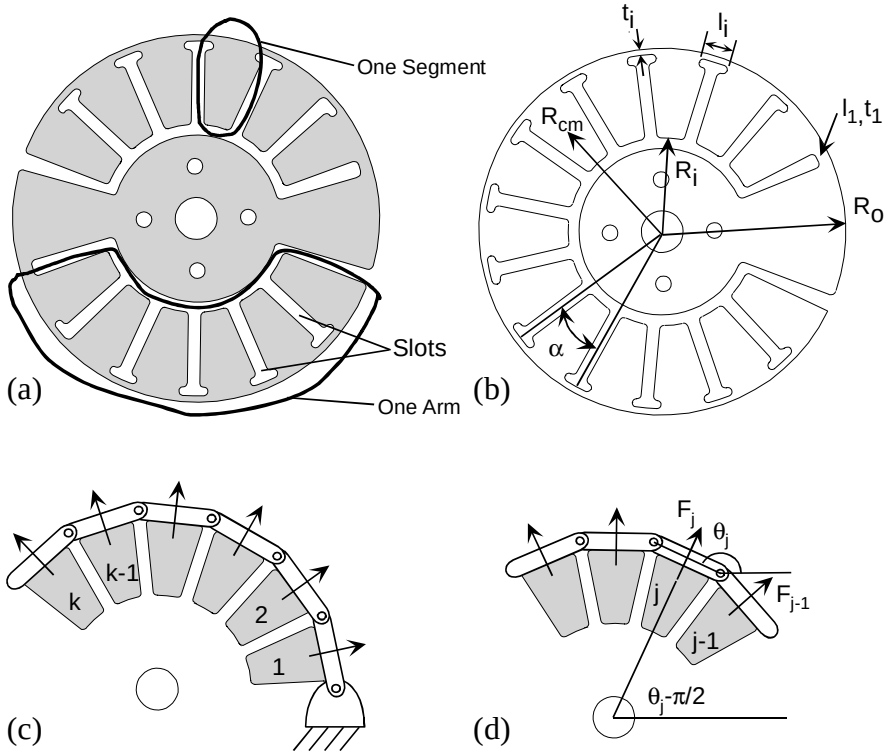


**Figure 4-10** The Split-arm clutch. (a) A two arm, six segment clutch. (b) A one arm, thirteen segment clutch. (c) The PRBM of a clutch arm with k segments with the centrifugal forces included. (d) Variables used in the deflection analysis of the clutch.

### 4.2.4 Split-arm

The split-arm clutch (Figure 4-10) is similar to a flexible trailing shoe clutch. The clutch is modeled as a series of rigid links connected by small-length-flexural pivots. As

the number of segments increases, the clutch more closely approximates the continuous compliance of a flexible-shoe. Therefore, increasing the number of segments decreases dependence of torque output on the friction coefficient as it approaches the relationship of a flexible shoe clutch. However, the slots that separate the segments decrease the centrifugal force and output torque by decreasing the overall mass of the clutch arm. Increasing the number of segments also increases the manufacturing difficulty.

The PRBM of the split-arm clutch is an open loop mechanism with a degree of freedom for every segment in the arm. However, under operating conditions the force applied to every arm is a function of speed. Therefore, as a clutch, the mechanism operates as though it has only one degree of freedom since the direction and magnitude of all of the applied forces are dependent. Virtual work may be applied to develop a general set of equations that relate speed and mechanism position.

The equations are developed for a clutch with $j$ segments on each arm with a centrifugal force at the center of the link. The formulation permits varying spring constants, link lengths, and segment masses. The centrifugal forces are assumed to act at on the center of the PRBM links since they act perpendicular to the PRBM links and the link rotations are small. The resulting virtual work equation is

$$\begin{aligned}\delta W \;=\; & \vec{F}_1 \bullet \delta\vec{z}_1 + \vec{F}_2 \bullet \delta\vec{z}_2 + \ldots + \vec{F}_{j-1} \bullet \delta\vec{z}_{j-1} + \vec{F}_j \bullet \delta\vec{z}_j + T_{01}\delta\theta_1 \\ & + T_{12}(\delta\theta_2 - \delta\theta_1) + T_{23}(\delta\theta_3 - \delta\theta_2) + \ldots + T_{(j-1)j}(\delta\theta_{j-1} - \delta\theta_{j-1})\end{aligned} \qquad \textbf{(4.26)}$$

where the forces, $F_k$, and the virtual displacements $\delta z_k$ are

$$\vec{F}_k \;=\; F_k\cos\left(\theta_k - \frac{\pi}{2}\right)\hat{i} + F_k\sin\left(\theta_k - \frac{\pi}{2}\right)\hat{j} \;=\; F_k\sin(\theta_k)\hat{i} - F_k\cos(\theta_k)\hat{j} \qquad \textbf{(4.27)}$$

$$\delta\vec{z}_k = \sum_{i=1}^{k-1}(-r_i\sin\theta_i\delta\theta_i\hat{i} + r_i\cos\theta_i\hat{j}) - \frac{r_k}{2}\sin\theta_k\delta\theta_k\hat{i} + \frac{r_k}{2}\cos\theta_k\delta\theta_k\hat{j} \quad \textbf{(4.28)}$$

Equations (4.27) and (4.28) are substituted into Equation (4.26). The principle of virtual work requires that the virtual work be zero for any combination of virtual displacements. This requires the sum of the terms associated with each virtual displacement to be zero. The resulting system of $j$ equations can be simplified with the angle difference formula to find

$$T_{k-1,k} - T_{k,k+1} - F_k\frac{r_k}{2}\cos(\theta_{k_o} - \theta_k) - \sum_{i=k+1}^{j}(F_i r_i\cos(\theta_k - \theta_i)) = 0,\ 0 < k < j \quad \textbf{(4.29)}$$

$$T_{k-1,k} - F_j\frac{r_j}{2}\cos(\theta_{j_o} - \theta_j) = 0 \quad \textbf{(4.30)}$$

These equations can be solved for the arm equilibrium position for a given force loading using numerical methods. Unlike other clutches, it is not possible to calculate the displacements separately from the forces. Since the arms have $j$ degrees of freedom, the actual arm position at contact can only be determined knowing all of the applied forces. The other clutches have only one degree of freedom per shoe/arm, permitting calculation of contact locations separately from force loading.

Once the arm begins to contact the clutch drum, the equations change. An additional unknown, $\left|\vec{F}_N + \vec{F}_f\right|$, is added for every link that contacts the clutch drum. However, each contacting link removes a degree of freedom as well. Since the links are generally short, the contact area can be modeled as a point at the center of every link.

*Test Results*

This design was tested in one and two arm versions to compare the relative torque transfer. The parameters of the tested prototypes are listed in Table 4-1. Figure 4-10 explains the parameter definitions. The one arm clutch is the least sensitive to changes in the coefficient of friction. However, it should be mounted in pairs to balance its non-symmetry. The two arm clutch does not have this limitation since it is symmetric.

The torque capacity of the split-arm clutches is generally higher than the existing designs, but not among the highest of the novel designs. It is also average in the profile perimeter metric.

**TABLE 4-6 Parameter values for prototype Split-arm clutches.**

| Clutch Parameters | #1 | #2 | #3 |
|---|---|---|---|
| $R_{clutch}$ (in) | 2.200 | 2.200 | 2.200 |
| n arms | 2 | 1 | 1 |
| n segments/arm | 5 | 8 | 13 |
| Segment Volume ($in^3$) | 0.137 | 0.261 | 0.148 |
| $R_{cm}$(in) | 1.702 | 1.611 | 1.655 |
| $\alpha$ (deg) | 24 | 40 | 24 |
| $l_1$ (in) | 0.796 | 0.559 | 0.1233 |
| $t_1$ (in) | 0.150 | 0.150 | 0.150 |
| $l_i$ (in) | 0.287 | 0.300 | 0.296 |
| $t_i$ (in) | 0.075 | 0.075 | 0.075 |
| $R_{drum}$ (in) | 2.250 | 2.250 | 2.250 |
| t (in) | 0.250 | 0.250 | 0.250 |
| $R_i$ (in) | 1.125 | 1.000 | 0.975 |
| $T_b$ (in*lb/1000 rpm) | 1.28 | 1.54 | 0.99 |
| Perimeter (in) | 49.55 | 44.92 | 57.05 |

## 4.3 Summary of Clutch Test Results

The $T_b$ values and the profile perimeter values for all of the tested clutches are summarized in Table 4-7. The bolded values mark the $T_b$ and perimeter values used in the clutch concept evaluations. With all of the clutch types except the FOA clutch, there is one test case that has the highest torque capacity with little or no increase in profile perimeter. Thus the choice of which data set to use in the evaluations becomes very easy. With the FOA clutch, there is a clear trade-off between torque capacity and profile perimeter. The best option depends on the relative weighting of the manufacturing and torque criteria. Therefore, two of the FOA prototypes will be evaluated as if they were different clutches.

## 4.4 Clutch Concept Evaluations

Using the established criteria, each of the novel clutch configurations and the two existing compliant centrifugal clutches underwent evaluation. The results of the clutch concept evaluation are given in Table 4-8. The total scores are listed and the ratio of each of the scores relative to the top score is calculated as the relative score. The top two scores belong to the FOA clutches while the S-clutch placed third, and the split arm placed fourth. The S-clutch excels despite its below average torque performance because of its

**TABLE 4-7 Clutch Test Result Summary**

| **Clutch name** | **$C^4$ 1** | **$C^4$ 2** | **$C^4$ 3** | **S 1** | **S 2** | **F1** | **FOA 1** | **FOA 2** | **FOA 3** | **FOA 4** | **GOA 1** | **GOA 2** | **Split 1** | **Split 2** | **Split 3** |
|---|---|---|---|---|---|---|---|---|---|---|---|---|---|---|---|
| **Tb** | 1.04 | **1.06** | 0.83 | 1.10 | **1.14** | 1.49 | 2.17 | **2.22** | **2.62** | 2.66 | 1.64 | **1.73** | 1.28 | **1.54** | 0.99 |
| **Perimeter & hub same operation** | 34.7 | **29.1** | 28.7 | 32.6 | **33.2** | 47.5 | 45.1 | **35.5** | **41.1** | 49.5 | 48.8 | **47.9** | 49.6 | **44.9** | 57.1 |
| **Perimeter,hub separate Operation** | 34.7 | **29.1** | 28.7 | 32.6 | **33.2** | 66.5 | 63.2 | **46.6** | **53.5** | 69.0 | 48.8 | **47.9** | 49.6 | **44.9** | 57.1 |

simplicity. The FOA clutch is decidedly more complicated, but offers improved performance through distributed loading, more wear points, and higher torque capacities.

It is not surprising that the S-clutch rated well in the evaluation. The S-clutch is the more widely used of the two pre-existing designs. It has been successfully incorporated in many inexpensive lawn and garden power tools. It is encouraging that the FOA design rates favorably with this commercially successful design. This suggests that the FOA clutch has good potential. The FOA clutch's higher $T_b$ rating enables size reduction relative to an S-clutch designed for the same application. The reduced size would reduce the profile perimeter size and the raw material required per clutch. This may increase its viability.

The split-arm clutch placed second among the novel configurations and was very close behind the S-clutch. It has average torque capacity for the group, but has unique advantages such as decreased dependence of torque transfer on the friction coefficient. It also has decreased operating stress since the compliance is distributed along the length of the arm. These advantages suggest that the clutch is likely to have useful applications. In

**TABLE 4-8 Clutch Concept Evaluation Results**

| | | **C^4** (Existing) | | **S-Clutch** (Existing) | | **F1** (Novel) | | **FOA 2** (Novel) | | **FOA 3** (Novel) | | **GOA** (Novel) | | **Split-Arm** (Novel) | |
|---|---|---|---|---|---|---|---|---|---|---|---|---|---|---|---|
| **Criteria** | Weight | Rating | Score | Rating | Score | Rating | Score | Rating | Score | Rating | Score | Rating | Score | Rating | Score |
| *Loading* | 2 | **3** | 6 | **4** | 8 | **2** | 4 | **3** | 6 | **3** | 6 | **1** | 2 | **3** | 6 |
| *Manufacturability* | 5 | **4** | 20 | **4** | 20 | **1** | 5 | **3** | 15 | **2** | 10 | **1** | 5 | **2** | 10 |
| *Torque Capacity* | 4 | **1** | 4 | **1** | 4 | **2** | 8 | **4** | 16 | **4** | 16 | **3** | 12 | **2** | 8 |
| *Retain Resilience* | 2 | **2** | 4 | **2** | 4 | **3** | 6 | **3** | 6 | **3** | 6 | **2** | 4 | **3** | 6 |
| *Wear* | 3 | **1** | 3 | **2** | 6 | **3** | 9 | **3** | 9 | **3** | 9 | **3** | 9 | **3** | 9 |
| *Other Advantages* | 1 | **0** | 0 | **0** | 0 | **0** | 0 | **1** | 1 | **1** | 1 | **1** | 1 | **1** | 1 |
| **Total Score** | | | **37** | | **42** | | **32** | | **53** | | **48** | | **33** | | **40** |
| **Relative Score** | | | **0.7** | | **0.792** | | **0.6** | | **1.00** | | **0.91** | | **0.62** | | **0.75** |

fact, the split-arm clutch scored better than the $C^4$ clutch which is already used successfully in several applications.

The GOA and F1 clutches did not score well relative to the other designs. Both designs have relatively modest torques and manufacturability. While they both performed adequately against the measures, neither has a strong advantage that would motivate further examination and analysis.

CHAPTER 5

# FOA Clutch Model and Application

The previous chapter showed that the FOA clutch scores well based on the clutch evaluation criteria, but more information is needed to design and develop these clutches for applications. Models for engagement speed and torque capacity ($T_b$) are required to design a clutch. For engagement speed, the model presented in Chapter 4 is expanded and a model for the torque capacity ($T_b$) is developed in this chapter. Predictions from both models are compared to prototype test data. The resulting equations are demonstrated by designing an FOA clutch to replace an existing S-clutch in a gas-powered string trimmer. The FOA string-trimmer clutch was prototyped and tested in the string trimmer.

## 5.1 Engagement Model

### 5.1.1 Equation Development

The clutch engagement speed is found by calculating the deflection for engagement and then solving the force equations to determine how much centrifugal force is required to deflect the clutch into contact with the drum. The variables used in the

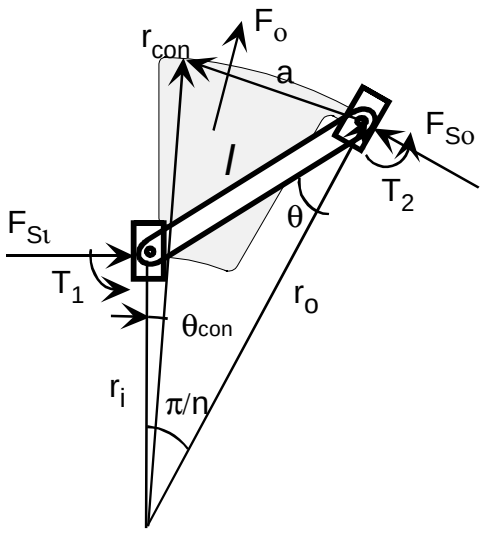


**Figure 5-1** Explanation of variables used in the FOA clutch engagement model.

analysis are shown in Figure 5-1. The change in outer clutch radius at the contact point ($\Delta r_{con}$) is approximately

$$\Delta r_{con} = (r_o - r_{o_o})\cos\left(\frac{\pi}{n} - \theta_{con}\right) + a(\sin(\theta - \theta_o)\cos\beta) \quad \textbf{(5.1)}$$

where

$$\beta = \text{asin}\left(\frac{r_{clutch} - r_o\cos\frac{\pi}{n}}{a}\right) \quad \textbf{(5.2)}$$

and $\theta_{con}$ is the angle from vertical to the contact location. Substituting for $r_o$ in terms of $\theta$ from Equation (4.19) results in

$$\Delta r_{con} = l\cos\left(\frac{\pi}{n} - \theta_{con}\right)\left(\left(\sin\theta\cot\frac{\pi}{n} + \cos\theta\right) - \left(\sin\theta_o\cot\frac{\pi}{n} + \cos\theta_o\right)\right) \quad \textbf{(5.3)}$$
$$+ a(\sin(\theta - \theta_o)\cos\beta)$$

This equation can be further simplified by assuming small angles to find

$$\Delta r_{con} = (\theta - \theta_o)\left[ l\left( \cos\theta \cot\frac{\pi}{n} - \sin\theta \right) \cos\left( \frac{\pi}{n} - \theta_{con} \right) + a(\cos\beta) \right] \quad \textbf{(5.4)}$$

At contact, $\Delta r_{con}$ equals $\delta$, the initial clearance between the clutch and the drum. Substituting for $\Delta r_{con}$, the angular deflection at contact is

$$\theta - \theta_o = \frac{\delta}{\left[ l\left( \cos\theta \cot\frac{\pi}{n} - \sin\theta \right) \cos\left( \frac{\pi}{n} - \theta_{con} \right) + a(\cos\beta) \right]} \quad \textbf{(5.5)}$$

A rough approximation for the angle of deflection can be obtained by assuming

$$\theta_{con} \approx 0 \quad \textbf{(5.6)}$$

$$a \approx 2 r_{clutch} \sin\frac{\pi}{2n} \quad \textbf{(5.7)}$$

The accuracy of these approximations improves as the number of segments and the width of the slots decrease. Once $\theta$ is known, the factors $T_1$ and $T_2$ in the force equations are easily calculated.

Recall from Chapter 4,

$$\vec{F_o} + k(_1 + k_2)(\theta_o - \theta) + l\angle\left( \frac{\pi}{2} - \frac{\pi}{n} - \theta \right) \times \vec{F}_{So} \quad \textbf{(5.8)}$$

An examination of Equation (4.21) and Equation (4.22) shows that both remaining terms are linear with $\omega^2$. Since the only remaining unknown in Equation (4.20) is the square of the rotational velocity, the equation can be solved directly for $\omega^2$ at engagement. Substituting for $T_1$ and $T_2$ from equations (4.24) and (4.25) respectively, the expression for $\omega^2$ is

$$\omega^2 = -\left( \frac{(k_1 + k_2)(\theta_0 - \theta)\hat{k}}{\vec{r}_{cm} \times \frac{\vec{F}_o}{\omega^2} + \vec{l} \times \frac{\vec{F}_{So}}{\omega^2}} \right) \quad \textbf{(5.9)}$$

$\frac{\vec{F}_o}{\omega^2}$ and $\frac{\vec{F}_{So}}{\omega^2}$ are expressions for the $\vec{F}_o$ and $\vec{F}_{So}$, respectively, due to an $\omega^2$ of one. The spring constants $k_1$ and $k_2$ are found from Equation (A.3). Since both flexible segments go through the same angular deflection, the spring constants of both segments equally influence the engagement speed. Therefore, the relative stiffness of the two segments can be adjusted so that the operating stress in both segments is similar.

### 5.1.2 Initial Test Data

These formulas were applied to the four prototype polypropylene FOA clutches to predict the engagement speeds. The calculated engagement speeds are compared to the measured engagement speeds in Table 5-1. The table includes the average and range of the measured speeds. The predicted engagement speeds for two different values of the modulus of elasticity are included to show its influence on the engagement speed.

Polypropylene, from which the designs were manufactured, experiences significant stress relaxation. Additionally, the modulus of elasticity varies due to size,

**TABLE 5-1 Measured and predicted engagement values for FOA clutches.**

| Clutch Name | Average Measured Speed (rpm) | Range of Measured Speeds (rpm) | Predicted Speed (rpm) (E=165 ksi) | Predicted Speed (rpm) (E=140 ksi) |
|---|---|---|---|---|
| FOA #1 | 715 | 693-718 | 799 | 735 |
| FOA #2 | 477 | 292-497 | 517 | 475 |
| FOA #3 | 535 | 521-548 | 540 | 497 |
| FOA #4 | 502 | 474-520 | 574 | 532 |

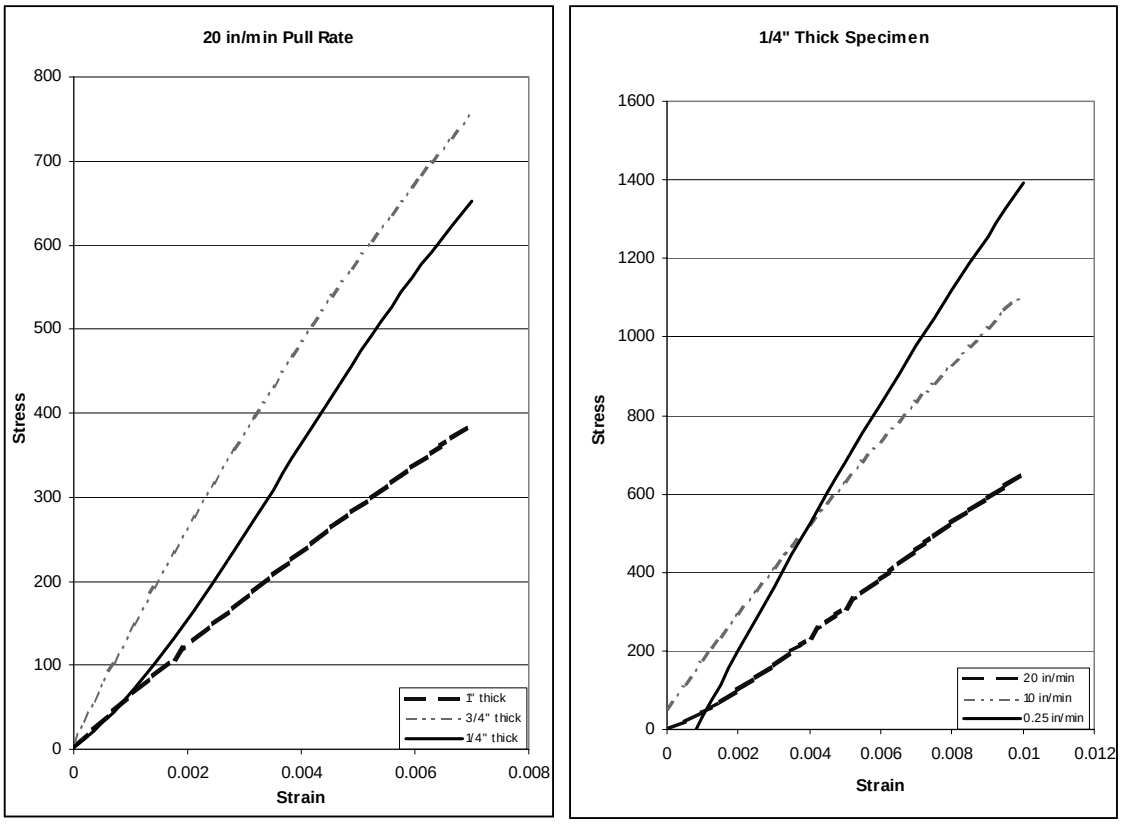


**Figure 5-2** Polypropylene stress strain curves for different specimen sizes and pull rates. The slope of the curves varies by a factor of two due to the variations in specimen size and pull rate (Cook & Parker, 1996).

temperature, loading rates, and many other factors. The material behavior is very nonlinear. Figure 5-2 shows the variation of measured stress strain curves for different pull speeds and specimen sizes. Due to this extreme variation, the predicted engagement speeds are shown using two different values for modulus of elasticity to calculate the spring constants in the model.

Table 5-1 shows that the range in the measured engagement speeds is large for FOA #2. One possible reason for this large variation is the existence of multiple stable configurations for the clutch. While the clutch is geometrically symmetric, random inputs may force it into other configurations that are also stable until the clutch begins contacting

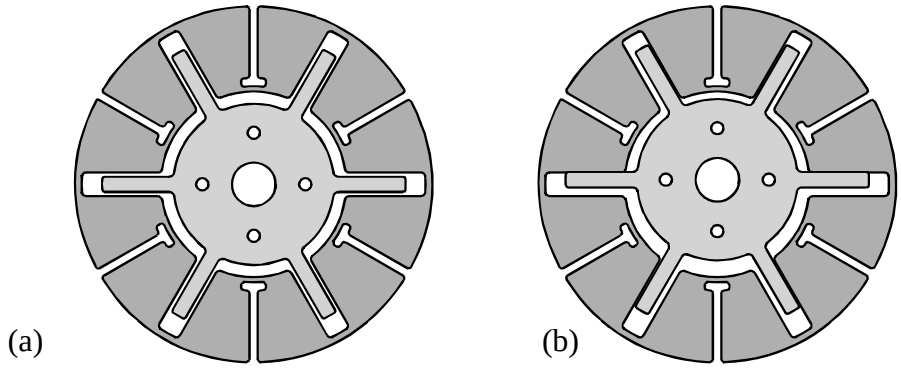


**Figure 5-3** (a) The assumed symmetrical position of the FOA clutch before engagement. The floating piece is centered on the hub with even spacing all the way around. (b) A likely configuration of the clutch before engagement. A non-symmetrical force such as gravity has caused the floating piece to rest against the hub on one side.

the drum. Once the clutch fully engages the drum, the circular drum should enforce geometric symmetry.

Figure 5-3 shows a likely non-symmetric configuration of the clutch. Under some operating conditions, the floating member may rest on one side of the hub as shown in Figure 5-3(b) rather than be centered on the hub as illustrated in Figure 5-3(a). Since the clearance between the hub and floating members is small (0.010-0.020 inches), the change in the applied forces should be small. However, for the tested clutches, this effect could reduce the clearance between the clutch and drum by twenty to forty percent. If the engagement model were applied with the clearance reduced by 0.015 inches, the engagement speed predictions for the prototype clutches would be reduced by 16.3 percent. The magnitude of this error depends on the relative size of the clearance between the clutch and drum and between the hub and floating member.

Other factors may contribute significant error as well. The largest factor is an irregularity in the outer diameter of the clutch after friction material is glued on the outside

edge. A variation of 0.025 inches in the gap between the clutch and drum could account for the systematic deviation from the predictions. Error might also be caused by a consistent tolerance error on the NC mill used to manufacture the clutches. The final dimensions are 0.002 inches below nominal for most clutches.

### 5.1.3 Engagement Speed Retest

An additional prototype was constructed to better test the validity of the engagement speed model by reducing several error sources. This prototype was produced from aluminum using wire EDM. The wire EDM was used to decrease the error due to machining tolerances and to reduce the radius sizes required for the tools. Error from stress relaxation in the polypropylene was eliminated by using aluminum. The stress relaxation in the aluminum should be minimal under test conditions.

Cotton webbing was glued on the contact surfaces of the aluminum clutch and it was tested using the same procedure as for the initial tests. The test was repeated five times. For each test, the engagement speed was determined by finding the roots of a quadratic fit to the clutch data. The average engagement speed was 844 rpm with a standard deviation of 30 rpm and a range of 75 rpm. The predicted engagement speed was 849 rpm. This represents an error of 0.5%.

The increased accuracy of the second test using higher machining tolerances and a material with a more constant modulus of elasticity supports the engagement speed model. This data suggests that most of the error in the initial tests is due to stress relaxation and machining tolerances.

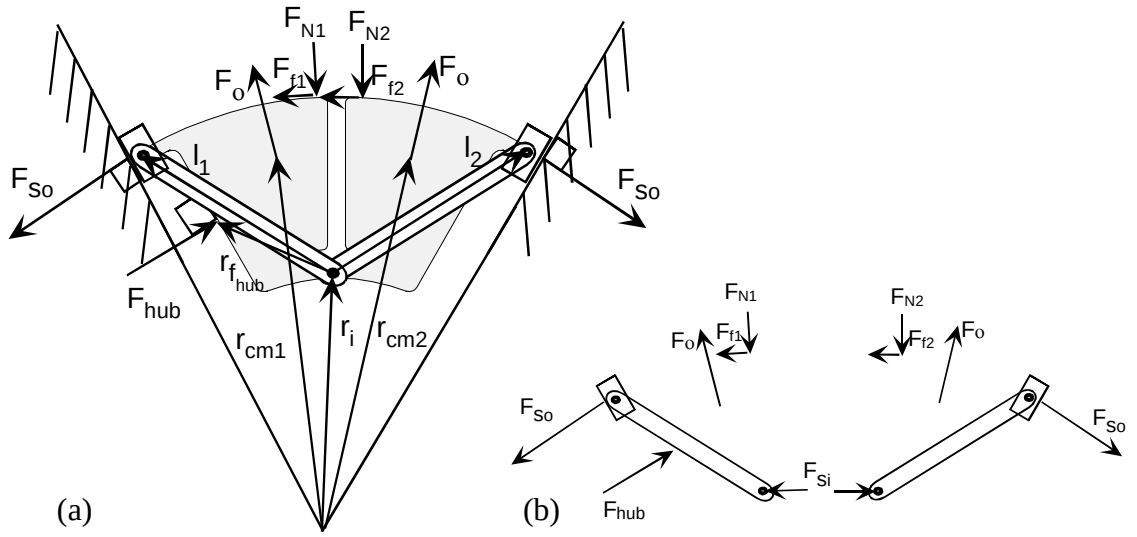


**Figure 5-4** Parameters used in calculating $T_b$ factor for the FOA clutches. (a) External forces and appropriate position vectors. (b) Free body diagrams of the two links.

## 5.2 FOA Torque Model

### 5.2.1 Equation Development

The $T_b$ value for the FOA clutches can be calculated using free-body diagrams of the two links that form a unit of symmetry for the clutch. Figure 5-4 explains the force and position vectors used in the model. The geometry of the two links is assumed to remain symmetric about the y-axis after contact. Reactions at the outer pin joints are assumed to be of equal magnitude and perpendicular to the plane on which the pin slides. The hub force acts at the tip of the hub and perpendicular to the face of the actual clutch segment. The geometrical symmetry of the clutch requires that the inner pin joint move along the y-axis. Since it moves like a slider, the reaction force at the pin is assumed to be normal to the plane of sliding motion. Given these assumptions, the unknown forces are the reactions at the outer slider, between the two links, and at the hub, and the normal forces

on both links. When calculating $T_b$, moments due to deflection of the compliant members are not included since $T_b$ represents the torque that would be transmitted if no springs were present.

The force equilibrium equations for both links and the moment equilibrium equation for link one are used to find the five unknowns. These five equations form the matrix equation

$$\begin{bmatrix} m\omega^2 r_{cm1x} \\ -m\omega^2 r_{cm1y} \\ (\vec{r}_{cm1} - \vec{r}_i\hat{j}) \times (m\omega^2 \vec{r}_{cm1}) \\ -m\omega^2 r_{cm2x} \\ -m\omega^2 r_{cm2y} \end{bmatrix} = \begin{bmatrix} f_{11} & 0 & f_{13} & f_{14} & -1 \\ f_{21} & 0 & f_{23} & f_{24} & 0 \\ f_{31} & 0 & f_{33} & f_{34} & 0 \\ 0 & f_{42} & 0 & f_{44} & 1 \\ 0 & f_{52} & 0 & f_{54} & 0 \end{bmatrix} \begin{bmatrix} F_{N1} \\ F_{N2} \\ F_{hub} \\ Fs_o \\ Fs_i \end{bmatrix} \quad \textbf{(5.10)}$$

where the elements of the matrix are:

$$f_{11} = (\sin\theta_{con} - \mu\cos\theta_{con}) \quad \textbf{(5.11)}$$

$$f_{13} = \cos\left(\frac{\pi}{n} + \theta - \theta_o\right) \quad \textbf{(5.12)}$$

$$f_{14} = \cos\frac{\pi}{n} \quad \textbf{(5.13)}$$

$$f_{21} = -(\cos\theta_{con} + \mu\sin\theta_{con}) \quad \textbf{(5.14)}$$

$$f_{23} = \sin\left(\frac{\pi}{n} + \theta - \theta_o\right) \quad \textbf{(5.15)}$$

$$f_{24} = \sin\frac{\pi}{n} \quad \textbf{(5.16)}$$

$$f_{31} = r_{drum}(-\sin\theta_{con}\hat{i} + \cos\theta_{con}\hat{j}) \times [(\sin\theta_{con} - \mu\cos\theta_{con})\hat{i} - (\cos\theta_{con} - \mu\sin\theta_{con})\hat{j}] \quad \textbf{(5.17)}$$

$$f_{33} = \vec{r}_{f_{hub}} \times \left(\cos\left(\frac{\pi}{n} + \theta - \theta_o\right)\hat{i} + \sin\left(\frac{\pi}{n} + \theta - \theta_o\right)\hat{j}\right) \quad \textbf{(5.18)}$$

$$f_{34} = \vec{l}_1 \times \left( \cos\frac{\pi}{n}\hat{i} + \sin\frac{\pi}{n}\hat{j} \right) \quad \textbf{(5.19)}$$

$$f_{42} = -(\mu \cos\theta_{con} + \sin\theta_{con}) \quad \textbf{(5.20)}$$

$$f_{44} = \cos\left(\pi - \frac{\pi}{n}\right) \quad \textbf{(5.21)}$$

$$f_{52} = \mu \sin\theta_{con} - \cos\theta_{con} \quad \textbf{(5.22)}$$

$$f_{54} = \cos\left(\pi - \frac{\pi}{n}\right) \quad \textbf{(5.23)}$$

The matrix equation is easily solved with standard methods. The torque output without any springs ($T_{ns}$) is

$$T_{ns} = \mu r_{drum}(F_{N1} + F_{N2}) \quad \textbf{(5.24)}$$

and the torque capacity is

$$T_b = \frac{T_{ns}}{\omega^2}10^6 = \frac{\mu r_{drum}(F_{N1} + F_{N2})}{\omega^2}10^6, \ \omega \text{ in rpm} \quad \textbf{(5.25)}$$

The torque output with springs is calculated from Equation (3.1).

### 5.2.2 Test Data

Table 5-2 summarizes the torque capacity ($T_b$) model predictions and measured values. All of the model predictions are within 10% of the measured values. The remaining variations are likely caused by variations in the coefficient of friction, outer diameter of the clutch with the friction material, or material density.

## 5.3 Other Design Issues

There are many important considerations in designing and developing centrifugal clutches. While this work does not undertake to analyze every important issue for the FOA clutches, the work does yield some insights into the areas of wear, material selection, and torque relationship to friction conditions. These insights are discussed in the following sections.

### 5.3.1 Wear

During starting and stopping, the centrifugal clutches are in sliding contact with the clutch drum. Over time, the sliding surfaces will abrade one another. The surface wear will influence the engagement speed and the torque capacity as the contact location

**TABLE 5-2 Measured and predicted torque capacities ($T_b$) for FOA clutches.**

| Clutch Name | Measured $T_b$ | Range of Measured Values | Predicted $T_b$ | Percent Error |
|---|---|---|---|---|
| FOA #1 | 2.20 | 0.156 | 2.32 | +5.5 |
| FOA #2 | 2.22 | 0.054 | 2.02 | -9.0 |
| FOA #3 | 2.60 | 0.051 | 2.57 | -1.2 |
| FOA #4 | 2.66 | 0.133 | 2.44 | -8.3 |

changes. The clutch response to wear can be divided into two main factors: relative speed of wear and sensitivity of clutch performance to wear.

*Relative Speed of Wear*

The speed of wear is primarily dependent on the particular materials in contact and the conditions at the contact point. This issue, material selection, will be considered in a later section. Over one hundred factors have been identified as important influences on wear. Some of the most important include contact pressure, slipping speed, temperature, and lubrication. Most of these factors are application specific. However, the relative contact pressure for different concepts can be compared.

Increasing contact pressure increases the rate of wear. Therefore, decreasing contact pressure is desirable. The contact pressure required to achieve a particular torque will decrease as the number of contacting points increases and the radius of the clutch drum increases. The FOA clutch prototypes had six to twelve contacting points compared to just two contacting points per clutch for the S-clutches. This would suggest that FOA clutches would have a longer wear life.

The contact pressure is also decreased by increasing the thickness of the clutch by a larger factor than the mass. If the profile remains the same while the thickness is increased, the torque capacity will increase while the contact pressure remains constant. The profile should be adjusted so that the mass does not increase as much as the contact area. This can be accomplished by drilling holes in the clutch shoes or otherwise decreasing the shoe mass.

*Performance Sensitivity to Wear*

As the contact surface wears, increased rotation of the clutch shoes is necessary for engagement. The mechanical advantage of the inertial force will also change as the location of the normal and friction forces changes. The increased rotation for engagement will always increase the speed at which the clutch engages. However, the mechanical advantage may increase or decrease. If the mechanical advantage increases with wear, the torque capacity will increase to compensate, at least partially, for the higher engagement speed.

The FOA clutch model indicates that as the contact location, indicated by $\theta_{con}$, moves with wear ($\theta_{con}$ increases), the torque capacity increases. The greater the difference between the engagement speed and the operating speed, the more significant the effect of the change in torque capacity. If the difference is large enough, the torque output would actually increase with wear. This is an important consideration in torque sensitive applications. Wear testing is necessary to understand the full effect of wear on FOA clutches.

### 5.3.2 Material Selection

Three important aspects of material selection are wear characteristics, centrifugal device suitability, and compliant mechanism suitability. Each of these issues is discussed briefly.

*Wear Characteristics*

The speed of wear is dependent on the particular materials in contact. Usually, in sliding contact between two different materials, one of the surfaces will lose more material than the other. Generally, the materials should be selected so that the clutch wears more

quickly than the drum. Testing will be necessary to verify that the clutch has sufficient wear life.

*Centrifugal Device Suitability*

Centrifugal devices are dependent on their mass for actuation force. Therefore, materials with higher densities will have larger actuation forces. Often, a clutch needs to fit within a limited space. If a higher density material is used, higher torque capacities are possible within the space constraints.

*Compliant Mechanism Suitability*

Generally, compliant mechanisms are required to sustain specific deflections rather than support a particular load. Therefore, the relative flexibility of the material is more important than the material's strength. The ratio of yield stress to the modulus of elasticity indicates the relative flexibility of a material. Higher ratios denote materials that can deflect farther before yielding (Howell, 1999).

In designing a centrifugal clutch, the magnitude of the modulus of elasticity is also important since the spring force varies linearly with modulus of elasticity. The relative magnitudes of the modulus of elasticity and the density will determine the relative magnitudes of the centrifugal actuating force and the restraining force of the compliant members. The relative magnitude limits the feasible combinations of engagement speed and operating speed and torque. The feasible design space of a clutch concept will be material dependent.

### 5.3.3 Torque Dependence on Coefficient of Friction

The torque output of the FOA clutches is not related linearly to the coefficient of friction. However, unlike the split arm clutches, the nonlinearity increases the dependence

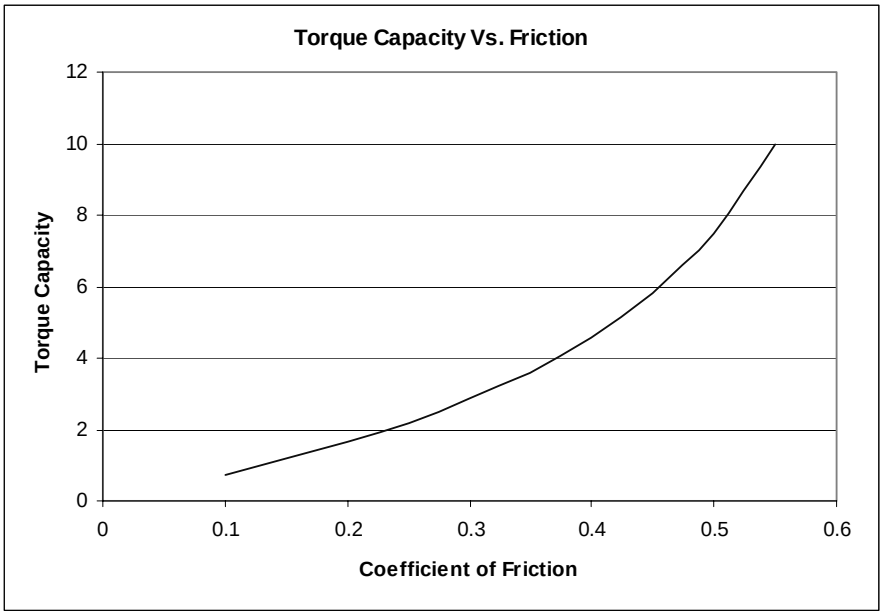


**Figure 5-5** Variation of torque capacity with the coefficient of friction for the FOA #3 clutch.

of torque output on the coefficient of friction. However, the nonlinearity is not extreme in the common ranges for the coefficient of friction. Figure 5-5 shows the torque capacity versus coefficient of friction for FOA #3. If the nominal coefficient of friction is 0.3, a deviation of ten percent in the coefficient of friction would cause a fifteen percent change in the torque capacity of the FOA #3. The FOA #4 clutch torque capacity would only vary twelve percent under the same conditions due to differences in its geometry.

The coefficient of friction is highly sensitive to operating conditions such as surface finish and particles between the mating surfaces. The nonlinearity of torque capacity with coefficient of friction serves to amplify this effect. This may make the FOA concept infeasible for some applications requiring precise torque outputs. However, the geometry of the clutches can be selected to minimize this effect and in many applications, the torque change with friction conditions is not a significant concern.

*Self-locking conditions*

In clutches and brakes with an aggressive, or self-energizing member, there is always a danger that the device could be self-locking. The friction forces on aggressive members apply moments that increase the normal force. This increases torque output, but if the actuating moment due to friction is larger than the opposing moment from the normal force(s), the clutch or brake will seize. This condition is called self-locking.

Self-locking disrupts the normal operating mode of a clutch and could destroy clutch, load, or other equipment in the powertrain. Therefore, it is vital that this condition be considered in designing any clutch with an aggressively oriented member. The FOA clutch has aggressively oriented members so it can experience self-locking conditions. However, each section of the FOA clutch has only one aggressive frictional force per section with two normal forces and one frictional force acting to oppose the aggressive force. This decreases the likelihood of achieving self-locking conditions with the FOA clutches.

Self-locking behavior is a function of geometry and the coefficient of friction. Self-locking friction conditions are easily identified from a graph of torque capacity versus the coefficient of friction. Such a graph can be created by varying the coefficient of friction input to the torque model. At the self-locking value of the coefficient of friction, the torque capacity curve is discontinuous. Figure 5-6 shows such a graph for the FOA #3. If the coefficient of friction is greater than or equal to the critical value, the clutch will lock. The approximate value of the coefficient of friction for self-locking behavior was identified for the prototype FOA geometries.

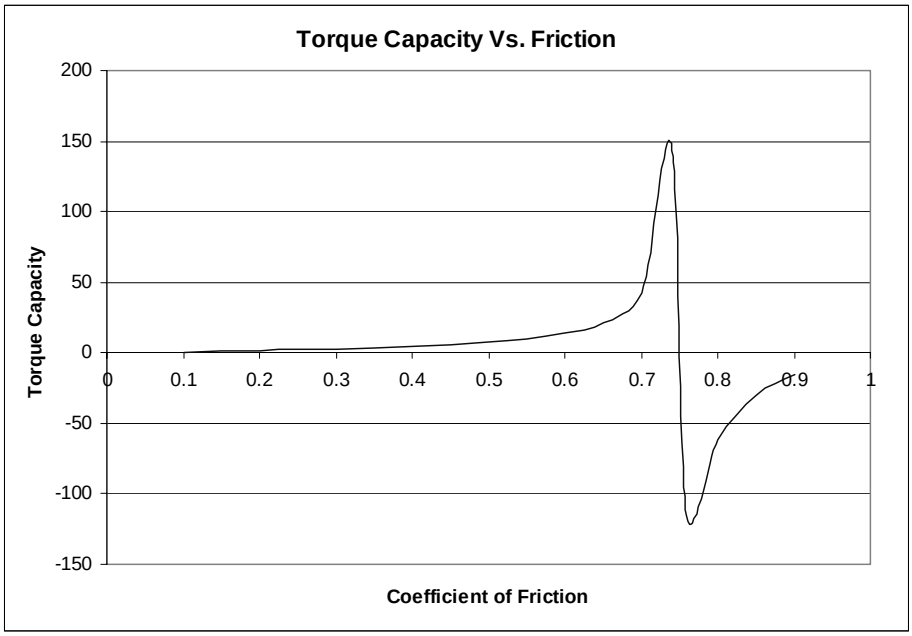


**Figure 5-6** Torque capacity versus coefficient of friction for the FOA #3 clutch. The torque capacity approaches infinity when the coefficient of friction is at the critical value for self-locking.

The approximate values of the self-locking coefficient of friction for each of the prototype FOA clutches is shown in Table 5-3. A good design will generally operate with a coefficient of friction well below the critical value for self-locking. It would also be advisable to estimate the critical value of the coefficient of friction after wear. Generally, the critical coefficient of friction decreases as the arm must rotate farther to contact the drum due to wear.

**TABLE 5-3 Critical Coefficient of Friction for Self-Locking**

| Clutch | $\mu_{crit}$ |
|---|---|
| FOA #1 | 0.95 |
| FOA #2 | 0.73 |
| FOA #3 | 0.75 |
| FOA #4 | 1.15 |

## 5.4 FOA Concept Enhancement

A major limitation of the FOA concept is the unpredictability observed in the engagement speed due to the clearance between the clutch and drum. A simple calculation showed that the clutch-hub clearance could decrease the engagement speed of the prototype clutches by over sixteen percent from ideal (page 90). The clutch performance might be improved by reducing or using the effect.

### 5.4.1 Reducing Effect of Clutch-Hub Clearance

If the effect of the clutch-hub clearance on engagement speed were reduced, this would increase the accuracy of the engagement speed model and the clutch reliability. This could be accomplished in at least four ways:

1. Modify the dimensions and reducing their tolerance. This could increase cost significantly.
2. Manufacture the hub larger than the floating member so that the floating member must be stretched for assembly. This would eliminate the clearance between the two pieces.
3. Place a layer of resilient material in several locations around the hub to fill the gap.
4. Increase the magnitude of the clearance between the clutch and drum relative to the clearance between the floating member and the hub. The amount of deviation in engagement speed due to the clutch-hub clearance is approximately equal to the square root of the ratio of the clutch-hub clearance to the clutch-drum clearance.

### 5.4.2 Using the Clutch-hub Clearance Effect

When the clutch assumes the non-symmetrical position shown in Figure 5-3(b), only one segment of the clutch engages initially. As the speed and the contact forces increase, more segments of the clutch will contact the drum until the clutch is in a symmetric configuration with all segments in contact with the drum. This effect might be adjusted or magnified to increase the starting smoothness of the FOA clutches.

**Figure 5-7** Two S-clutches from a Homelite Versatool string trimmer. The outer diameter of the clutches is 2.41 inches.

## 5.5 String Trimmer Design Example

String trimmers are common applications for low-cost centrifugal clutches. Many string trimmers already use an S-clutch, but may benefit from an FOA clutch. To show the advantages of an FOA clutch, the S-clutch of a Homelite VersaTool string trimmer was replaced with an FOA clutch. This trimmer actually uses a stack of two identical S-clutches each 1/8 inch thick shown in Figure 5-7. A potential advantage of the FOA clutch is the possibility of using just one 1/8 inch thick FOA clutch because of its higher torque capacity.

### 5.5.1 Design Requirements

The design requirements specified for the string trimmer example are engagement speed, operating speed, torque capacity, and maximum clutch diameter. The idle speed and operating speed parameters were measured for the trimmer. The torque capacity was estimated from the maximum torque capacity of the original S-clutch. Maximum diameter was determined from the size of the current clutch drum. The torque capacity ($T_b$) of the

existing S-clutch was estimated using the method outlined in “S-Clutch” on page 63. The values for the design requirements are shown in Table 5-4.

### 5.5.2 Proposed Design

The FOA concept was chosen because it ranked highest in the evaluation. A clutch with four symmetrical sections was selected for its higher torque capacity while maintaining a reasonable profile perimeter. The outer radius of the clutch was chosen as the outer radius of the S-clutch. The thickness was chosen as 1/8 inch thick to illustrate the potential space and weight savings of an FOA clutch. The design was manufactured from low carbon steel ($E \approx 30x10^6$) to match the S-clutch that it replaces. The exact parameters of the proposed design are listed in Table 5-5.

### 5.5.3 Design Predictions

The models were applied to the FOA design to verify that it would meet the required performance parameters. The calculated value of $T_b$ for a coefficient of friction of 0.25 is 0.718 in*lb/1000 rpm. The clutch was designed for a $T_b$ higher than required to allow for the nonlinearity in the torque output due to changes in the coefficient of friction. The model predicts an engagement speed of 6480 rpm. This is well above the engine idle

**TABLE 5-4 Design Requirements for FOA string trimmer clutch.**

| Requirement | Value |
|---|---|
| Idle Speed | 5500 RPM |
| Operating Speed | 9500 RPM |
| $T_b$ | 0.575 in*lb/1000 rpm |
| Max Thickness | 0.420 in |
| Shaft Diameter | 0.330 in |

speed to allow for no-load idling. Since the torque curve of the engine was not available to permit evaluation of the motor-clutch dynamics, this high engagement speed was selected to assure that the motor would have adequate torque at the engagement speed. However, this may reduce the output torque excessively. The estimated coefficient of friction for self-locking is 1.01. This value is much higher than the actual coefficient of friction and there should be no danger of self-locking even after significant wear. The design was manufactured using wire EDM. The prototype is shown in Figure 5-8(a).

### 5.5.4 Prototype Testing

The prototype string trimmer clutch was manufactured and installed in the string trimmer as shown in Figure 5-8(b). The string trimmer was reassembled and tested. For

**TABLE 5-5 Parameter values for String Trimmer FOA.**

| Clutch Parameters | Values |
|---|---|
| $R_{clutch}$ (in) | 1.205 |
| Arm Volume ($in^3$) | 0.01097 |
| $R_{cm}$(in) | 12.0 |
| $\theta_{cm}$ (deg) | 21.0 |
| $l_i$ (in) | 0.140 |
| $t_i$ (in) | 0.050 |
| $l_o$ (in) | 0.240 |
| $t_o$ (in) | 0.050 |
| $R_{drum}$ (in) | 1.2175 |
| n | 4 |
| t (in) | 0.125 |
| $R_i$ (in) | 0.484 |
| $\mu$ | 0.25 |

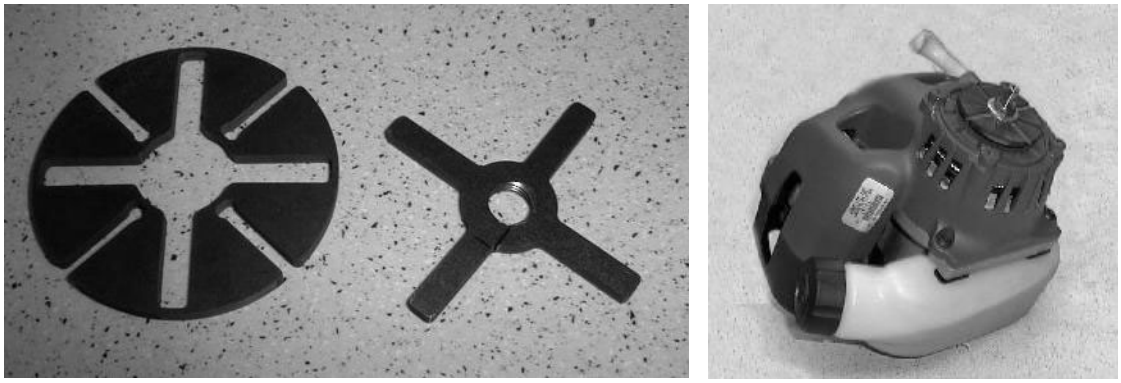

(a) (b)

**Figure 5-8** (a) The prototype FOA clutch for the string trimmer. (b) The FOA clutch mounted on the string trimmer.

the test, the string trimmer was used to cut lawn grass, edge along a sidewalk, and trim overhanging bush branches. The test was recorded using a video camera.

During the initial test, the FOA clutch performed adequately. The string would remain largely motionless while the clutch was idling. At times, the string did turn, but when the head was placed against the ground or some other resistance, the string stopped readily. During engagement, the engine sometimes stalled. This may be because the clutch engages too hard or at too low of a speed. The torque output from the string trimmer was adequate for all of the trimming tasks performed. It continued to trim very well even when the resistance was increased by pressing the head against the ground. When disassembling the trimmer after testing, grease from the shaft was found inside the clutch drum.

The test was repeated with a different mounting arrangement after it was noted that there was axial friction between the drum and the clutch mounting hardware. The mounting hardware was modified for the second test. With the modified mounting hardware, the clutch performance was greatly improved. At idle, the trimming head was

motionless and the engine accelerated the trimmer head to operating speed without difficulty.

For comparison, the FOA clutch was replaced with an S-clutch and the test was repeated. With the S-clutch, the engagement was smooth with a noticeable delay between engine and string acceleration. The torque seemed adequate for the tests performed.

### 5.5.5 FOA String Trimmer Conclusions

The FOA design performs the basic clutch functions in the string trimmer. The torque output of the clutch may have been affected significantly by the grease in the clutch drum but was still adequate for the tests performed. Due to the nonlinearity of the FOA torque with friction coefficient, the grease may have a much more significant torque capacity impact on the FOA clutch than the original S-clutch. Further work is also needed to improve the clutch-engine dynamics so that the clutch engages smoothly without overloading the engine and supplies all necessary torque.

More work is needed to fully assess the potential of the FOA clutch. The engagement speeds of the FOA clutch and the S-clutch should be compared. The engagement speed of the FOA clutch may need adjustment to better approximate the S-clutch performance. A wear test of the FOA clutch is also needed to see whether it can maintain performance for the required clutch life. If the clutch wear life is not adequate, a lining of friction material on the contact surface may be added to increase the life.

CHAPTER 6

# Conclusions and Recommendations

Compliant mechanism design techniques were used to analyze compliant centrifugal clutches and to develop effective new centrifugal clutch concepts. The pseudo-rigid-body model (PRBM), rigid-body replacement synthesis, force-deflection analysis, compliance potential evaluation, and compliant concept evaluation were employed in this work. These methods were instrumental in developing and modeling four novel compliant centrifugal clutch designs, modeling two existing designs, and identifying a concept with excellent potential for low-cost centrifugal clutch applications. Additional novel designs developed through this work also show good potential. All of the designs were prototyped and tested to measure their torque-speed relationships.

## 6.1 Contributions

### 6.1.1 Modeling Two Existing Clutches

Two existing compliant centrifugal clutches were modeled using the pseudo-rigid-body model. The PRBM permits quick evaluation of initial designs with much less time and cost than is possible with finite element methods. This simplicity will allow these

clutches to be applied to new applications with relatively little effort. The new model is a significant improvement over trial and error methods used previously.

### 6.1.2 Floating Opposing Arm (FOA) Clutch

After modeling, testing, and evaluation, the floating opposing arm (FOA) clutch emerged as the most promising clutch concept developed through this work. This clutch combines the high torque output of an aggressively oriented clutch shoe with the smoother starting of a non-aggressive shoe by connecting both together. This permitted an increase of over two hundred percent in torque capacity relative to existing compliant centrifugal clutches of the same size and material. The clutch also consists of a separate hub which transfers torque from the drive shaft to reduce force in the flexible segments. This increases the design space of the FOA clutches. The clutch also performs equally well when rotated either direction.

Models were developed for predicting the torque transfer and engagement speed of the clutch. These models successfully predicted the performance of the prototype clutches. Other design issues such as material selection and wear were discussed briefly. Finally, the FOA concept was designed and tested in a gasoline-engine-powered string trimmer. The test demonstrated that the FOA clutch has the potential to replace an existing compliant centrifugal clutch and reduce required space and material due to its higher torque capacity.

### 6.1.3 Split-Arm Clutch

The split-arm clutch is another novel design developed through this work. Preliminary tests show that the clutch can generate more torque than the existing compliant centrifugal clutch types for a given size and material. This clutch has the added

advantage of simulating flexible trailing shoe clutches but with a reduced part count. This clutch is only one piece. The primary advantage of this clutch is that it is less sensitive to changes in coefficient of friction than the other compliant designs. This allows the split-arm clutch to perform more consistently under varying friction conditions.

### 6.1.4 Demonstration of Compliant Mechanism Techniques

The whole of the work demonstrates many new methods for developing, analyzing, and evaluating compliant mechanisms. They were successfully integrated together to develop, analyze, and evaluate new design solutions to an old device: the centrifugal clutch. The new designs formulated through this work demonstrate clear advantages over the existing designs, both compliant and rigid-body.

## 6.2 Recommendations

### 6.2.1 Advance the Promising Novel Designs

As mentioned, several promising designs have been developed through this work. Preliminary analysis, modeling, and testing have been performed. However, further design, analysis, and testing is necessary to apply them to specific applications. The work to be done includes wear testing, fatigue testing, and material selection.

### 6.2.2 Apply the Clutch Concepts to Overspeed Brakes

By securing the clutch drum, a centrifugal clutch becomes an overspeed brake. Therefore, any of the designs discussed in this work might work well as an overspeed brake. However, a good centrifugal clutch is not always a good overspeed brake. Further work should be done to identify the characteristics of a good overspeed brake and evaluate the relative potential of the various clutch concepts as brakes.

### 6.2.3 Explore Other Centrifugal Clutch Concepts

There are always numerous solutions to a design problem. However, two promising solution classes have not yet been examined. These two design areas deserve further attention.

*Clutches with Reduced Torque at High Speed*

The torque output of centrifugal clutches increases with the square of the rotational velocity indefinitely. The only factor to limit torque output of many centrifugal clutches is the ultimate strength of the members carrying the load. However, even then, broken components of the clutch may wedge between the remaining clutch and the drum to continue transferring power. This effect can be very dangerous in many applications. If the clutch is accelerated beyond the normal operating speed, it may easily transmit dangerous amounts of torque that could damage other machinery or injure its operators.

Centrifugal clutches can be made with torque capacity that levels off or even decreases at excessive speeds. Such clutches have been developed already. One example is documented in Patent Number 4446954 (Weiss, 1984). This design is shown in Figure 6-1.

This clutch concept acts much like a normal clutch at lower speeds. It has a large mass that provides the centrifugal actuation force. It also has a smaller secondary mass located closer to the clutch center to limit its input force. However, the centrifugal force at the second mass has a high mechanical advantage. As the speed increases beyond the safe operating range, the force on the secondary mass increases until it disengages the clutch.

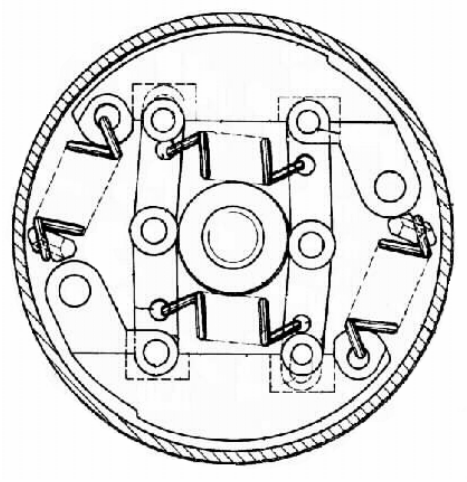

**Figure 6-1** A patented clutch concept that reduces torque at high speeds. The joints near the rotational axis are weighted to overcome the restraining springs to move outward at high speeds. Small forces at the weights have a large effect because the links are near toggle.

This idea should be examined and compliant configurations for achieving this behavior should also be sought. Designing a compliant clutch with this safety feature could drastically reduce the part count and cost of such a clutch. The patented design has at least seventeen parts. A compliant design might be possible with only one or two parts. This part count reduction is much more dramatic than the reduction achieved for the centrifugal clutches analyzed in this work.

*Improved Starting Smoothness Through a Multi-input Clutch*

This work did not present any methods for improving the starting smoothness of compliant centrifugal clutches. All of the clutches considered in this work maintained a quadratic relationship between torque and speed. However, several rigid-body designs were reviewed which had torque responses that were a function of both speed and time. The addition of time as a variable in the torque response increases starting smoothness. The time variability of those clutches was achieved by forcing fluid to flow through an

orifice. This principle could be applied to compliant clutches, but the additional complexity from incorporating a fluid would likely remove the cost advantage of compliant clutches.

A similar increase in starting smoothness could be achieved by adding a second input force to the mechanism that is proportional to the difference in the speeds of the driver and the driven (clutch and drum). This force would act against the energizing centrifugal force to limit torque output while there was a speed difference. When the difference in speeds is greatest, the limiting force would limit the torque the most. As the load approaches the input speed, the clutch would reach the operating torque as the second force went to zero. This transitory effect would slow the response of the clutch torque to changes in speed.

The second input force proportional to the speed difference might be created by means of a viscous friction between elements rotating at the two different speeds. Such a force could be generated by a bearing. One bearing race could be fixed to the drum and the other attached to an element of the clutch with significant mechanical advantage to limit the torque output. Such a clutch is illustrated in Figure 6-2(a). Figure 6-2(b) shows the PRBM for one half of the clutch and the opposing input forces that would increase its starting smoothness. The clutch arm is the same as for the $C^4$ design except that a second link is connected between the bearing and the clutch arm. This second link applies a force away from the clutch drum during start-up conditions.

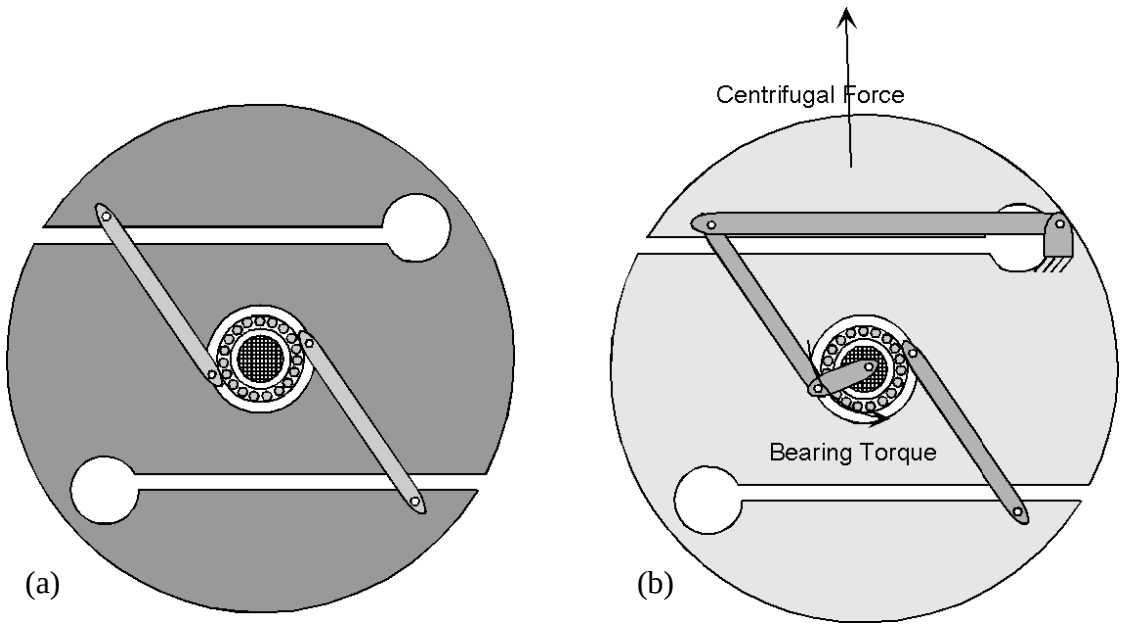


**Figure 6-2** (a) A clutch concept with improved starting smoothness. (b) A PRBM for half of the clutch showing the two counteracting input forces that would slow the clutch's torque response.

### 6.2.4 Improve Torque Model

The torque model for the clutches only includes two parameters, a torque capacity ($T_b$) and engagement speed. This model was satisfactory for most of the clutches, but some had linear terms that weren't accounted for by this model. A new model should be developed to better model these clutches.

## 6.3 Conclusion

This thesis demonstrates that compliant mechanism design methods can produce new design concepts, even for a simple, existing design challenge. This work has developed four original concepts that have several potential advantages beyond existing designs—FOA, GOA, Split-arm, and F1. The FOA design is particularly promising because it doubles torque capacity relative to the S-clutch, a commercial compliant design

currently produced, while maintaining reasonable manufacturability. This exercise in developing and analyzing new compliant solutions to a design problem demonstrates the value of the methods used—pseudo-rigid-body model, rigid-body replacement synthesis, force-deflection analysis, compliance potential evaluations, and compliant concept evaluation. In particular, this work shows that each of these methods, though developed individually for specific parts of the design process, can be unified into an effective development process.

# REFERENCES


Achi, P. B. U., 1986, “Design and Testing of an Automatic Clutch”, *Sadhana*, Vol. 9, No. 3, pp. 23-238.

Ananthasuresh, G.K., Kota, S. and Gianchandani, Y., 1994, “A Methodical Approach to the Design of Compliant Mechanisms,” *Solid-State Sensor and Actuator Workshop,* Hilton Head Island, South Carolina, pp. 189-192.

Ananthasuresh, G.K., and Kota, S., 1995, “Designing Compliant Mechanisms,” *Mechanical Engineering*, Vol. 117, No. 11, pp. 93-96.

Bisshopp, K.E. and Drucker, D.C., 1945, “Large Deflection of Cantilever Beams,” *Quarterly of Applied Mathematics*, Vol. 3, No. 3, pp. 272-275.

Boronkay, T., and Mei, C., 1970, “Analysis and Design of Multiple Input Flexible Link Mechanisms,” *Journal of Mechanisms*, Vol. 5, No. 1, pp. 29-49.

Berglund, M. D., 1998, “A Methodology for the Evaluation and Selection of Acceptable Design Concept Alternatives for Compliant Mechanisms,” M.S. Thesis, Brigham Young University, Provo, Utah.

Burns, R.H., 1964, “The Kinetostatic Synthesis of Flexible Link Mechanisms,” Ph.D. Dissertation, Yale University, New Haven, Connecticut.

Burns, R.H. and Crossley, F.R.E., 1968, “Kinetostatic Synthesis of Flexible Link Mechanisms,” ASME Paper No. 68-MECH-36.

Chase, T. R., Erdman, A. G., and Marier, G., 1991, “Design of an Improved Variable-Sheave V-Belt Drive,” *Mechanism and Machine Theory*, Vol. 26, No. 6, pp. 579-592.

Cook, B., and Parker, B. “Tensile Test Analysis of Polypropylene at Different Sizes and Pull Speeds”, Unpublished class project for Mechanical Engineering 352, December 1996.

Cragun, R., Jensen, B., Lyon, S. M. Unpublished research data used with permission of authors, 1998.

Dekhanov, V. I. and Makhtinger, V. L., 1987, "Variable Drive of Centrifugal Separator," *Chemical and Petroleum Engineering*, Vol. 23, No. 1-2, pp. 3-5.

Derderian, J.M., Howell, L.L., Murphy, M.D., Lyon, S.M., and Pack, S.D., 1996, "Compliant Parallel-Guiding Mechanisms," *Proceedings of the 1996 ASME Design Engineering Technical Conferences*, 96-DETC/MECH-1208.

Dietzsch, G., Frers, G., Henning, K., and Lux, H., 1977, "Rotor for Centrifugal Clutch," United States Patent No. 4016964.

Edwards, B.T., Jensen, B. D., and Howell, L.L., 1996, "A Pseudo-Rigid-Body model for Functionally Binary Pinned-Pinned Segments Used in Compliant Mechanisms," *Proceedings of the 1999 ASME Design Engineering Technical Conferences*, DETC99/DAC-8644.

Erdman, A.G. and Sandor, G.N., 1997, *Mechanism Design: Analysis and Synthesis*, Vol. 1, 3rd Ed., Prentice Hall, New Jersey.

Frecker, M.I., Kikuchi, N., and Kota, S., 1996, "Optimal Synthesis of Compliant Mechanisms to Meet Structural and Kinematic Requirements - Preliminary Results," *Proceedings of the 1996 ASME Design Engineering Technical Conferences*, 96-DETC/DAC-1497.

Frecker, M.I., Kota, S., and Kikuchi, N., 1997, "Use of Penalty Function in Topological Synthesis and Optimization of Strain Energy Density of Compliant Mechanisms," *Proceedings of the 1997 ASME Design Engineering Technical Conferences*, DETC97/DAC-3760.

Gandhi, M. and Thompson, B., 1980, "The Finite Element Analysis of Flexible Components of Mechanical Systems Using a Mixed Variational Principle," ASME Paper No. 80-DET-04.

Goodling, E. C., 1974, "Fighting High Energy Costs with Centrifugal Clutches," *Machine Design*, Vol. 46, No. 23, pp. 119-124.

Goodling, E. C., 1977, "Trailing Shoe Type Centrifugal Clutch-Design Principles and Characteristics," *ASME Papers*, DET-126.

Gorski, W., 1976, "A Review of Literature and a Bibliography on Finite Elastic Deflections of Bars," *Transactions of the Institute of Engineers, Australia, Civil Engineering Transactions*, Vol. 18, No. 2, pp. 74-85.

Gruden, J. M., and Brooks, R. B., 1999, "Centrifugal Clutch for Power Door Locks" United States Patent No. 5862903.

Hartenberg, R.S. and Denavit, J., 1964, *Kinematic Synthesis of Linkages*, McGraw-Hill Book Company, New York, New York.

Her, I., 1986, "Methodology for Compliant Mechanism Design," Ph.D. Dissertation, Purdue University, West Lafayette, Indiana.

Hill, T.C., Midha, A., 1990, "A Graphical User-Driven Newton-Raphson Technique for use in the Analysis and Design of Compliant Mechanisms," *Journal of Mechanical Design*, Trans. ASME, Vol. 112, No. 1, pp. 123-130.

Howell, L.L. and Midha, A., 1994a, "A Method for the Design of Compliant Mechanisms with Small-Length Flexural Pivots," *ASME Journal of Mechanical Design*, Vol. 116, No. 1, pp. 280-290.

Howell, L.L. and Midha, A., 1994b, "The Development of Force-Deflection Relationships for Compliant Mechanisms," *Machine Elements and Machine Dynamics*, DE-Vol. 71, 23rd ASME Biennial Mechanisms Conference, pp. 501-508.

Howell, L.L., Midha, A., and Murphy, M.D., 1994a, "Dimensional Synthesis of Compliant Constant-Force Slider Mechanisms," *Machine Elements and Machine Dynamics*, DE-Vol. 71, 23rd ASME Biennial Mechanisms Conference, pp. 509-515.

Howell, L.L. and Midha, A., 1995a, "Parametric Deflection Approximations for End-Loaded, Large-Deflection Beams in Compliant Mechanisms," *ASME Journal of Mechanical Design*, Vol. 117, No. 1, pp. 156-165.

Howell, L.L. and Midha, A., 1995b, "Determination of the Degrees of Freedom of Compliant Mechanisms Using the Pseudo-Rigid-Body Model Concept," *Proceedings of the Ninth World Congress on the Theory of Machines and Mechanisms*, Milano, Italy, Vol. 2, pp. 1537-1541.

Howell, L.L. and Midha, A., 1995c, "The Effects of a Compliant Workpiece on the Input/Output Characteristics of Rigid-Link Toggle Mechanisms," *Mechanism and Machine Theory*, Vol. 30, No. 6, pp. 801-810.

Howell, L.L, Midha, A., and Norton, T.W., 1996, "Evaluation of Equivalent Spring Stiffness for Use in a Pseudo-Rigid-Body Model of Large-Deflection Compliant Mechanisms," *ASME Journal of Mechanical Design*, Vol. 118, No. 1, pp. 126-131.

Howell, L.L. and Midha, A., 1996a, "Parametric Deflection Approximations for Initially Curved, Large-Deflection Beams in Compliant Mechanisms," *Proceedings of the 1996 ASME Design Engineering Technical Conferences*, 96-DETC/MECH-1215.

Howell, L.L. and Midha, A., 1996b, “A Loop-Closure Theory for the Analysis and Synthesis of Compliant Mechanisms,” *Journal of Mechanical Design*, March 1996, Vol. 118, pp. 121-125.

Howell, L., 1999, “Compliant Mechanisms,” Notes for MeEn 538, Brigham Young University, Provo, Utah.

Jensen, B., 1998, “Identification of Macro- and Micro- Compliant Mechanism Configurations Resulting in Bistable Behavior,” M.S. Thesis, Brigham Young University, Provo, Utah.

Kellerman, R. and Fischer, J. L., 1976, “Centrifugal Clutch with One Piece Rotor,” United States Patent No. 3945478.

Kramer, M., Schmid, W., and Cramer, H., 1982, “Electric Centrifugal Switch,” United States Patent No. 4315118.

Mettlach, G.A. and Midha, A., 1996, “Using Burmester Theory in the Design of Compliant Mechanisms,” *Proceedings of the 1996 ASME Design Engineering Technical Conferences*, 96-DETC/MECH-1181.

Midha, A., Norton, T.W., and Howell, L.L., 1994, “On the Nomenclature, Classification, and Abstractions of Compliant Mechanisms,” *Journal of Mechanical Design*, March 1994, Vol. 116, pp. 270-279.

Moore, H. O., 1980, “Centrifugal Switch,” United States Patent No. 4182952.

Murphy, M.D., Midha, A., and Howell, L.L., 1994a, “Type Synthesis of Compliant Mechanisms Employing a Simplified Approach to Segment Type,” *Mechanism Synthesis and Analysis*, DE-Vol. 70, 23rd ASME Biennial Mechanisms Conference, pp. 51-60.

Murphy, M.D., Midha, A., and Howell, L.L., 1994b, “Methodology for the Design of Compliant Mechanisms Employing Type Synthesis Techniques with Example,” *Mechanism Synthesis and Analysis*, DE-Vol. 70, 23rd ASME Biennial Mechanisms Conference, pp. 51-60.

Nielson, A.J. and Howell, L.L., 1998, “Compliant Pantographs via the Pseudo-Rigid-Body Model,” *Proceedings of the 1998 ASME Design Engineering Technical Conferences*, DETC98/MECH-5930.

Norton, R. L., 1999, *Design of Machinery, Second Edition*, McGraw-Hill Inc., Boston.

Norton, R. L., 1998, *Machine Design: An Integrated Approach*, Prentice-Hall, New Jersey, 959-988.

Orthwein, W.C., 1986, *Clutches and Brakes Design and Selection,* Marcel Dekker, Inc., New York, New York.

Opdahl, P.G., 1996, "Modeling and Analysis of Compliant Bi-Stable Mechanisms Using the Pseudo-Rigid-Body Model," M.S. Thesis, Brigham Young University, Provo, Utah.

Opdahl, P.G., Jensen, B.D., and Howell, L.L., 1998, "An Investigation into Compliant Bistable Mechanisms", ASME 25th Biennial Mechanisms Conference, to be held in Atlanta, Georgia, August 1998.

Parkinson, M.B., Howell, L.L, and Cox, J., 1997, "A Parametric Approach to the Optimization-Based Design of Compliant Mechanisms," *Proceedings of the 1997 ASME Design Engineering Technical Conferences*, DETC97/DAC-3763.

Paul, B., 1979b, *Kinematics and Dynamics of Planar Machinery,* Prentice-Hall, Inc., Englewood Cliffs, New Jersey.

Roach, G.M., 1998,"An Investigation of Compliant Over-Running Ratchet and Pawl Clutches," M.S. Thesis, Brigham Young University, Provo, Utah.

Roach, G. M. and Howell, L. L., 1999, "Evaluation and Comparison of Alternative Compliant Over-running Clutch Designs," 1991 ASME Design Engineering Technical Conferences, DETC99/DAC-8619.

Roach, G.M., Lyon, S.M., and Howell, L.L., 1998, "A Compliant, Over-Running Ratchet and Pawl Clutch with Centrifugal Throw-Out," *Proceedings of the 1998 ASME Design Engineering Technical Conferences,* DETC98/MECH-5819.

Salamon, B.A., 1989, "Mechanical Advantage Aspects in Compliant Mechanisms Design," M.S. Thesis, Purdue University, West Lafayette, Indiana.

Salamon, B.A. and Midha, A., 1998, "An Introduction to Mechanical Advantage in Compliant Mechanisms," *Journal of Mechanical Design,* Trans. ASME, Vol. 120, No. 2, pp. 311-315.

Saxena, A., Kramer, S. N., 1998, "A Simple and Accurate Method for Determining Large Deflections in Compliant Mechanisms Subjected to End Forces and Moments", *Journal of Mechanical Design,* Trans. ASME, Vol. 120, No. 3, pp. 392-400. Erratum Vol. 121, No. 2, pp. 194.

Sevak, N.M., McLarnan, C.W., 1974, "Optimal Synthesis of Flexible Link Mechanisms with Large Static Deflections," AME Paper No. 74-DET-83.

Shigley, J. E. and Mischke, C. R., 1989, *Mechanical Engineering Design,* Fifth Edition, pp. 627-664.

Shimizu, Y. and Ogura, M., 1987, "Centrifugal Clutch Instantly Engageable and Disengageable," United States Patent No. 4687085.

Shoup, T.E., 1972, "On the Use of the Nodal Elastica for the Analysis of Flexible Link Devices," *Journal of Engineering for Industry,* Trans. ASME, Vol. 94, No. 3, pp. 871-875.

Shoup, T.E. and McLarnan, C.W., 1971a, "A Survey of Flexible Link Mechanisms Having Lower Pairs," *Journal of Mechanisms,* Vol. 6, No. 3, pp. 97-105.

Shoup, T.E. and McLarnan, C.W., 1971b, "On the Use of the Undulating Elastica for the Analysis of Flexible Link Devices," *Journal of Engineering for Industry,* Trans ASME, pp. 263-267.

Shultz, W. L., 1996, "Bi-directional centrifugal clutch," United States Patent No. 5503261.

South, D.W. and Mancuso, J.R., 1994, *Mechanical Power Transmission Components,* Marcel Dekker, Inc., New York, New York.

St. John, R. C., 1975, "Centrifugal Clutch Has Gentle Touch," *Power Transmission Design,* Vol. 17, No. 3, pp. 40-42.

St. John, R. C., 1979, "Centrifugal Clutch Basics," *Power Transmission Design,* Vol. 21, No. 3, pp. 52-55.

Suchdev, L. S. and Campbell, J. E., 1989, "Self Adjusting Rotor for a Centrifugal Clutch," United States Patent No. 4821859.

Timoshenko, S. and Young, D.H., 1948, *Advanced Dynamics,* 1st Edition, McGraw-Hill Book Company, Inc., New York.

Timoshenko, S. and Young, D.H., 1951, *Engineering Mechanics,* 3rd Edition, McGraw-Hill Book Company, Inc., New York.

Town, H. C., 1988, "Clutches for Machine Control," *Power International,* Vol. 34, No. 401, pp. 247-249.

Weiss, H., 1984, "Centrifugal Clutch for Power Saws," United States Patent No. 4446954.

Young, W.C., 1989, *Roark's Formulas for Stress & Strain*, McGraw-Hill Book Company, New York, New York.

APPENDIX A

# Pseudo Rigid Body Model

Due to the importance of the Pseudo Rigid Body Model (PRBM) in this work, the basics of this method will be reviewed here. This appendix is not meant to be a full treatment of the subject but merely a brief overview. As such, no theoretical development or testing validation will be presented here. Some material may also be treated in only its simplest cases. Where further information or clarification is desired, consult the appropriate technical literature (Howell, 1999).

## A.1 PRBM Overview

The premise of the PRBM is that most compliant mechanisms behave sufficiently similarly to a particular rigid-body mechanism that most analysis can be performed on the corresponding rigid-body mechanism. Indeed, many of the segment types commonly encountered in compliant mechanisms are very well approximated by known configurations of rigid-body mechanisms. Remarkably, this equivalence holds up throughout all of the kinematic properties such as displacement, velocity, acceleration, and energy storage.

This model then permits analysis and design of compliant mechanisms using the techniques developed for rigid-body mechanisms. This opens a rich toolbox of analysis and synthesis methods. In designing a mechanism, the rough design can be generated using the PRBM and these rigid-body tools. Then, a more exact analysis and design cycle can be executed, if necessary, using other tools such as nonlinear finite element analysis to see a more exact solution for the kinematics or to look at the stresses in the design.

The basics of the PRBM consist of a series of rules for converting specific compliant segment types into equivalent rigid-body links. These rules can be easily inverted to find a compliant segment type that will approximate a rigid-body link. These rules in their simplest forms will be presented here.

A consistent set of parameters will be used where possible. Force loads will be parameterized as a vertical load $P$ and a horizontal load $nP$. The horizontal and vertical coordinates of the beam tips will be given by $a$ and $b$ respectively. For most segments, a pseudo-rigid-body angle ($\Theta$) will be defined that denotes the angle of the pseudo rigid link used in the model to approximate the deflection of a compliant member. In some cases, the pseudo-rigid-body angle ($\Theta$) deviates from the actual angle of the flexible beam tip ($\theta_o$) for some compliant segment types.

## A.2 Small Length Flexural Pivot

A small length flexural pivot is a relatively short segment of a link that is significantly more flexible than the remainder of the link, as shown in Figure A-1. The conditions for classification as a small length flexural pivot may be expressed as

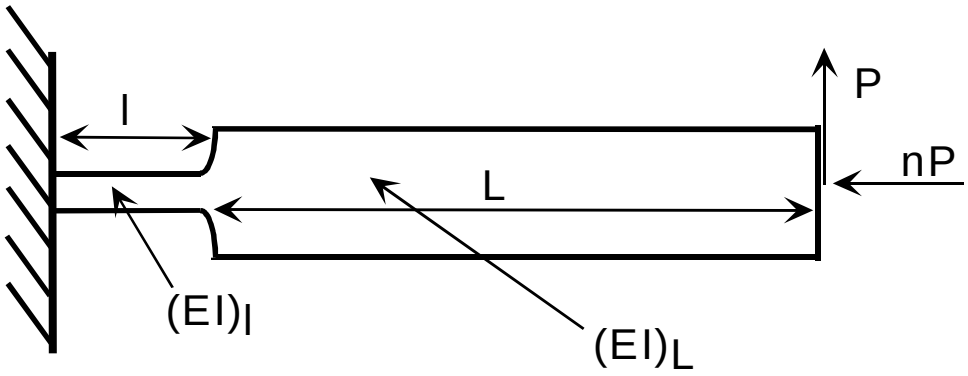


**Figure A-1** A small length flexural pivot.

$$L \gg l \tag{A.1}$$

$$(EI)_L \gg (EI)_l \tag{A.2}$$

Generally, accuracy is sufficient when $L$ is at least ten time larger than $l$. When this link is loaded with a force at its end, the variation in moment across the flexible section is small. This small variation allows the deflection of the flexible segment to be accurately approximated by applying a constant moment equal to the average moment applied to the segment. Moreover, the linear deflections of the flexible beam tip are insignificant compared to the beam angle in determining the path of the end of the rigid segment. This segment type then can be modeled as a rigid link pinned to a another rigid link with this pseudo pin located at the center of the flexible segment. This pin is called the characteristic pivot. The angle of the rigid segment, the pseudo-rigid-body angle ($\Theta$), is equal to the angle of the end of the flexible beam. The model is illustrated in Figure A-2.

The energy required to deflect the flexible segment is modeled by a torsional spring placed at the characteristic pivot. The spring constant is derived from the equations for deflection of a moment loaded cantilever beam. The spring constant and the torque required to rotate the rigid link to $\Theta$ are given by the following equations:

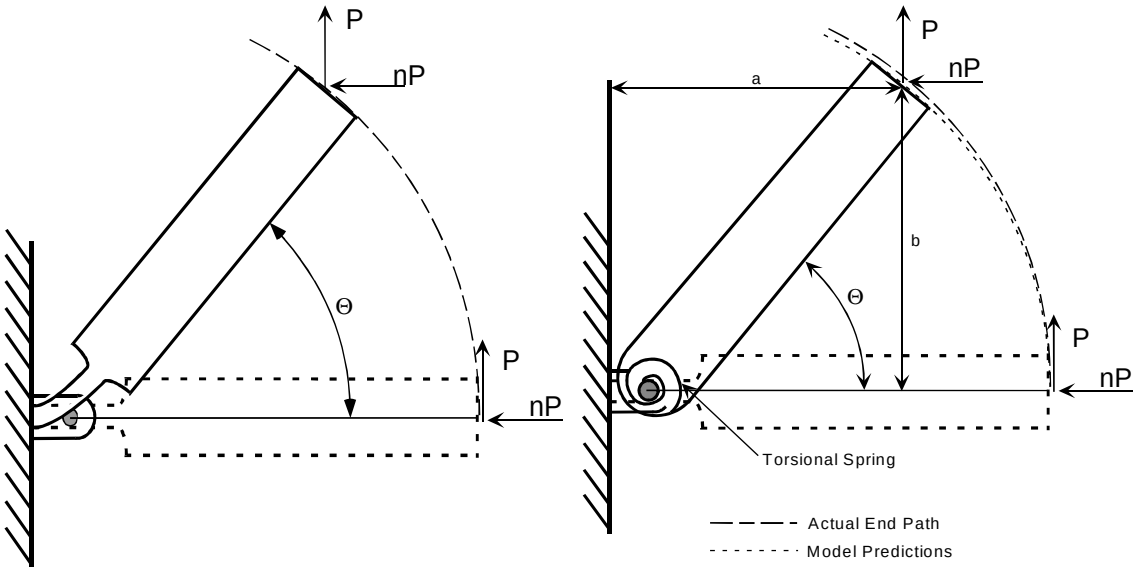


**Figure A-2** A small length flexural pivot in its undeflected and deflected positions and the corresponding pseudo rigid body model.

$$K = \frac{(EI)_l}{l} \tag{A.3}$$

$$T = K\Theta \tag{A.4}$$

The coordinates of the end of the beam can be solved for directly from this approximation. In their nondimensional form, the x and y coordinates are respectively,

$$\frac{a}{l} = \frac{1}{2} + \left(\frac{L}{l} + \frac{1}{2}\right)\cos\Theta \tag{A.5}$$

$$\frac{b}{l} = \left(\frac{L}{l} + \frac{1}{2}\right)\sin\Theta \tag{A.6}$$

Stress in the flexible segment must also be considered. If the force on the free end is parameterized as a vertical component ($P$) and a horizontal component ($nP$), then the stress at the top and bottom of the beam at the base of the cantilever is

$$\sigma_{top} = \frac{-(Pa + nPb)c}{I} - \frac{nP}{A} \quad \textbf{(A.7)}$$

$$\sigma_{bot} = \frac{(Pa + nPb)c}{I} - \frac{nP}{A} \quad \textbf{(A.8)}$$

where $c$ is the distance to the outer fiber of the flexible segment from the neutral axis.

Due to the large deflections, some solutions of these equations can require the solution of nonlinear equations. Generally, solving for the angle of deflection from a force input will require an iterative solution. When the pseudo-rigid-body angle is known ($\Theta$), the solutions are generally linear.

In some cases, the section properties of the small length flexural pivot are such that the force required to deflect the beam is negligible. In these cases, the torsional spring at the characteristic pivot can be neglected if there are other sources of significant potential energy. These segments are called living hinges.

## A.3 Cantilever Beam with Force at Free End

There is also a pseudo-rigid-body model for a cantilever of uniform cross section and linear material properties loaded by a force at the free end that accurately reflects its large deflection behavior. Under large deflections, the tip of a cantilever beam traces out a nearly circular arc. This is the basis of the pseudo rigid body model of a cantilever beam with a force at the free end. The center of the arc is defined as the segment *characteristic pivot.* The distance of the characteristic pivot from the free end is given by a *characteristic radius factor* ($\gamma$), where $\gamma l$ is the *characteristic radius*, the radius of the circular arc approximating the path of the beam tip. These parameters are illustrated in Figure A-3.

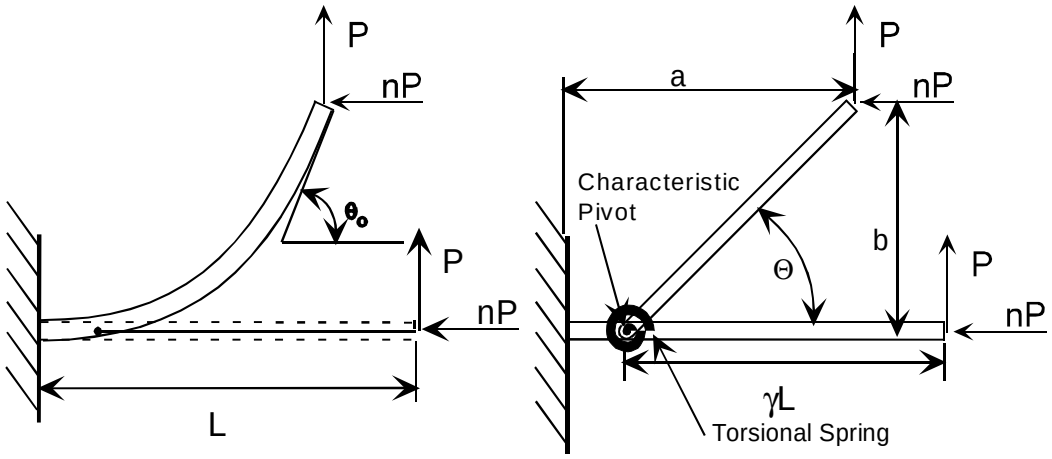


**Figure A-3** A cantilever beam with end forces and its pseudo rigid body model. Both are shown in their deflected and undeflected positions.

The value of the characteristic radius factor is a function of the direction of the force loading. This can be expressed as a function of $n$ as follows:

$$\gamma = 0.841655 - 0.0067807n + 0.000438n^2; \quad (0.5 < n < 10.0) \qquad \textbf{(A.9)}$$

$$\gamma = 0.852144 + -0.0182867n; \quad (-1.8316 < n < 0.5) \qquad \textbf{(A.10)}$$

$$\gamma = 0.912364 + 0.0145928n; \quad (-5 < -1.8216) \qquad \textbf{(A.11)}$$

These values of $\gamma$ will approximate the end deflection of the beam accurately for beam end deflection angles from 75 to 150 or more degrees for values of $n$ greater than zero. A graph of the values of $\gamma$ with respect to $n$ shows that the value of $\gamma$ is relatively constant across most values of $n$. For values of $n$ between -0.5 and 1.0,

$$\gamma_{avg} \approx 0.85 \qquad \textbf{(A.12)}$$

The torsional spring constant that models the energy storage of the flexible beam is given as

$$K = \gamma K_\Theta \frac{EI}{l} \quad \textbf{(A.13)}$$

$$K_\Theta \approx 2.65 \quad \textbf{(A.14)}$$

where $K_\Theta$ is termed the stiffness coefficient. More exact value of $K_\Theta$ are available from (Howell,1999), but this is sufficiently accurate for most purposes. The error in $K_\Theta$ increases more rapidly than the error in beam path with increasing $\Theta$. This means that path approximations are significantly more accurate than force and potential energy approximations as the amount of deflection increases.

The deviation between $\Theta$ and the actual beam end angle ($\theta_o$) is nearly linear for a given value of $n$. The relationship between the two angles may be approximated as

$$\theta_o = c_\theta \Theta \quad \textbf{(A.15)}$$

$$c_\theta \approx 1.24 \quad \textbf{(A.16)}$$

The value of $c_\theta$, the parametric angle coefficient, varies between 1.256 and 1.179. Exact values for different values of $n$ are available from Howell, 1995a.

Stress calculations are the same as for the small length flexural pivot and equations (A.7) and (A.8) apply.

## A.4 Cantilever Beam with End Moment Loading

End moment loaded cantilever beams can be modeled using the same approach as was used on force loaded cantilever beams. Reference Figure A-4 for a graphical representation of an cantilever beam with an end moment and its pseudo rigid body model. The appropriate characteristic radius factor is

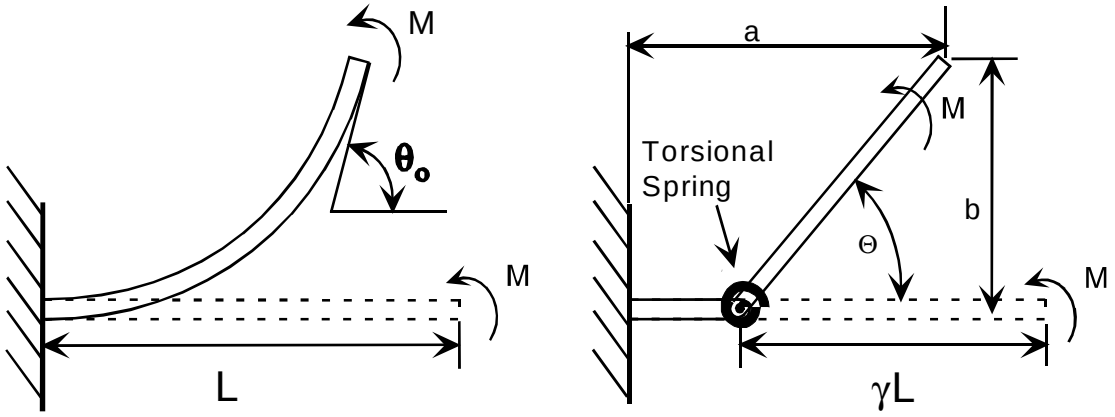


**Figure A-4** A cantilever beam with an end moment load is shown with its corresponding pseudo rigid body model.

$$\gamma = 0.7346 \quad \textbf{(A.17)}$$

This results in error less than 0.5% in the deflection path approximation for end angles less than 124.4 degrees. The parametric angle coefficient is

$$c_\theta = 1.5164 \quad \textbf{(A.18)}$$

and the stiffness coefficient is

$$K_\Theta = 2.0643 \quad \textbf{(A.19)}$$

The resulting spring constant is given by equation (A.13). Equations (A.5) to (A.8) from the small length flexural pivot still apply to the beam tip locations and stress calculations.

APPENDIX B

# Experiment Data

This appendix includes graphs of data taken for this work. Not all of the test data is included, but representative plots are shown for every class of clutch tested. Calibration data and summaries of the bearing torque data are included.

## B.1 Calibrations

### B.1.1 Torque Sensor

The torque sensor was a TQ103-125 from Omega Engineering Incorporated with a range from -125 inch pounds to +125 inch pounds. The calibration from the sensor manufacturer is

$$T = (K_1 + K_2 Output)Output \quad \textbf{(2.1)}$$

where

$$K_1 = 55.9306 \quad \textbf{(2.2)}$$

$$K_2 = 0.11771 \quad \textbf{(2.3)}$$

$Output$ is expressed in millivolts output per volt excitation and $T$ is in inch pounds. The manufacturer guarantees that the sensor is accurate to within 0.37% of full scale torque. The gauge's full scale torque is 125 inch pounds. The output from the torque sensor was then input to a signal conditioning circuit. The primary purpose of this circuit was to scale the output for computer sampling. The gain of the circuit was 532, and the excitation voltage was 10.0 volts. Thus, in terms of the voltage read from the computer ($V_c$), the torque is

$$T = (1.0513x10^{-2} + 2.2126x10^{-5}V_c)V_c \quad \textbf{(2.4)}$$

**B.1.2 Tachometer**

The tachometer was a Maxon DC motor. The motor was mounted in the lathe so that it was driven at the same speed as the clutch and the voltage output of the motor was measured. A 0.1 micro-farad capacitor was placed in parallel with the voltage measurement to protect the computer data acquisition system from voltage extremes.

The tachometer was calibrated by mounting the motor shaft in a lathe and fixing the motor body with the tailstock. The lather was cycled through its speed range. At each speed, the voltage out of the motor the lathe speed were measured. The data is recorded in Table B-1.The data was fit with a line to relate voltage and speed. The relationship was

$$RPM = 718.6681V \quad \textbf{(2.5)}$$

where $RPM$ is the speed in revolutions per minute and $V$ is the voltage out of the motor.

## B.2 Friction Coefficient

The friction coefficient of cotton webbing on steel was measured as described in 3.3.1 “Test Setup” . The average measured value of $\mu$ was 0.276. Due to the potential for error and variability, this value was rounded to two significant figures. The torque models were verified using 0.28 for $\mu$ .

## B.3 Bearing Torques

Bearing torque is the torque applied to the torque sensor due to the friction in the bearings mounting the clutch drum on the driving shaft. The bearing torque was measured

**TABLE B-1. Tachometer Calibration Data**

| Speed (RPM) | $V_{out}$ Tachometer |
|---|---|
| 367 | 0.511 |
| 674 | 0.939 |
| 866 | 1.206 |
| 1039 | 1.450 |
| 1170 | 1.631 |
| 1229 | 1.712 |
| 1333 | 1.858 |
| 1498 | 2.085 |
| 915 | 1.275 |
| 830 | 1.155 |
| 680 | 0.947 |
| 742 | 1.036 |
| 640 | 0.890 |
| 587 | 0.818 |
| 521 | 0.726 |
| 383 | 0.533 |
| 328 | 0.456 |
| 240 | 0.335 |

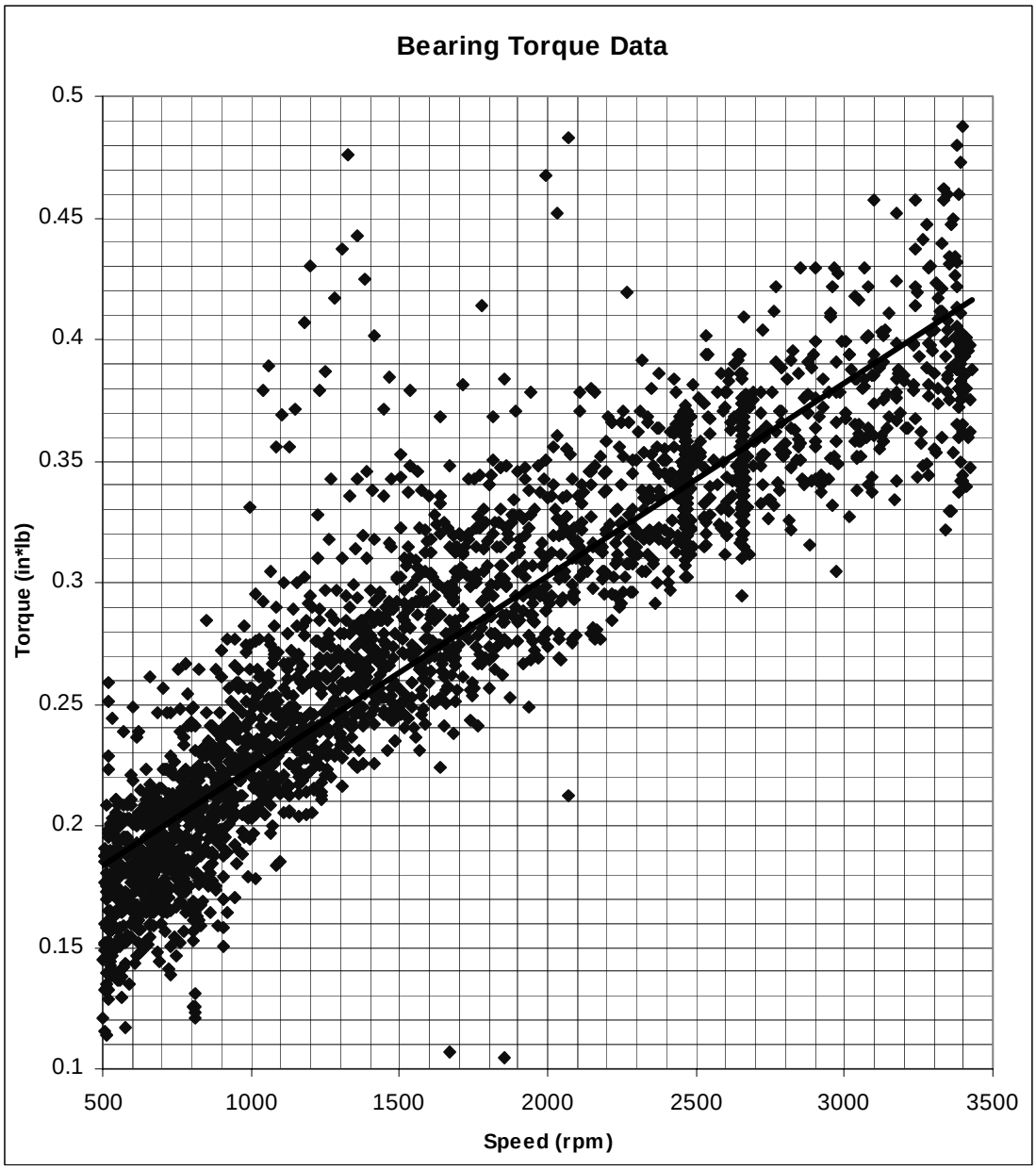


**Figure B-1** Bearing torque data from six tests. The solid line is the best-fit line for the bearing data used for subtracting off the bearing torque.

numerous times. A representative group of bearing torque tests are shown in Figure B-1.

This data was fit with the linear equation

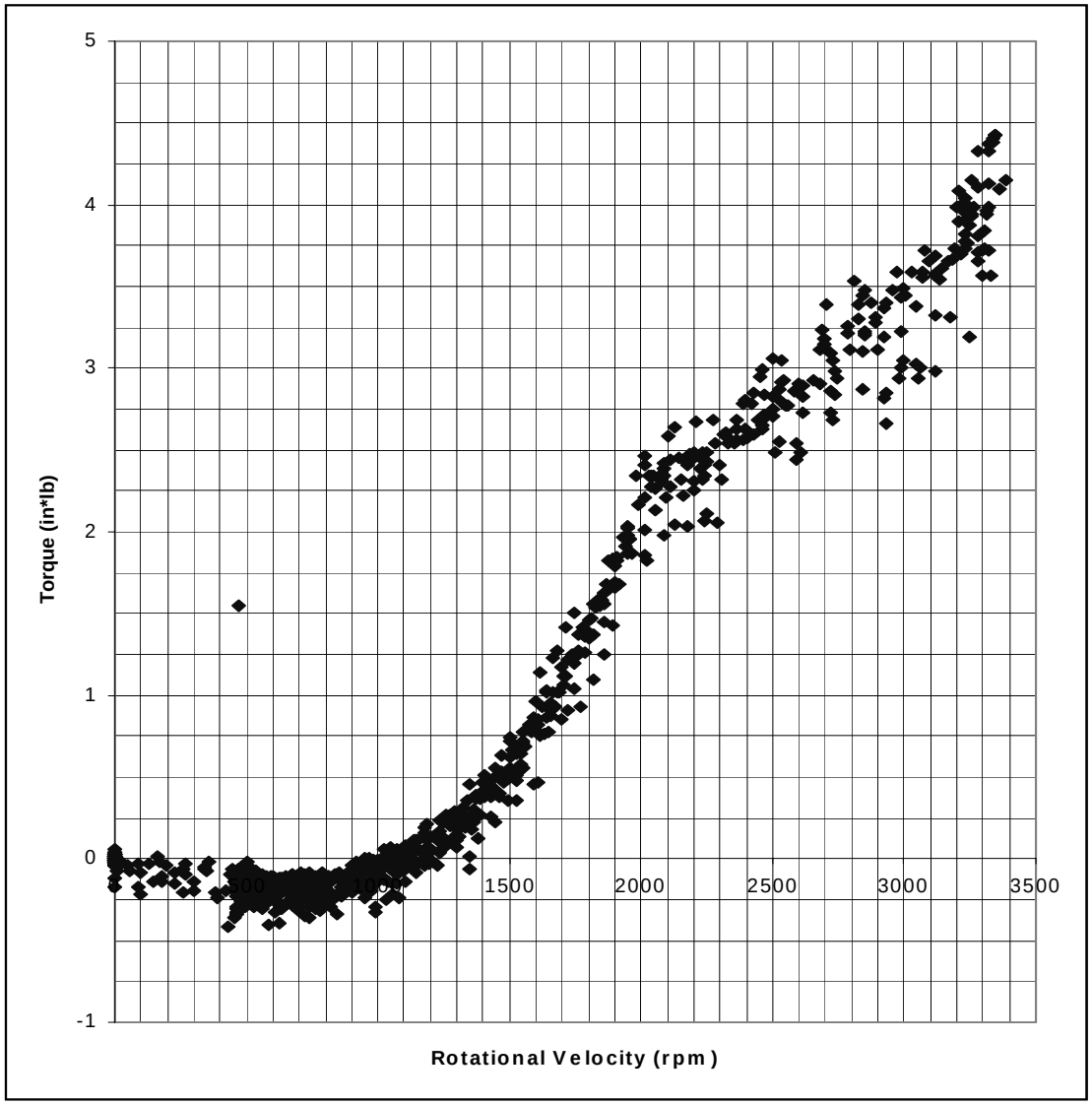


**Figure B-2** Bearing data with unusual values. The peak values are far in excess of the expected torques for the bearings.

$$T_b = 7.931x10^{-5} + 0.144 \quad \textbf{(2.6)}$$

This function was subtracted from all of the measured torque values to approximate the actual bearing torque.

In two tests, the bearing torque deviated substantially from this behavior as shown in Figure B-2. The two tests were not taken sequentially but were almost identical. After

this behavior was noted, efforts were made to replicate it, but to no avail. It is probable, the there was a problem in the setup that caused this phenomena because the measured torques are well above reasonable expectations.

## B.4 Oscillations in Test Setup at Start-up

The torque-speed data sets for several of the clutches show several high readings near 500 rpm. These readings are due to oscillations as play in the measurement system was absorbed.

During the tests, the lathe would immediately accelerate to approximately 500 rpm. Bearing torque and the clutch torque, if the clutch was engaged at this speed, were then applied. The torque loads would move the drum until it absorbed the play in the connections between the drum and the torque gauge. If the applied torques were low at the speed, the drum would oscillate briefly causing several high torque measurements.

This phenomena was observed most in the FOA clutch measurements.

## B.5 Conventional Compliant Centrifugal Clutch ($C^4$)

There were three prototypes of the $C^4$ clutches. A representative data set for each clutch is shown.

### B.5.1 $C^4$ #1

Data is shown in Figure B-3 on page 139.

### B.5.2 $C^4$ #2

Data is shown in Figure B-4 on page 140.

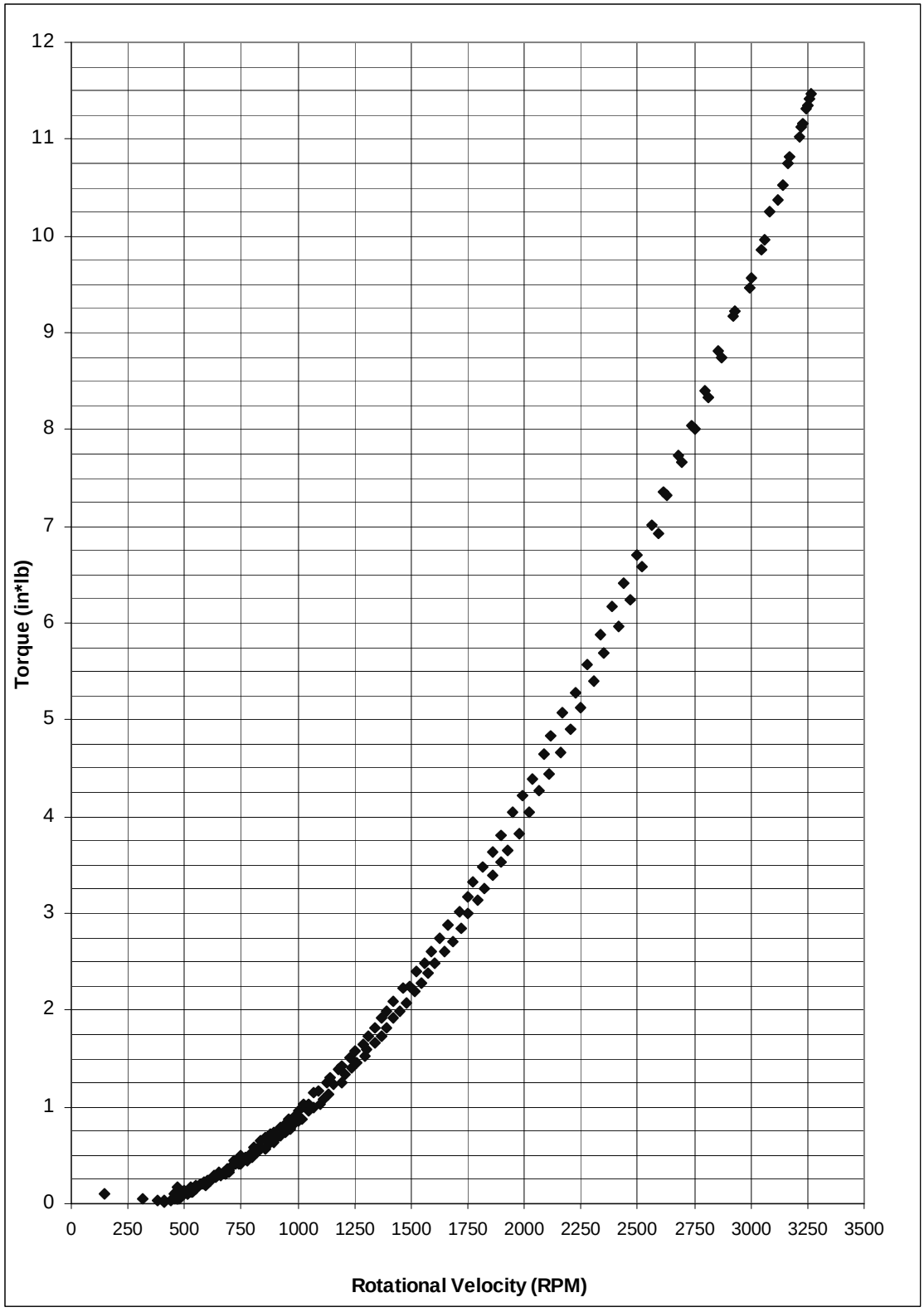


**Figure B-3** Experimental Data for $C^4$ clutch #1.

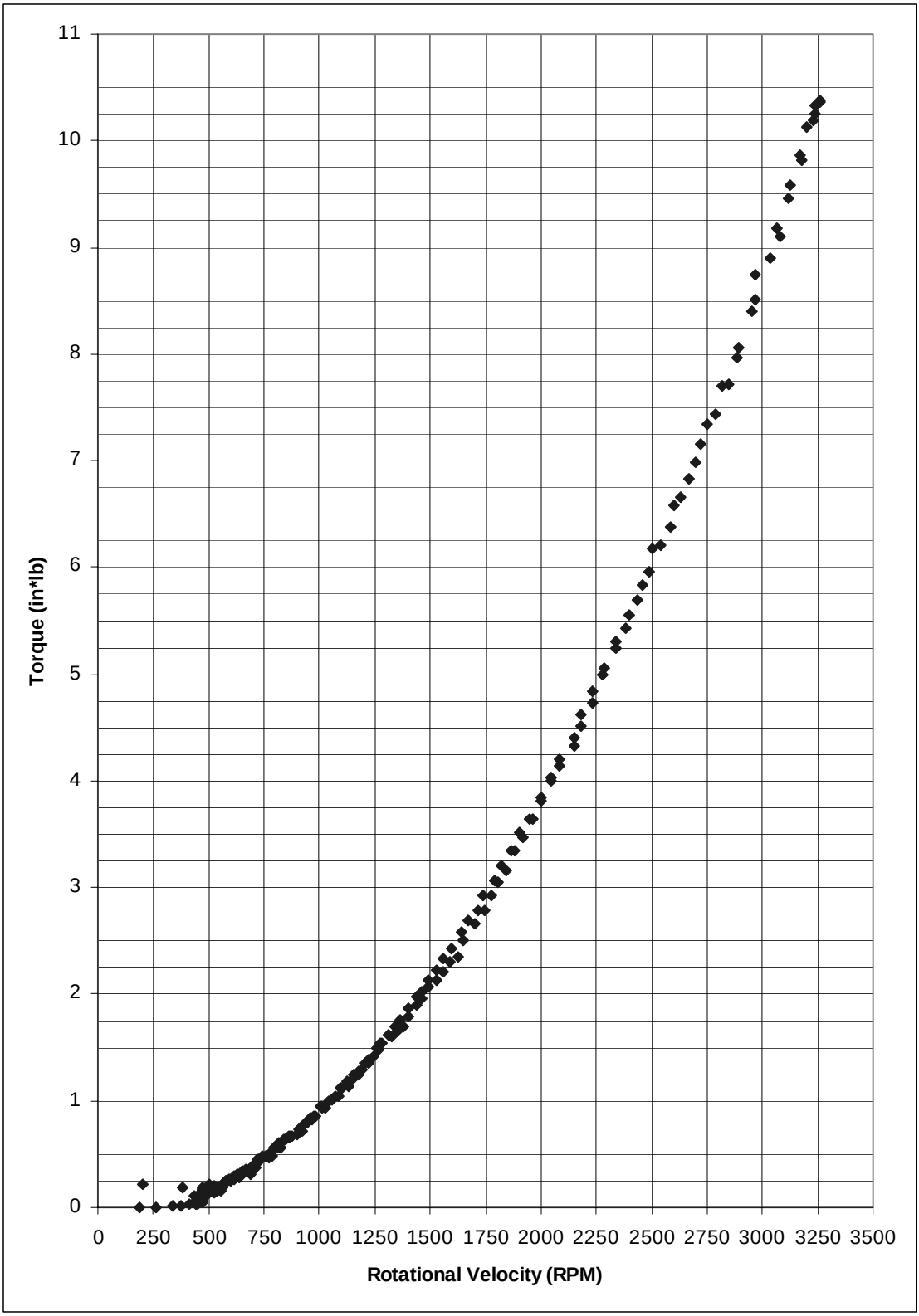


**Figure B-4** Test data for $C^4$ clutch #2.

### B.5.3 $C^4$ #3

Data is shown in Figure B-5 on page 142.

## B.6 S-clutch

### B.6.1 S-clutch #1

Data is shown in Figure B-6 on page 143.

### B.6.2 S-clutch #2

Data is shown in Figure B-7 on page 144.

## B.7 F1 Clutch

### B.7.1 F1 clutch #1

Data is shown in Figure B-8 on page 145.

## B.8 Floating Opposing Arm (FOA) Clutch

### B.8.1 FOA #1

Data is shown in Figure B-9 on page 146.

### B.8.2 FOA #2

Data is shown in Figure B-10 on page 147.

### B.8.3 FOA #3

Data is shown in Figure B-11 on page 148.

### B.8.4 FOA #4

Two very different sets of results were obtained from this clutch. Initially, the data shown in Figure B-12 on page 149 was obtained. The torque capacity calculated from this data is 3.44 in*lb/1000 rpm. However, this was far from the model predictions. A second

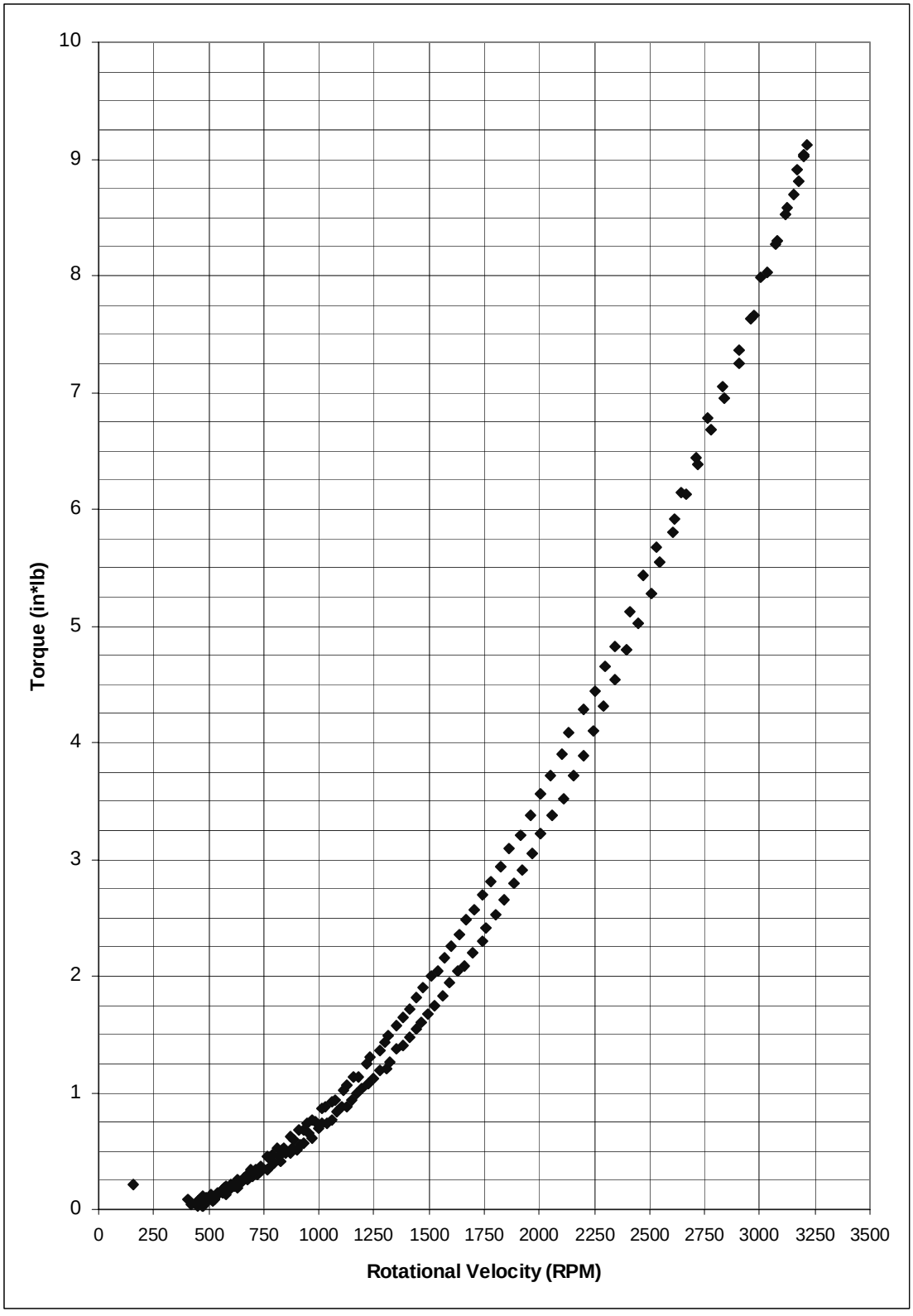


**Figure B-5** Test data for $C^4$ clutch #3.

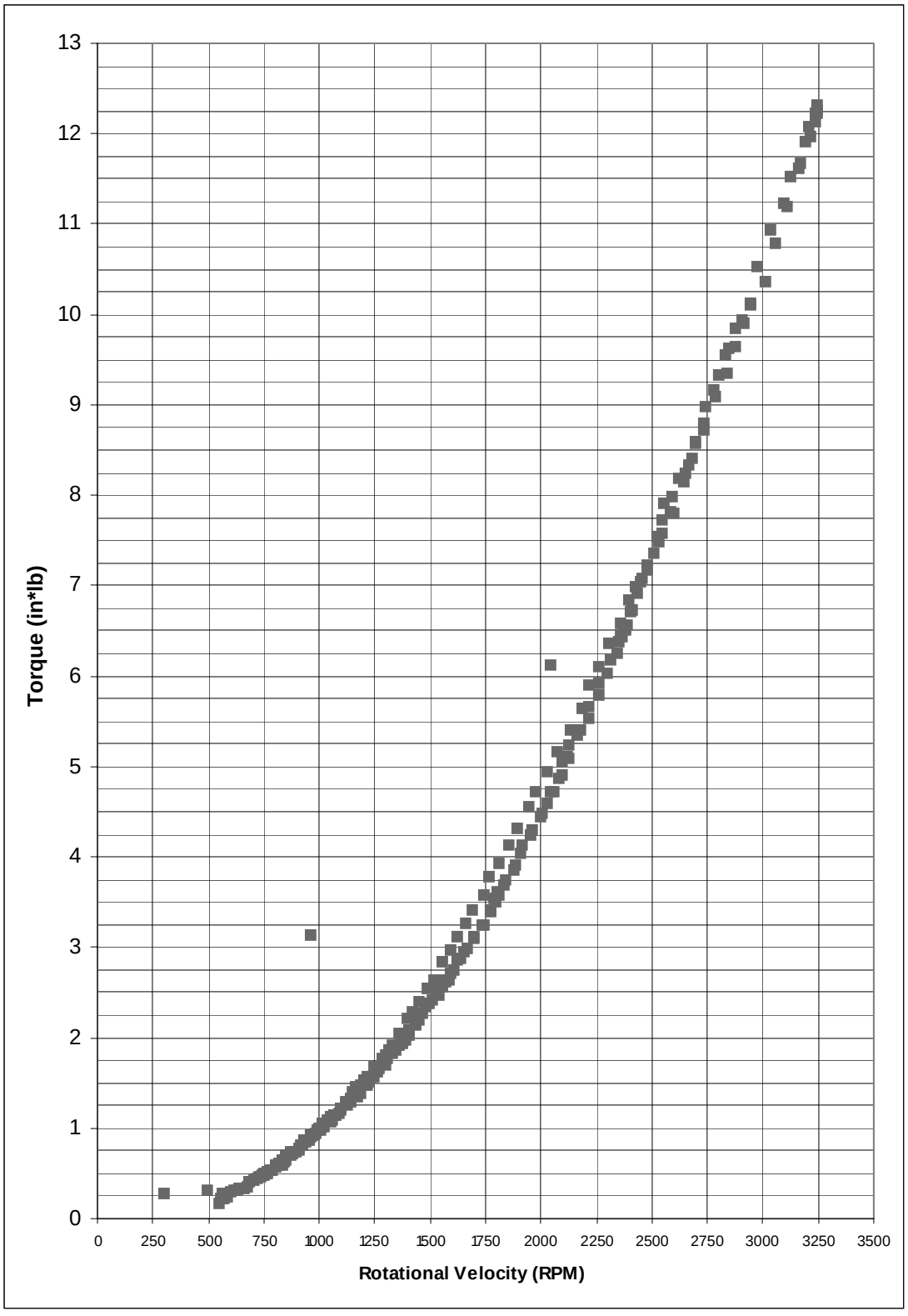


**Figure B-6** S-clutch #1 data.

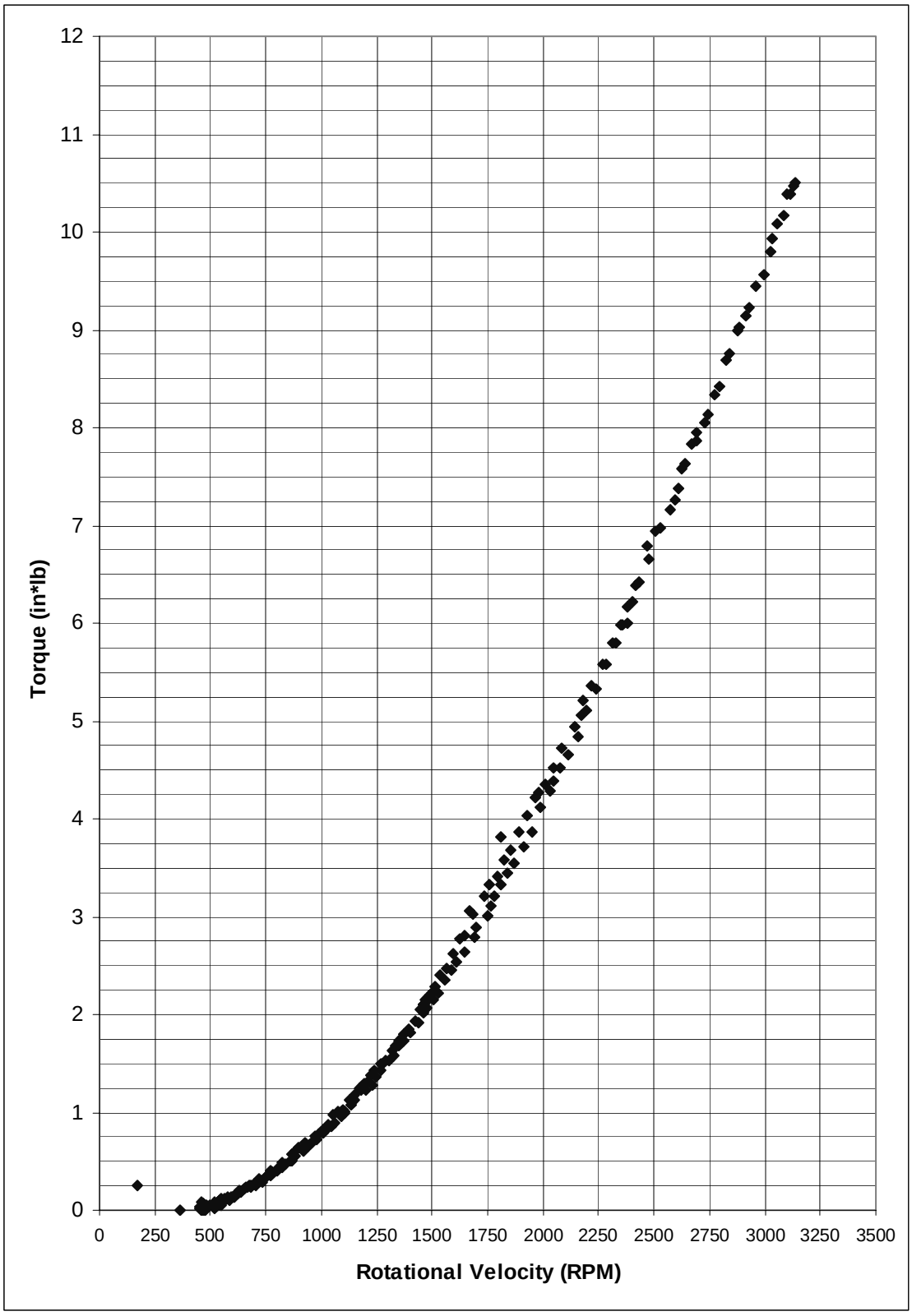


**Figure B-7** S-clutch #2 data.

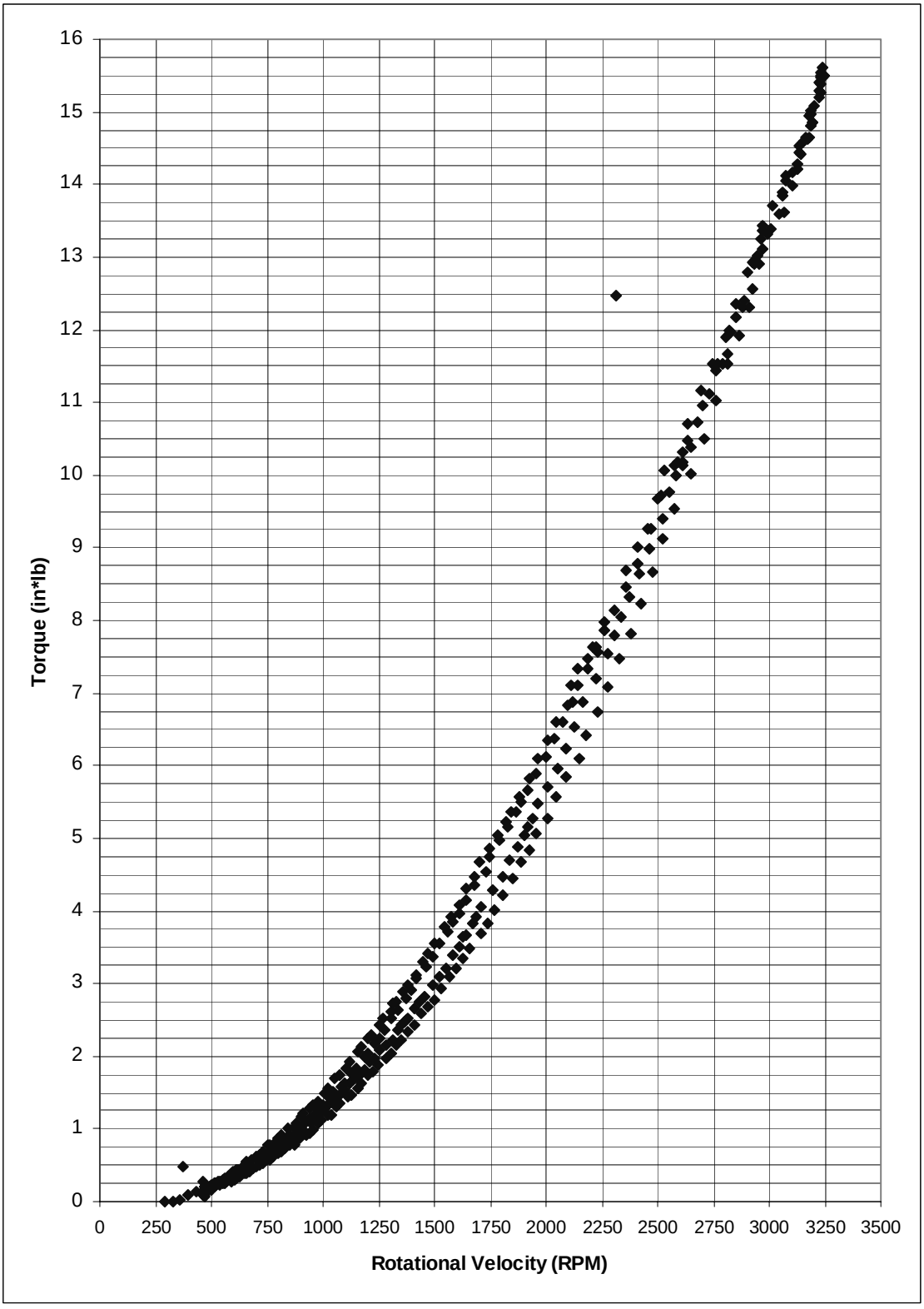


**Figure B-8** F1 clutch #1 data from two speed cycles.

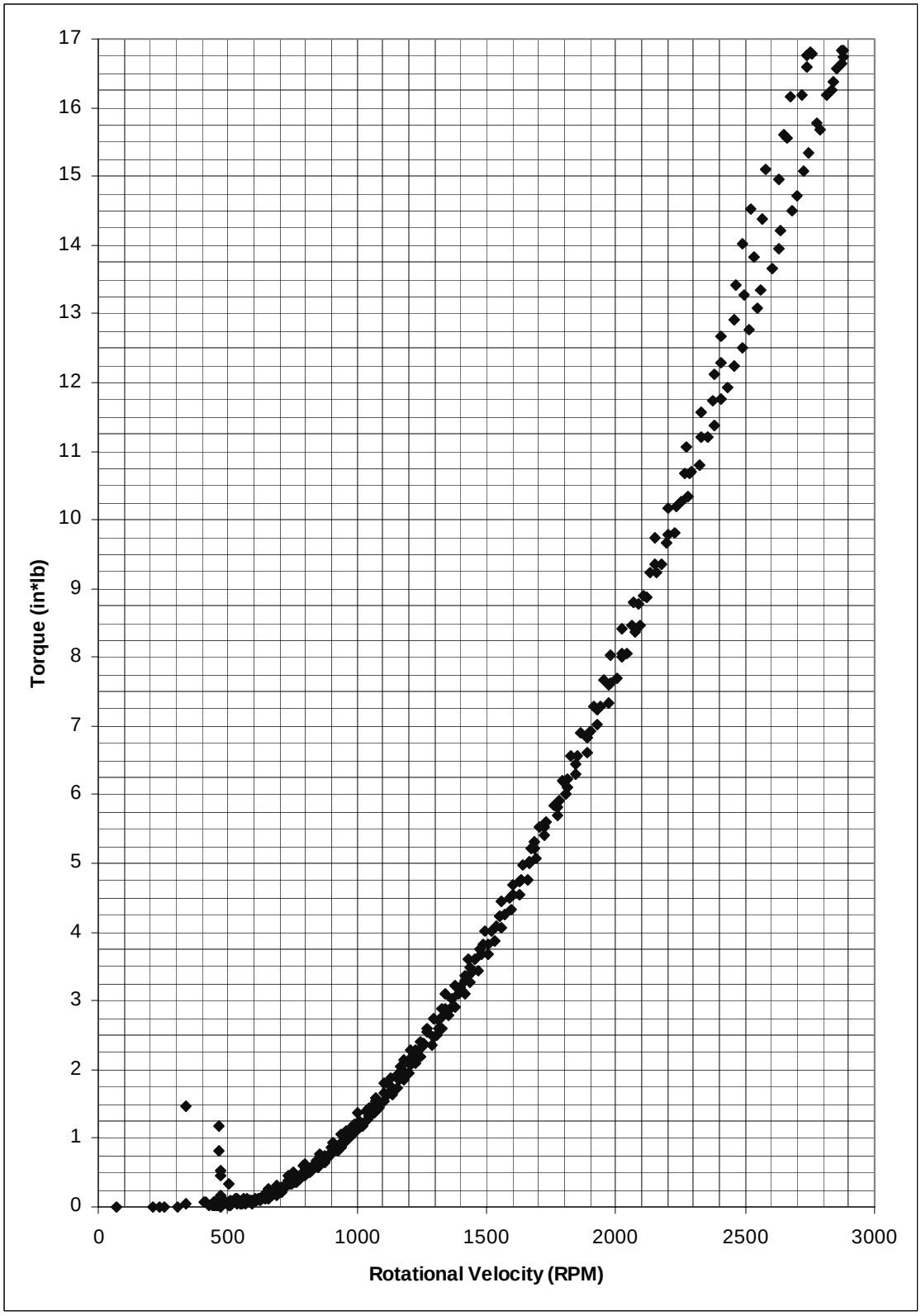


**Figure B-9** FOA clutch #1 data.

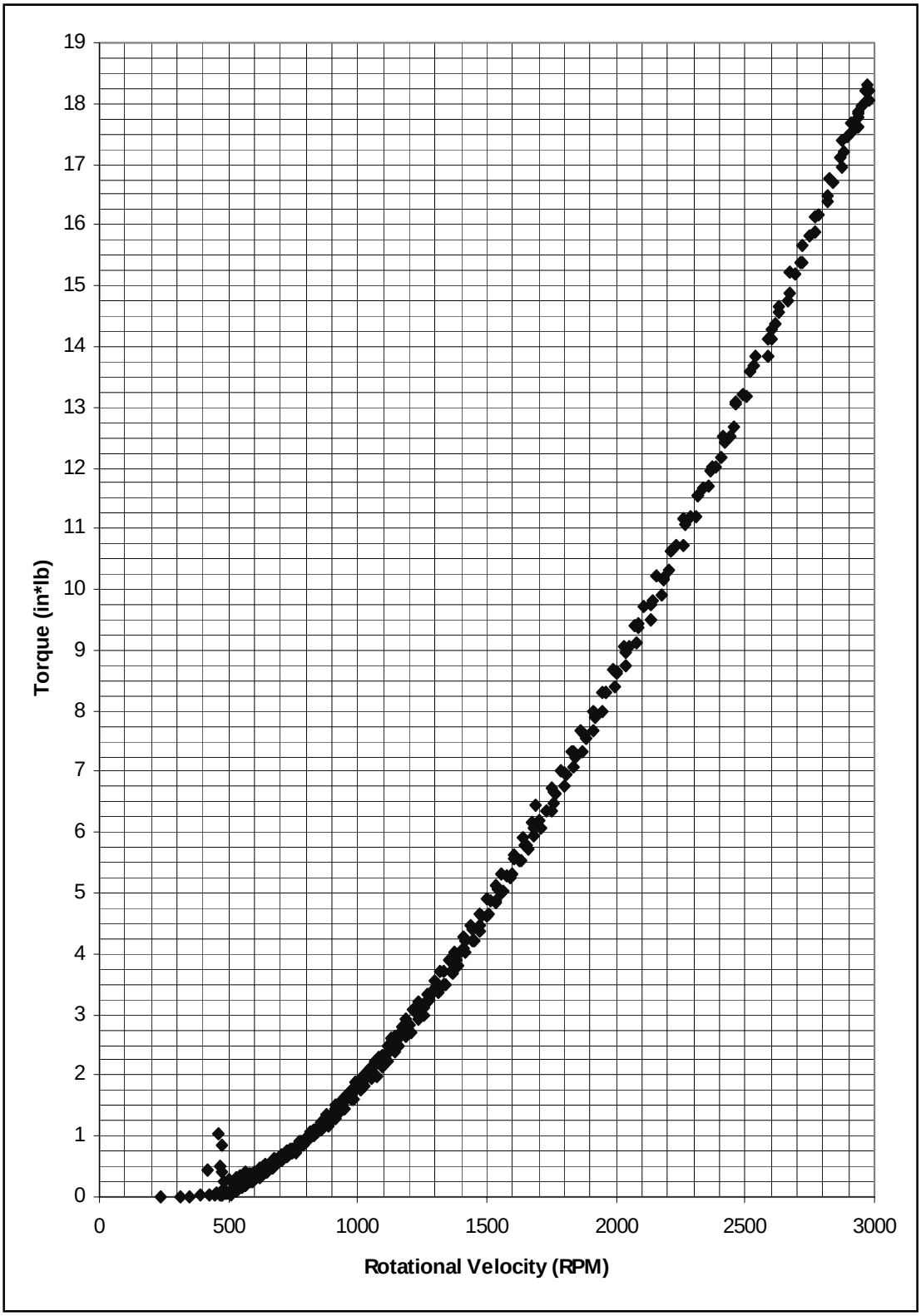


**Figure B-10** FOA clutch #2 data.

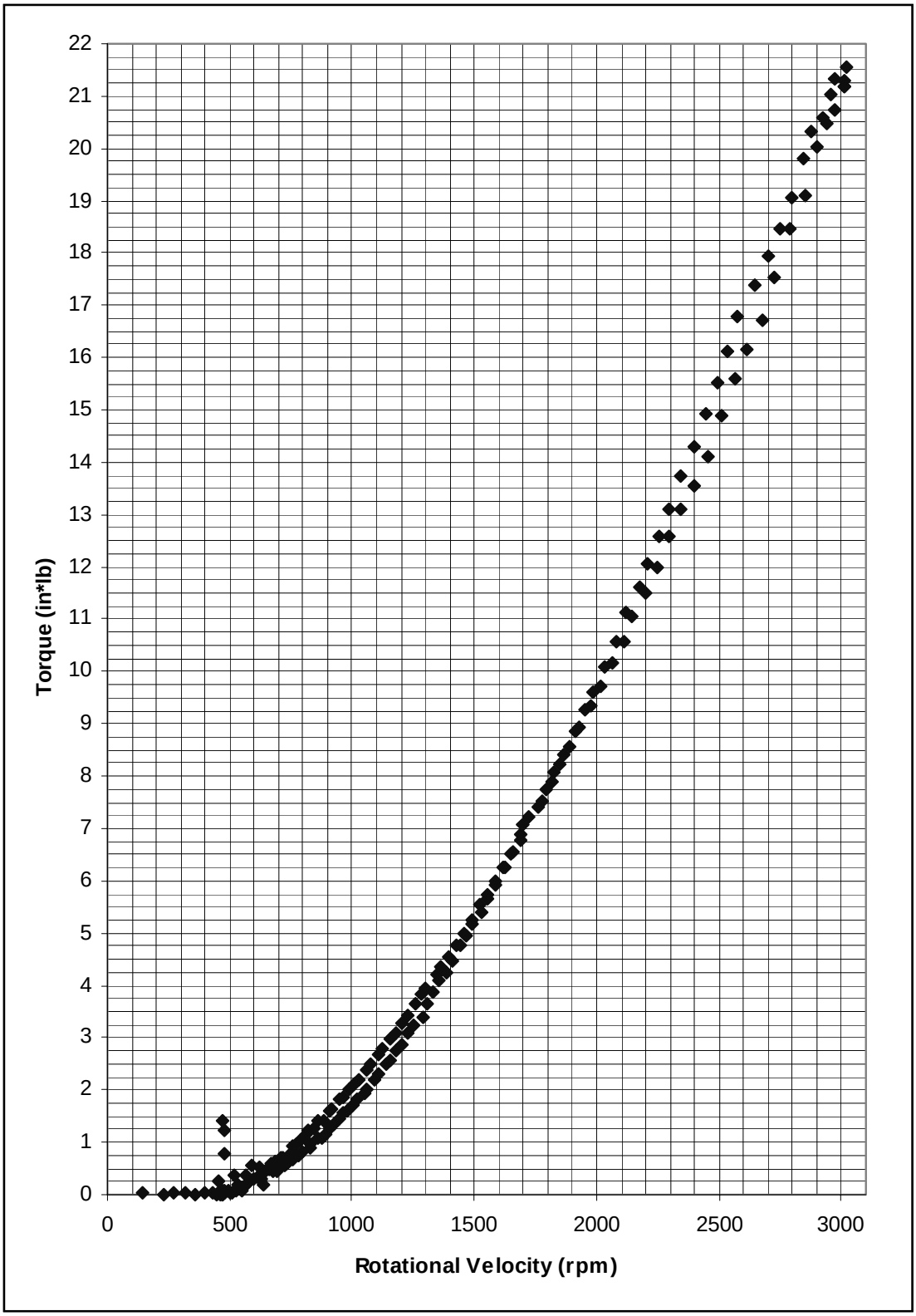


**Figure B-11** FOA clutch #3 data.

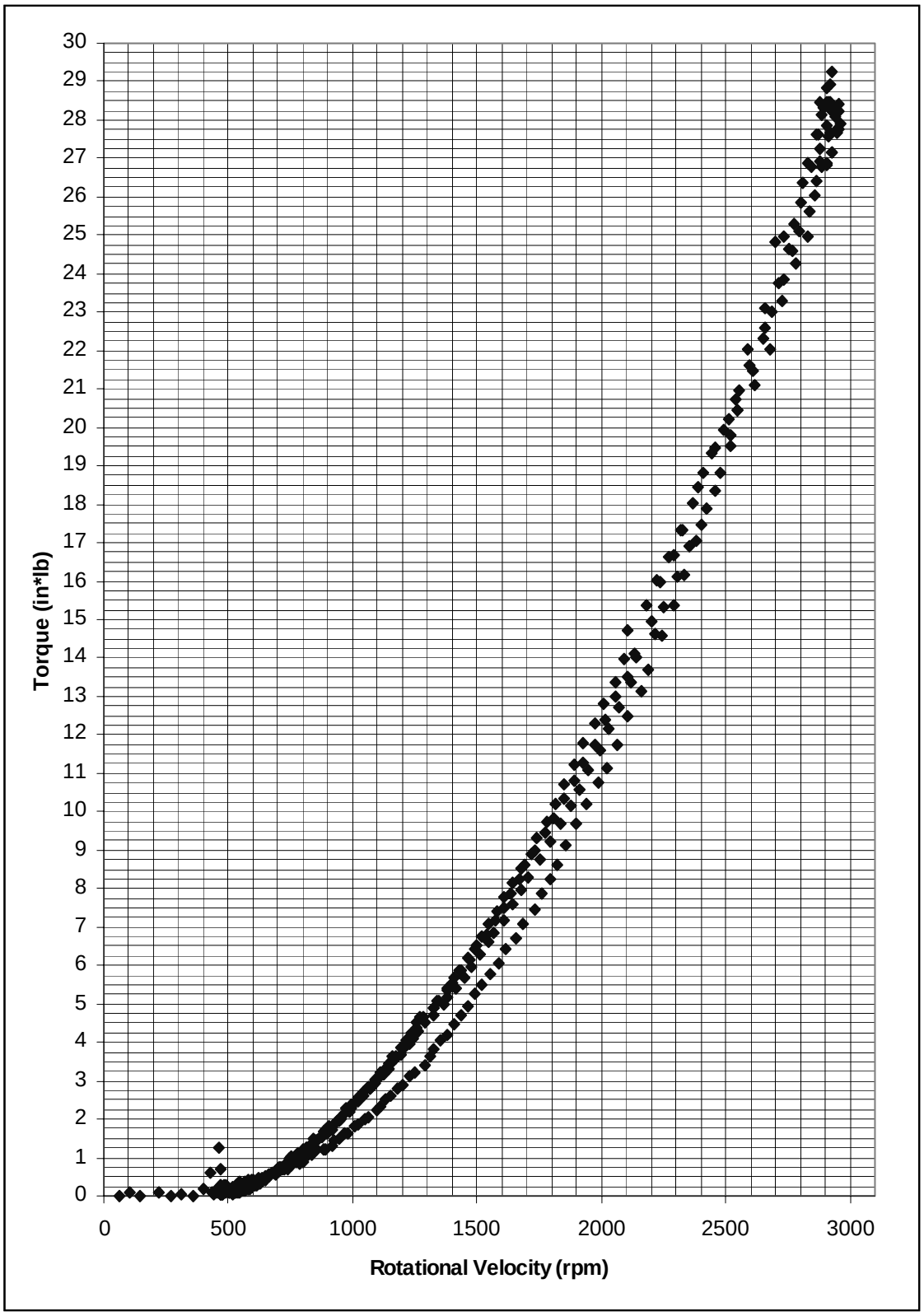


**Figure B-12** FOA clutch #4 initial results.

set of tests repeatedly recorded torques such as shown in Figure B-13 on page 151 with a corresponding average torque capacity of 2.66 in*lb/1000 rpm. This value is within nine percent of the model predictions.

The error is likely due to excessive bearing torque as was measured in Figure B-2 on page 137. A fifth order polynomial was fit to the bearing torque curve shown in Figure B-2 and subtracted from the torque data shown in Figure B-12 on page 149. The $T_b$ value calculated from this data is 2.64 in*lb/1000 rpm. This torque capacity is in good agreement with the second set of torque data. However, only the torque capacities and engagement speeds from the second set of data were used to calculate the average values reported in Chapter 5.

## B.9 Grounded Opposing Arm (GOA) Clutch

### B.9.1 GOA #1

Data is shown in Figure B-14 on page 152.

### B.9.2 GOA #2

Data is shown in Figure B-15 on page 153.

## B.10 Split-arm Clutch

### B.10.1 Split-arm #1

Data is shown in Figure B-16 on page 154.

### B.10.2 Split-arm #2

Data is shown in Figure B-17 on page 155.

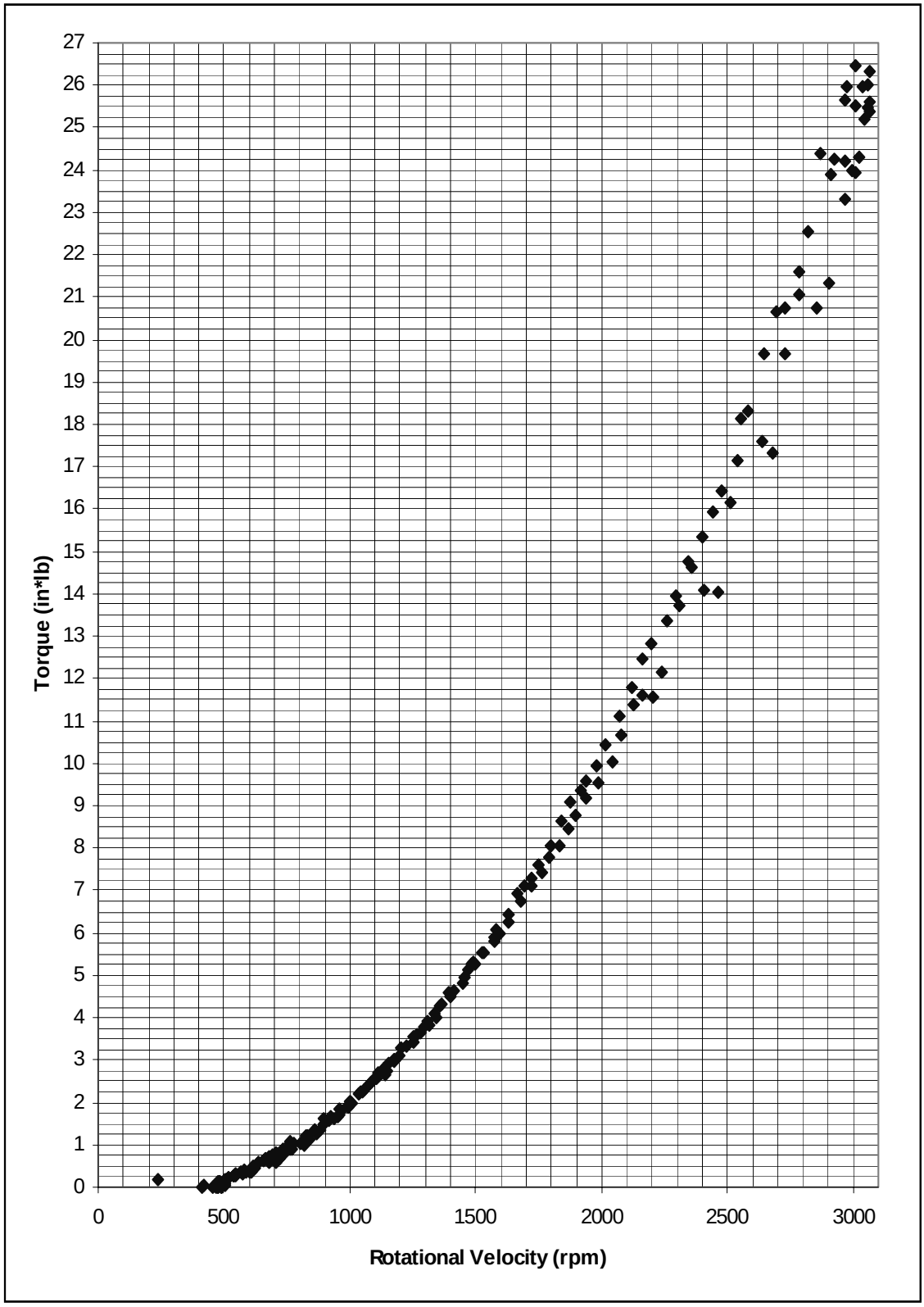


**Figure B-13** FOA clutch #4 secondary results.

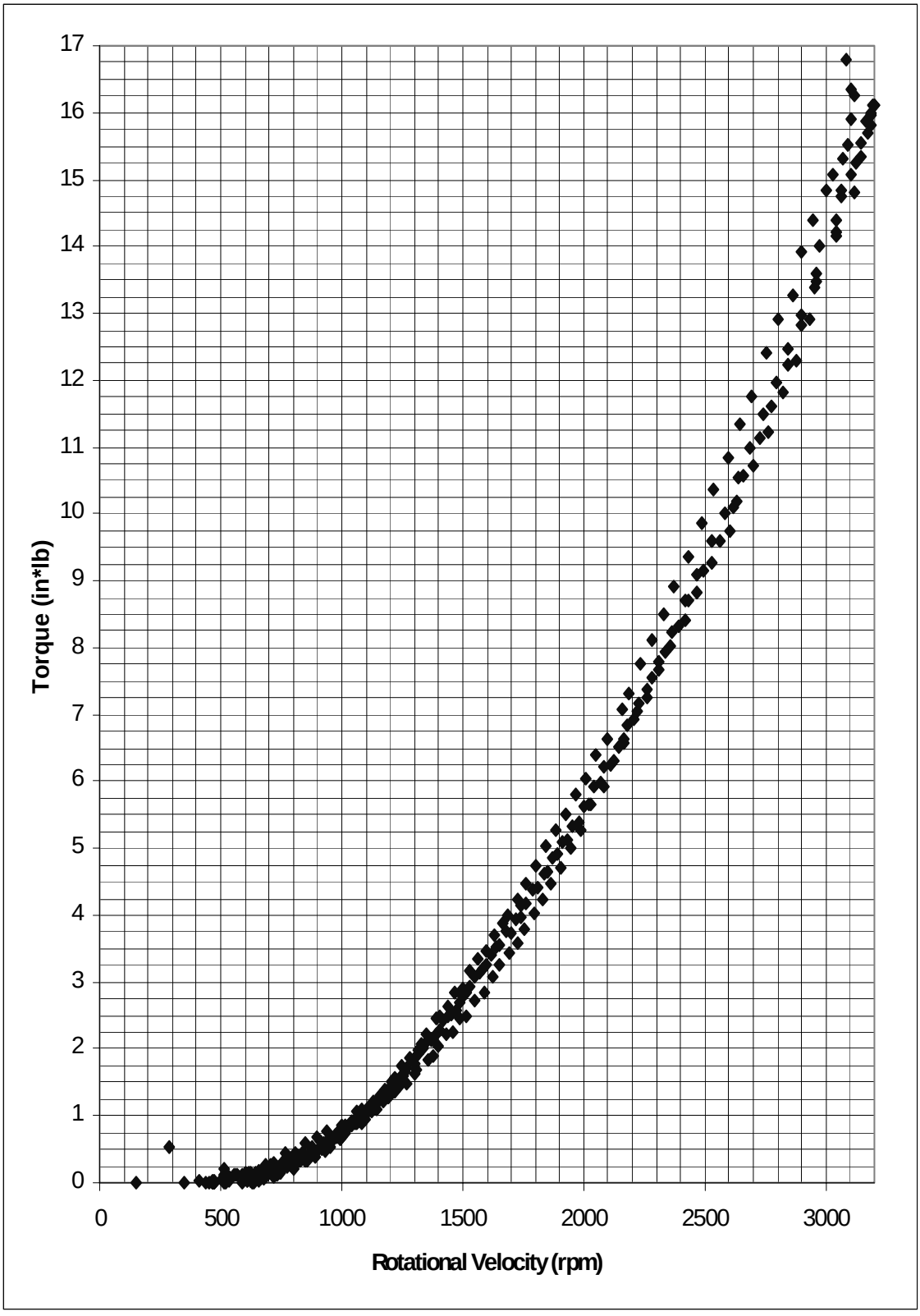


**Figure B-14** GOA clutch #1 data.

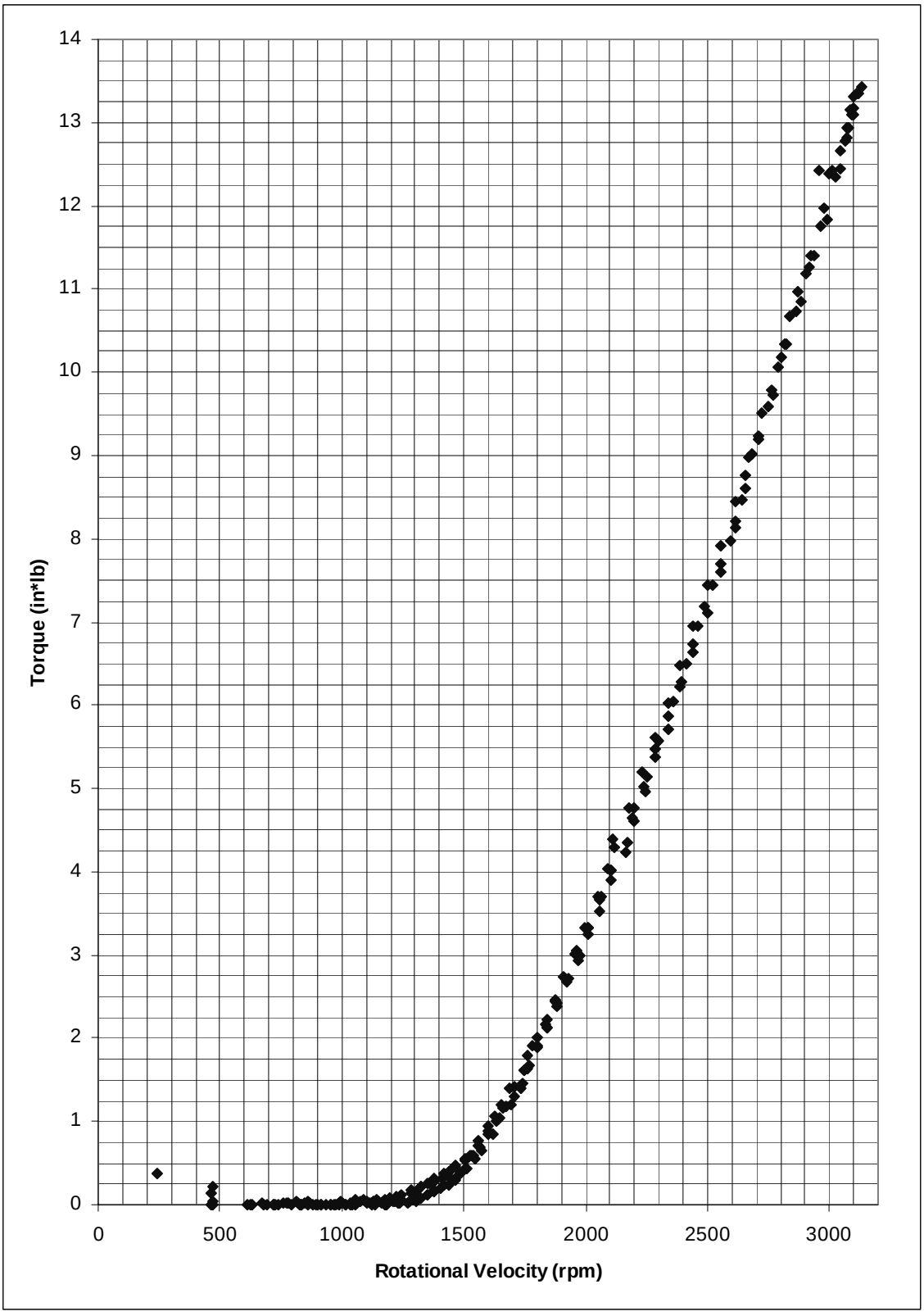


**Figure B-15** GOA clutch #2 data.

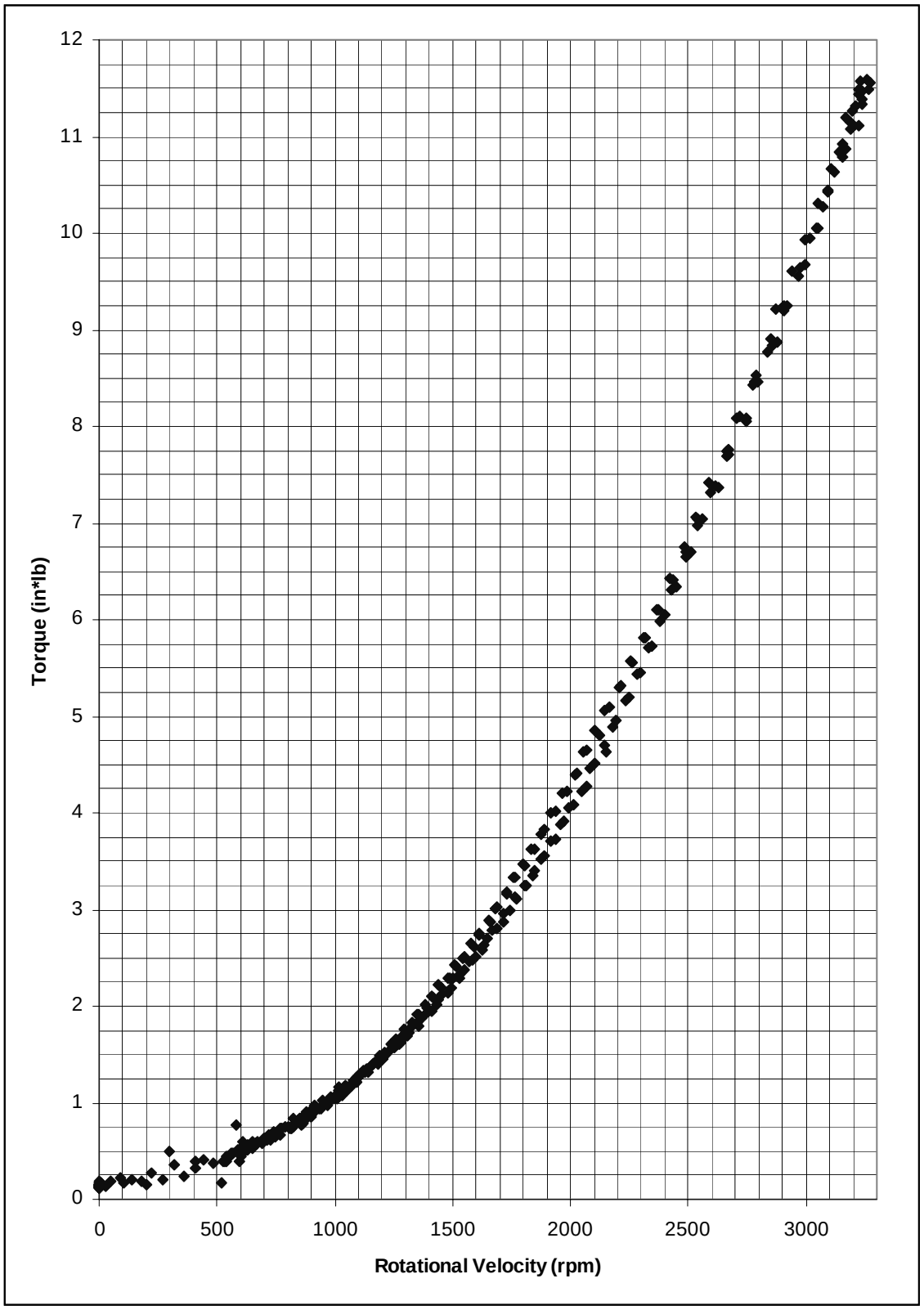


**Figure B-16** Split-arm clutch #1 data.

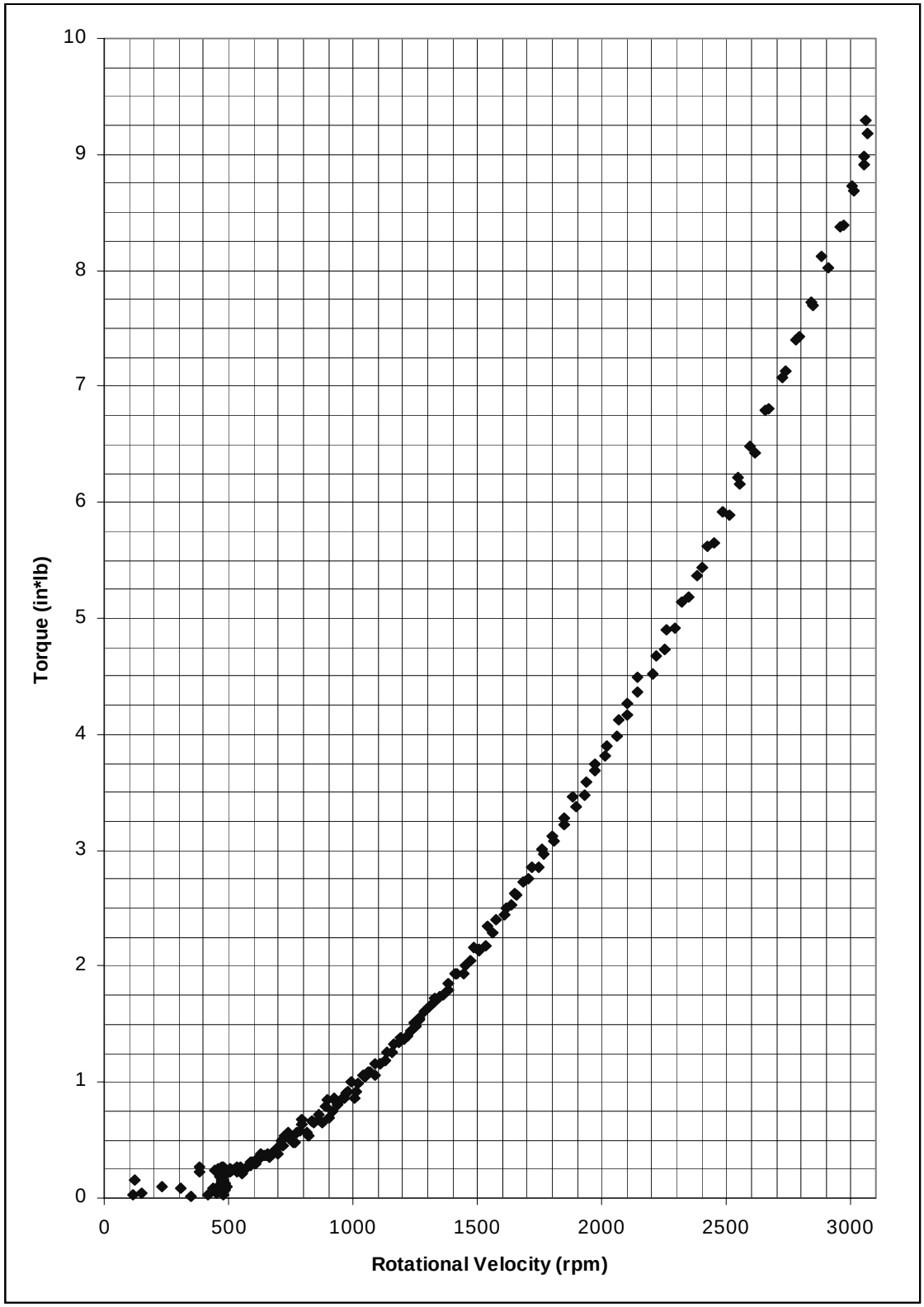


**Figure B-17** Split-arm clutch #2 data.

### B.10.3 Split-arm #3

Data is shown in Figure B-18 on page 157.

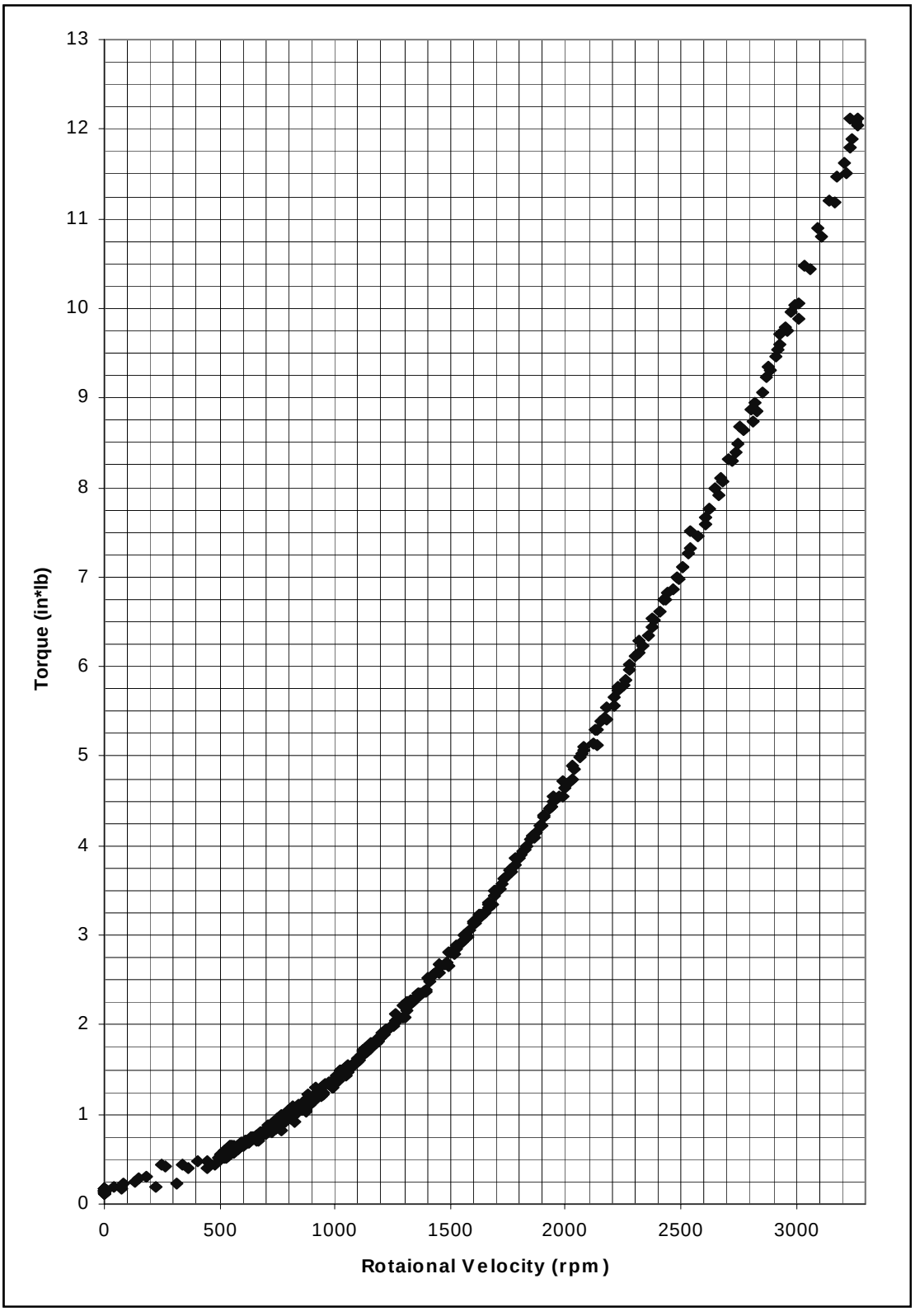


**Figure B-18** Split-arm clutch #3 data.